The status of scientific development on the application of biosorption of heavy metals at laboratory and pilot-scale: a review

Clint Sutherland*, Beverly S. Chittoo, Amar Samlal

*Project Management and Civil Infrastructure Systems, The University of Trinidad and Tobago, Trinidad and Tobago (WI),
Tel.: +1 868 497 5744; Fax: +1 868 643 1617; email: clint.sutherland@utt.edu.tt (C. Sutherland), Tel.: +1 868 770 3004;
email: beverly.chittoo@utt.edu.tt (B.S. Chittoo), Tel.: +1 868 342 0337; email: amarsamlal@hotmail.com (A. Samlal)*

ABSTRACT

Biosorption continues to grasp the attention of researchers worldwide for its potential to remediate and recover a wide spectrum of contaminants from the environment. In spite of 120 y since its first reported study, the commercialisation of biosorption technology has been somewhat slow, although we have made great strides in understanding this complex phenomenon. Many forms of life are fatally affected by heavy metal ions, mainly due to their non-biodegradability, and thus, their concentrations rise up the food chain. The presence of these contaminants in waste streams continues to present a costly remediation challenge, particularly for small and medium-sized industries. The aim of this study is to present the status of scientific development in biosorption of heavy metals. The review offers a brief history of biosorption developments, types of reported biosorbents, fundamental parameters affecting biosorption, biosorption modelling, desorption and mechanisms. In addition, the process of scaling-up from laboratory to pilot scale is considered as well as the main factors which continue to affect the evolution of biosorption as a useful method for heavy metals removal. Finally, we provided a summary of the key points of recent biosorption research as well as recommendations for its future lines of inquiry.

Keywords: Biosorption; Kinetic modelling; Heavy metal; Equilibrium modelling; Desorption; Biosorption mechanisms

1. Introduction

The quality of our water continues to degenerate due to anthropogenic activities, population growth, unplanned urbanisation, and rapid industrialisation. A number of contaminants, including heavy metals, dyes, pesticides and toxic organic compounds, have greatly increased water pollution as a result of expanded industrial and agricultural operations [1]. Contaminants ultimately accumulate throughout the food chain, turning this phenomenon into a severe environmental danger [2]. Further, when hazardous metals are present in the environment, they cycle between abiotic and biotic components, causing toxicity in the latter. The term heavy metal has been in use for over 80 y.

This term encompasses metal and their compounds and assumes they possess the same toxicological, biological, and physicochemical properties, which is misleading [3]. To date, a new classification system for heavy metals has not been universally adopted, and thus, in this study, the term heavy metal is continued to be used.

Mining, metallurgical, electrical, electroplating, and metal finishing are just a few of the industries that employ metals. Heavy metal ions are poisonous to both lower and higher organisms; thus, their presence in final industrial effluents is highly undesirable. Under some environmental circumstances, heavy metals may build up to unsafe concentrations and harm the environment [4]. Among these metals, mercury, lead, cadmium, arsenic, and chromium(VI) are deemed hazardous metals; other metals, such as cobalt,

* Corresponding author.

nickel, zinc, and copper, are non-toxic metals, but their widespread use and rising concentrations in the environment are raising concerns [5–7]. Further, due to the fact that they are not biodegradable and can accumulate in living organisms, these heavy metals have the potential to cause disease in the parts per billion (ppb) level [8].

Traditional physicochemical techniques for removing heavy metals from solutions include ion exchange, reverse osmosis, chemical precipitation, membrane filtration, adsorption using activated carbon and evaporation. However, most of these methods are often ineffective or uneconomical when heavy metal concentrations are higher than permissible concentrations [9]. Specifically, these techniques have high running costs, high capital costs (a drawback of ion exchange, chemical coagulation and adsorption using activated carbon), low efficiency (membrane process and ultrafiltration), inability to effectively recover heavy metals and high waste generation, creating yet another disposal problem.

Over the past decades, researchers have successfully demonstrated biosorption removal of heavy metals such as chromium, lead, zinc, arsenic, copper, nickel, cobalt, cadmium, mercury, iron, selenium and gold. The technique continues to gain prominence in scientific research as a potential basis for developing innovative wastewater treatment technologies [10]. Organic and inorganic substances have been effectively recovered or removed from solutions via biosorption, which uses biological material like live or dead microbes and their components [11]. A wide variety of biosorbents have been studied for their ability to sorb metals with varying degrees of effectiveness [12–14]. Common types of biosorbents have been derived from bacteria, industrial wastes, fungi, algae, agricultural wastes, and chitosan. Depending on how the biomass is processed, the species that are employed, where they came from, and the solution chemistry, one or more mechanisms, including ion exchange, adsorption, chelation, and diffusion through cell membranes, may be involved in biosorption [15].

The foregoing study's main objectives are: (1) to review the application of biosorption for heavy metal uptake at the laboratory (batch and column) and pilot-scale; (2) to report on pertinent recorded literature on the modelling of biosorption kinetics, equilibrium, and columns under several process conditions and highlight the best suited for a given biosorbent–sorbate interaction; (3) to review different operational factors affecting heavy metal biosorption, such as pH, temperature, biomass dosage, initial concentration, contact time and agitation speed; and (4) to identify the different mechanisms influencing a given biosorbent–sorbate interaction.

2. Biosorption

2.1. Biosorption overview

According to Fourest and Roux [16], "Biosorption can be defined as the ability of biological materials to accumulate heavy metals/contaminants through metabolically mediated or physico-chemical pathways of uptake". A biological entity, such as a living organism, component, or product made from or generated from a living organism, is indicated by the prefix "bio" [17]. While life scientists primarily focused on the toxicological effects and accumulation of heavy metals in microorganisms, environmental scientists

and engineers used this ability of microorganisms as a way to monitor heavy metal pollution as well as for removal/recovery of metals from metal-bearing wastewaters [18]. According to Ramachandra et al. [10], in the 1970s, there was a rise in environmental consciousness and concern, which sparked research into innovative, cost-effective technology for treating wastewater contaminated with metals and dyes. Muraleedharan et al. [18] conducted a detailed historical account of major developments in biosorption which is presented in tabular form in Table 1. In the past three decades, several patents have been granted for breakthroughs in biosorption technologies. Some of the noted breakthroughs include a patent granted to Landell [19] for the development of a hydrogel chitosan-derived biosorbent. Patents based on the use of bacteriological-derived biosorbents such as *Pseudomonas alcaliphila* by Li et al. [20], *Bacillus* sp. by Tadic et al. [21], *Cupriavidus metallidurans* by Pfeiffer et al. [22], and *Pseudomonas stutzeri* by Lewis et al. [23]. Algal-derived biosorbents have been patented by Oberholster and Cheng [24] for the use of *Chlorella protothecoides* and *Chlorella vulgaris* and Rivasseau et al. [25] for a specie of *Coccomyxa*. Fungal-derived biomass such as *Fusarium oxysporum* have been patented by Kozubal et al. [26] and *Rhizopus stolonifer* by Prigione et al. [27]. These developments serve to support the value and effectiveness of biosorption technologies. Volesky [28] iterated that the technology of biosorption has more advantages when compared to conventional techniques such as reverse osmosis, ion exchange, electrodialysis, ultrafiltration, and chemical precipitation. The author went on to explain that some of the main advantages include low-cost, the ability of biosorbents to be selective for different contaminants, regeneration ability, no sludge generation and the possibilities of metal recovery.

There are noted biosorption drawbacks, particularly, biosorbent leaching of organics into treated effluent. Some studies have attempted to elucidate the extent of leaching and pre-treatment techniques to mitigate or reduce leaching. Notably, Chen and Yang [29] reported on the pre-treatment of *Sargassum* sp. using 0.2% formaldehyde, which resulted in an 80% reduction in leached organic content during biosorption of Cu(II) ions. Further, the authors confirmed that the fraction of biomass removed in the modification did not contribute significantly to metal biosorption. Davis et al. [30] showed that at higher Cd(II) concentrations, reduced organic leaching by *Sargassum fluitans* was observed, possibly due to cross-linking of Cd(II) ions with alginate. Matheickal and Yu [31] pre-treated *Durvillaea potatorum* and *Eucalyptus radiata* using 0.2 M CaCl₂ solution to produce a sorbent with low to negligible organic leaching and increased stability. Sorbent leaching is not a major focal point in current biosorption research. However, the release of biosorbent organics can cause biosorption columns to clog, negatively impact the quality of treated effluent and introduce an additional burden on treatment costs. Thus, greater research attention is warranted.

The ability of biosorbents to remove heavy metals can be improved by pre-treating the material, which can result in stretching biopolymer rings, thereby increasing porosity and stability [32–34]. Physical alterations (such as steam activation, drying, or heating) are simple and inexpensive but are rarely used because they are ineffective at enhancing heavy

Table 1
Summary of historical overview of biosorption as presented by Muraleedharan et al. [18]

Year	Description of work
1902	Hecker as cited in [18], published the first quantitative investigation on the uptake of copper by fungal spores of *Tilletia tritici* (the cause of common bunt of wheat) and *Ustilago crameri*
1922	Pichler and Wobler as cited in [18], reported the uptake of silver (Ag), mercury (Hg), copper (Cu), and cerium (Ce) by corn smut
1949	Ruchloft as cited in [18], reported that activated sludge efficiently removed plutonium-239 from wastewater
1953	Rudolf and Zuber as cited in [18], investigated the influence of sludge volume index on the removal of metals in the activated sludge process
1966	Polikarpov as cited in [18], reported that radionuclides present in seawater were accumulated by marine microorganisms
1968	Friedman and Dugan as cited in [18], reported on the concentration and accumulation of metallic ions by the bacterium *Zoogloea*
1971	Goldman and Roberts as cited in [18], reported on the use of moss for monitoring heavy metal pollution
1973	Brown et al. as cited in [18], investigated the relationship between metal concentration and uptake of metals by sludge floc
1975	Cheng et al. as cited in [18], reported on the uptake of heavy metals by activated sludge where the authors concluded metal uptake was dependent on pH, concentrations of sludge, soluble organic matter, and metal ions in the system
1975	Neufeld and Hermann as cited in [18], reported on the kinetics of sorption of metals onto acclimated activated sludge
1979	Brown and Lester as cited in [18], reported on the removal of metal ions in activated sludge systems by the accumulation in the cytoplasm of a bacterial cell or adsorption onto the cell wall
1979	Sakaguchi et al. as cited in [18], reported on the adsorption of uranium from seawater by *Chlorella* dry cells, orange peel, chitin, chitosan, cellulose and starch
1980	Muzzarelli et al. as cited in [18], reported on hot-alkali treatment of different fungal masses originating from food and pharmaceutical industries for the removal of heavy metals
1981	Tsezos and Volesky as cited in [18], reported on the uptake of uranium and thorium by dead fungal mycelia
1985	Macaskie and Dean as cited in [18], investigated the removal of uranium using immobilised cells of a *Citrobacter* sp. The authors were able to desorb and recover greater than 90% of the sorbed metal
1987	Muraleedharan et al. as cited in [18], investigated the use of *Ganoderma lucidum* as a biosorbent for copper uptake. The authors reported a rapid uptake of 90% within the first 10 min
1990	Sharma and Venkobachar as cited in [18], reported on the copper-binding ability of dried anaerobic sludge generated from a UASB reactor

metal sorption on the surface of the biosorbent [35,36]. On the other hand, chemical modifications are given priority since they are successful in increasing the stability of biosorbents and their capacity for metal sorption [37]. Chemical treatment is used to change the water sorbency, ion exchange capability, conductivity, hydrophilicity, and hydrophobicity of cellulosic materials. To boost the adsorption capacity of agricultural wastes, most researchers recommend simply washing with acid, alkali, or another solvent [37–40]. The physical characteristics of biosorbents can vary depending on the nature of the sorbent and the type and degree of pre-treatment. Biosorbent pre-treatment is usually carried out to free occluded pores, thereby increasing the pore volume and specific surface area. Generally, biosorbents possess varying degrees of compressibility, mechanical strength, size, rigidity and density. These characteristics can also change after successive sorption/desorption runs. Consequently, physical parameters of biosorbents such as porosity, pore volume, pore diameter and surface area are often overlooked by researchers. Industrial-derived biosorbents such as tea factory waste possessed Brunauer–Emmett–Teller (BET) specific surface area (SSA) of 1.0 m^2/g [41] and raw eggshells of 1.61 m^2/g [42]. While acid-treated *Aspergillus niger* [43] and *Rhizopus arrhizus* [44] exhibited SSA of 1.9 and 0.7 m^2/g,

respectively. Non-viable bacteria cells exhibited BET surface area of 1.06 m^2/g, pore volume of 0.004 cm^3/g and pore size of 2.5 nm [45]. Agricultural-derived biosorbent as coconut tree sawdust and sugarcane bagasse reveal BET surface area of 0.4 and 2.8 m^2/g and pore diameter of 1.9 and 7.2 nm, respectively [46]. It is notable that despite the varying nature of these biosorbents, parameters such as specific surface area and pore size do not appear to differ significantly.

2.2. Batch biosorption systems

A well-mixed aqueous medium (including a target metal ion) is typically used in batch investigations. A small quantity of biosorbent is then added, and the metal-saturated biomass is removed from the mixture after a period of time [47,48]. The metal ion concentrations are then determined by analysing the filtrate. Data from batch systems, such as the various operational factors affecting biosorption (pH, temperature, initial concentration, particle size etc.), are then used to scale-up either to a pilot or a full-scale system.

2.3. Column biosorption systems

The continuous or column mode of operation is commonly used to assess the technical viability of biosorption
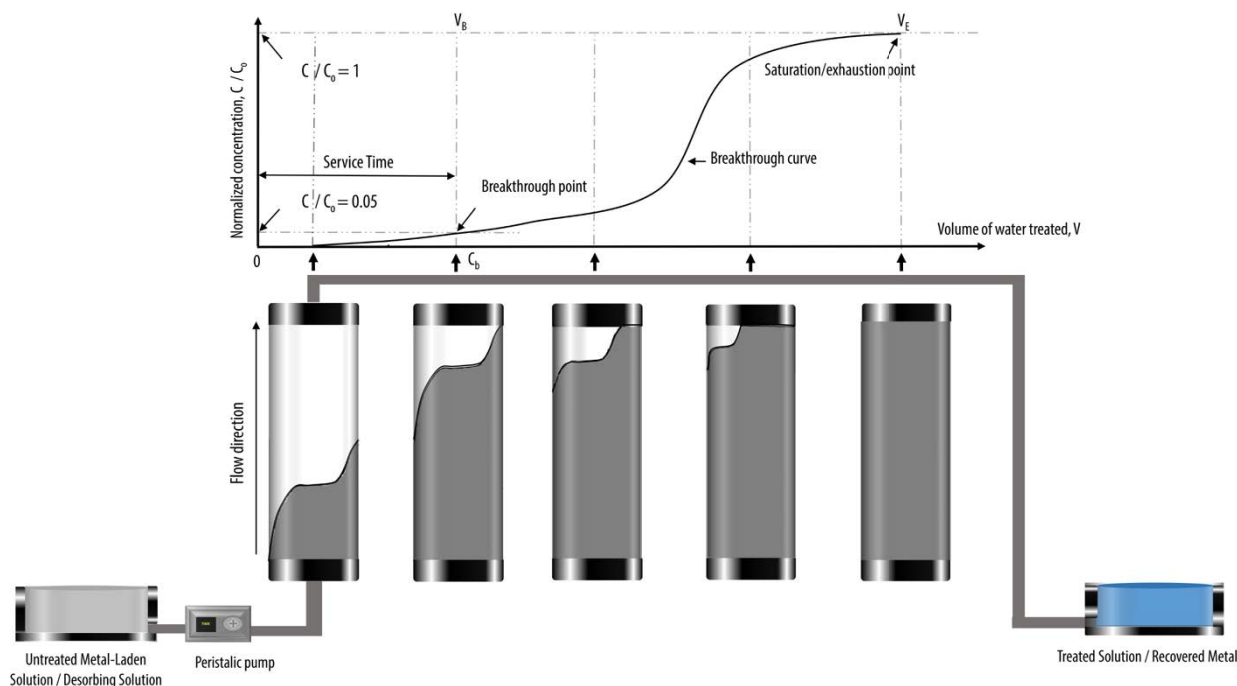
Fig. 1. Biosorption breakthrough curve shown in a schematic illustration of a packed column configuration.

for real-world applications. A packed bed system (Fig. 1) is the simplest, most successful, and most economical column system for biosorption [49–52]. Sag [53] reviewed the application of biosorption capability using four distinct column operation techniques under identical circumstances. Biosorption capacity decreased as follows: packed column (fixed-bed) reactor (PCR) followed by three batch stirred-tank reactors in series (BSTRS), continuous flow stirred-tank reactor (CFST) and finally batch stirred-tank reactor (BSTR). Fixed-bed reactors continue to be the configuration of choice by researchers [54]. The effluent quality is improved by packed bed systems because they maximise the concentration difference, which is thought to be the key factor in sorption. They also make better use of the available sorbent capacity [55]. Packed bed sorption also provides advantages such as a high operating yield and relative simplicity of scaling-up operations [56]. A packed bed experiment, as its name says, is a cylindrical column filled with sorbent that allows wastewater to flow through it by gravity or pressure. Initially, when the solute is exposed to the new biosorbent bed, the majority of it will be sorbed (bind to the surface of biomass), leading to a nearly zero concentration in the column output; supposedly, this is the point where the majority of mass is transferred in the mass transfer zone or adsorption zone [57,58]. Over time the bed will get saturated with solute and the concentration will progressively increase at the column exit; the breakthrough concentration is dependent on the solute toxicity [57]. Papirio et al. [59] explained that a valuable technique for assessing the effectiveness of biosorbents is the breakthrough curve, which is often S-shaped and is obtained by graphing the normalised effluent concentration C/C_o vs. time. Additionally, the amount of solute removed at saturation may be easily determined in the region above the breakthrough curve

(Fig. 1), where the slope gives information on the column service time.

3. Biosorbents

3.1. Bacterial-derived biosorbents

The method of biosorption was found to allow inactive/dead microbial biomass to passively bind metal ions. The advantages of dead microbial biomass over living microbial biomass include affordability, reduced toxicity, ease of regeneration, and operation within a wide range of pH and temperature [60]. The three main shapes of the most prevalent bacteria are spherical or ovoid (coccus), rod-shaped (*Bacillus*), and spiral (*Spirillum*). However, there are many different shapes because of variations in genetics and ecology [61]. Bacterial biomass is typically created as a waste product from industrial processes or it can be purposefully propagated on a big scale. Because of their small size, prevalence, ability to thrive under controlled settings, and tolerance to a wide variety of variable environmental conditions, bacteria are utilised as biosorbents [62–64]. Among the group of bacteria, we can distinguish gram-positive and gram-negative. The prokaryotic cell's diameter ranges from 0.5 to 1.0 μm, and nearly all of them are unicellular [60]. The cell has four major components, cytoplasm, cell wall, nuclear and cell membrane [60]. Thick peptidoglycans connected by amino acids are found in gram-positive bacteria. By producing lipoteichoic acids, which are necessary for effective membrane bonding, the teichoic acids contained in the cell wall are joined to the lipids of the cytoplasmic membrane. The biosorption of divalent cations is linked to the total negative charge produced by the presence of phosphodiester linkages between the monomers of teichoic acid [65]. Bacteria such as *Microcystis novacekii*, *Bacillus xiamenensis*,

Pseudomonas spp. and *Bacillus subtilis* have demonstrated a strong affinity for heavy metals (Table 2).

Bacteria frequently create extracellular polymeric substances (EPS) as a defensive reaction to challenging environmental conditions, including the presence of toxic heavy metals and antibiotics [71]. Bacterial EPS are high molecular weight, naturally occurring polymers that bacteria produce into their surroundings and can exist as slime on

Table 2
Biosorptive performance by bacterial-derived biosorbents for the removal of heavy metals

Nature of biosorbent	Heavy metal	Biosorbent	Experimental conditions	Results description	References
Bacterial-derived	Pb(II)	*Micrococcus* sp.	pH: 5.0–9.0, initial metal concentration: 20–100 mg/L, biomass concentration: 0.25–1.25 g/L, temperature: 30°C	There was an 84% removal efficiency with a contact time of 1,440 min, pH of 6.0, and temperature of 30°C	[66]
	Pb(II)	*Bacillus xiamenensis*	Contact time: 0–400 min, pH 4.0–9.0, initial metal concentration: 100 mg/L, biomass concentration: 0.1–2 g/L, temperature: 25°C–40°C	Maximum biosorption obtained was 216.8 (for live) and 207.4 mg/g (for dead) at a pH of 6.0 and biosorbent dose of 1 g/L	[67]
	Pb(II)	*Microcystis novacekii*	Contact time: 0–240 min, pH: 5.0–7.0, initial metal concentration: 10–50 mg/L, biomass concentration: 1.0 g/L, temperature: 21°C	The maximum sorption capacity was found to be 70.0 mg/g at a temperature of 21°C, contact time of 60 min, and pH of 5.0	[68]
	Cu(II)	*Bacillus* sp.	pH: 5.0–9.0, initial metal concentration: 20–100 mg/L, biomass concentration: 0.25–1.25 g/L, temperature 30°C	There was a 69% removal efficiency with a contact time of 1,440 min, pH of 7.0, and temperature of 30°C	[66]
	Cr(VI)	*Bacillus licheniformis*	Contact time: 0–48 h, pH: 2.0–4.5, initial metal concentration: 150 mg/L, temperature: 20°C–37°C	There was a 52% removal efficiency with a contact time of 2,880 min, pH of 3.5, temperature of 28°C, agitation speed of 120 rpm, and an initial concentration of 150 mg/L	[69]
	Cd(II)	*Pseudomonas* sp.	pH 5.0–9.0, initial metal concentration: 20–100 mg/L, biomass concentration: 0.25–1.25 g/L, temperature: 30°C	There was a 90% removal efficiency with a contact time of 1,440 min, pH of 6.0, and temperature of 30°C	[66]
	Ni(II)	*Bacillus subtilis*	Contact time: 10–90 min, pH 4.0–8.0, initial metal concentration: 2–32 mg/L, biomass concentration 0.1–0.8 mg dry mass/mL, temperature: 25°C–45°C	There was a 99% (185.0 mg/g) removal efficiency with a pH of 5.0, temperature of 35°C, initial concentration of 2 mg/L, and a contact time of 10 min	[69]
	Au(III)	*Bacillus megaterium*	pH 1.0–7.0, initial metal concentration: 10 mg/L, biomass concentration: 5–20 mg dry wt., temperature: 25°C	The maximum biosorption capacity was found to be 13.2 mg/g with a pH of 3.0, temperature of 25°C, initial concentration of 10 mg/L, and a biomass dosage of 0.15 g/L	[70]
	Au(III)	*Pseudomonas aeruginosa*	pH 1.0–7.0, initial metal concentration: 10 mg/L, biomass concentration: 5–20 mg dry wt., temperature: 25°C	The maximum biosorption capacity was found to be 32.7 mg/g with a pH of 3.0, temperature of 25°C, initial concentration of 10 mg/L, and a biomass dosage of 0.15 g/L	[70]
	Au(III)	*Pseudomonas maltophilia*	pH 1.0–7.0, initial metal concentration: 10 mg/L, biomass concentration: 5–20 mg dry wt., temperature: 25°C	The maximum biosorption capacity was found to be 37.6 mg/g with a pH of 3.0, temperature of 25°C, initial concentration of 10 mg/L, and a biomass dosage of 0.15 g/L	[70]

microbial surfaces or as attached capsular polysaccharides [72]. Several studies have reported high removal capacities of the EPS produced by strains such as *Paenibacillus jamilae* [73], *Bacillus licheniformis* [74], *Oceanobacillus profundus* [71], *Pseudomonas fluorescens* [75], *Escherichia coli* [76], and *Bacillus vallismortis* [77] for various heavy metals including Zn^{2+}, Pb^{2+}, Ni^{2+}, Cu^{2+}, Cd^{2+}, Co^{2+}, Hg^{2+}, Al^{3+}, Cr^{4+}. Results presented in the literature even suggest that EPS contributes far more to metal ion sorption than bacterial cells. According to Lu et al. [78], studies analysing *Desulfovibrio vulgaris* found that living cells exhibited an adsorption capacity for Ca^{2+} of up to 44.4 mg/g, while tightly bound EPS and loosely bound EPS had adsorption capacities for Ca^{2+} of up to 64.5 and 136.7 mg/g, respectively. The ability of EPS to sorb metal cations was generally attributed to the presence of negatively charged functional groups such as carboxyl, sulfate, phosphate, phosphoryl and hydroxyl groups in these macromolecules' structures [79,71]. According to Saba et al. [80] and Concórdio-Reis et al. [79], the immobilisation of heavy metals within the EPS is caused by the deprotonation of these functional groups into anionic species, which interact with cationic metal ions through electrostatic interactions.

3.2. Algal-derived biosorbents

Algae are abundantly available in seas and oceans and have a high metal-sorption capacity [81,82]. Being autotrophic, it also has low food requirements and produces a lot of biomass, in contrast to other biomass and microorganisms like bacteria and fungi. In most cases they do not produce any harmful materials. The two most prevalent types of algae are microalgae and macroalgae; macroalgae are frequently referred to as seaweeds [83]. Seaweeds are multicellular plants that may grow in salt or fresh water and are categorised into three kinds based on their colour, viz. red, brown, and green [84]. Alginate, with its carboxyl and hydroxyl groups, is found in the cell walls of brown and green algae [85,86]. Due to the composition of sulfated polysaccharides consisting of galactans (which include significant amounts of hydroxyl and carboxyl groups), red algae have drawn recent interest for biosorption. Microalgae, on the other hand, are unicellular photosynthetic plants that thrive in both fresh and salt water. They are grouped according to their pigmentation, the configuration of their photosynthetic membranes, or other physical characteristics [84]. It also has a slightly distinct cell wall, with polysaccharides, proteins, and lipids as the main components. Components such as carboxyl, hydroxyl, phosphate, and sulfate groups provide a net negative charge on the cell surface and promote metal cation binding through counter-ion interactions [84]. Examples of microalgae are green-blue, golden algae, diatoms, *Chlorella* spp., *Chlamydomonas* spp., and freshwater algae (Table 3).

3.3. Fungal-derived biosorbents

According to Abbas et al. [61], fungi have the benefit of having a high percentage of cell wall materials, which makes it possible for them to quickly and affordably biosorb dangerous heavy metals from diluted aqueous solutions. The cell wall of fungi is made up of chitin, cellulose, glucan, chitosans, polyuronides, glycoproteins, lipids, inorganic salts, and pigments. The antibiotic and food industries both produce substantial quantities of fungi [101]. Three groups of fungi (Table 4) are of major practical importance in biosorption, moulds (*Aspergillus* spp., *Rhizopus* spp.), yeasts (*Saccharomyces* spp., *Candida* spp.) and mushrooms (*Agaricus* spp., *Trichaptum* spp.) [37]. Adewuyi [60] opined that using yeast for environmental studies has increasing appeal due to its ability to be genetically altered. These genetic alterations can be done either chemically or physically to boost the biosorbent capability. The modification can be carried out by removing the functional groups from the surface or concealing them, which can result in creating readily accessible biosorption sites [101,102]. Additionally, modifications to the cell wall can result in derivatives with varying sorption capabilities and affinities [101]. The free cells of fungus utilised in biosorption have small particle sizes and low mechanical strength, requiring the application of excessive hydrostatic pressure to produce a tolerable flow rate in column applications [60]. Furthermore, due to disintegration and attrition, when employed in industrial processes, the biosorbent, despite maybe performing well in a batch system, is unsuited for column packing procedures [103]. Due to the difficulty with disintegration and attrition, immobilisation techniques like cross-linking and trapping have been recommended as means of modification [60]. The biosorbent improves and gains an advantage when it is mounted on a polymeric matrix in terms of particle size, high biomass loading, little clogging, high regeneration, and simplicity of separation [104].

3.4. Chitosan-derived biosorbents

Chitosan, which is produced by deacetylating chitin, the most common amino-polysaccharide in nature, is less expensive than commercial activated carbon and has a strong affinity for pollutants, especially metals [11]. Chitosan has received wide attention in treating a large number of aquatic pollutants, including heavy metals (Table 8), due to its high contents of amino and hydroxyl functional groups [108]. Various natural sources, including crustaceans, fungi, insects, annelids, and molluscs, include chitin, a naturally occurring mucopolysaccharide [10]. However, chitin and chitosan are only commercially produced from crustaceans (crab, krill, and crayfish) primarily because a considerable volume of the crustacean's exoskeleton is available as a by-product of food processing [10]. Chitosan may be modified because it is not suitable for practical usage in its natural state due to its low mechanical strength and solubility in acidic environments. Physical modifications (radiation or UV light) and chemical alterations (cross-linking agents) allow the chitosan to remain stable in acid for metal sorption [109]. Cross-linking agents such as sodium trimetaphosphate, sodium tripolyphosphate, or carboxylic acids have been recommended to accomplish a safe and environmentally acceptable biosorbent [110].

3.5. Industrial-derived biosorbents

Numerous sectors, particularly those in the food industry, dispose of considerable amounts of waste and by-products [65]. By employing these industrial wastes (Table 5) as

Table 3
Biosorptive performance by algal-derived biosorbents for the removal of heavy metals

Nature of biosorbent	Heavy metal	Biosorbent	Experimental conditions	Results description	References
Algal-derived	As(III)	*Maugeotia genuflexa*	Contact time: 5–90 min, pH: 2.0–10.0, initial metal concentration: 10–400 mg/L, biomass concentration: 0.4–16 g/L, temperature: 20°C–50°C	The maximum monolayer biosorption capacity was found to be 57.5 mg/g (97% maximum biosorption efficiency) at a pH of 6.0, biomass concentration of 4 g/L, contact time of 60 min, and temperature of 20°C	[87]
	As(V)	*Lessonia nigrescens*	Contact time: 10–1,580 min, pH: 2.5–6.5, initial concentration: 50–600 mg/L, temperature: 20°C	The maximum adsorption capacity was found to be 45.2 mg/g at a pH of 2.5, temperature of 20°C, and contact time of 300 min	[88]
	Pb(II)	*Chlamydomonas reinhardtii*	Contact time: 0–120 min, pH: 2.0–7.0, initial metal concentration: 100 mg/L, biomass concentration: 0.2–1 g/L, temperature 5°C–35°C	The maximum adsorption was 96.3 mg/g dry biomass at a pH of 5.0, contact time of 60 min, and temperature of 25°C; regenerated using 0.1 M HCl with 98% recovery	[89]
	Pb(II)	*Nizimuddinia zanardini*	Contact time: 15–1,440 min, pH: 2.5–7, initial metal concentration: 0.0625, 0.125, 0.25, 0.5, and 1 mmol/L, temperature: 20°C–50°C, particle size: 0.5–1 mm	The maximum sorption capacity was 51.8 mg/g at a pH of 5.5, contact time of 120 min, temperature of 25°C, and a biomass dosage of 2 g/L	[90]
	Pb(II)	*Anabaena sphaerica*	Contact time: 5–120 min, pH: 2.0–6.0, initial metal concentration: 50–300 mg/L, biomass concentration: 0.25–2.5 g/L, temperature: 25°C	The maximum biosorption capacity was 122.0 mg/g (88% removal efficiency) at a pH of 3.0, contact time of 90 min, temperature of 25°C, initial metal concentration of 50 mg/L, and 1.0 g/L biosorbent dosage	[91]
	Pb(II)	*Laminaria japonica*	Contact time: 5–1,400 min, pH: 1.4–5.3, initial metal concentration: 1 mmol/L, biomass concentration: 1 g/L, room temperature	There was a 1.7 mmol/g removal at a pH of 5.2 with a contact time of 120 min, biomass concentration of 1 g/L, and at room temperature	[92]
	Cu(II)	*Scenedesmus quadricauda*	Contact time: 0–175 min, pH: 2.0–7.0, initial metal concentration: 25–600 mg/L, temperature: 5°C–40°C	The maximum adsorption capacity was 75.6 mg/g with a pH of 5.0 and a temperature of 25°C	[93]
	Cr(III)	*Laminaria digitata*	Contact time: 0–50 h, pH: 2.5–4.0, initial metal concentration: 5–200 mg/L, biomass concentration: 2 g/L, temperature: 25°C and 40°C	The maximum uptake capacity was 42 mg/g at a pH of 4.0, initial concentration of 250 mg/g, and temperature of 25°C	[94]
	Cr(VI)	*Sargassum muticum*	Contact time: 0–30 h, pH: 2.0–7.0, initial metal concentration: 10–50 mg/L, biomass concentration: 0.5–2 g/L, temperature: 20°C–50°C	There was 84% maximum removal (196.1 mg/g) at 50°C, 20 mg/L of metal concentration, and a sorbent dosage of 2 g/L	[95]
	Cr(VI)	*Oedogonium hatei*	Contact time: 10–160 min, pH: 1.0–4.0, initial metal concentration: 10–100 mg/L, biomass concentration: 0.1–1 g/L, temperature: 20°C–50°C	The raw and acid-treated algae produced biosorption capacities of 31 and 35.2 mg/g, respectively. Optimum conditions were 0.8 g/L biomass dose, 110 min contact time, pH of 2.0, and 45°C temperature	[96]

Table 3

Nature of biosorbent	Heavy metal	Biosorbent	Experimental conditions	Results description	References
Algal-derived	Co(II)	*Corallina mediterranea*	Contact time: 0–120 min, pH: 2.0–8.0, biomass concentration 1–40 g/L, temperature: 20°C–50°C	The maximum biosorption capacity of metal ions was 76.2 mg/g (86% removal) at a biomass dosage of 10 g/L, pH of 5.0, and contact time of 60 min	[97]
	Zn(II)	*Scenedesmus quadricauda*	pH: 2.0–6.0, initial metal concentration: 25–600 mg/L, temperature: 5°C–40°C	The maximum adsorption capacity was 55.2 mg/g with a pH of 5.0 and a temperature of 25°C	[93]
	Hg(II)	*Chlamydomonas reinhardtii*	Contact time: 0–120 min, pH: 2.0–7.0, initial metal concentration: 100 mg/L, biomass concentration: 0.2–1 g/L, temperature: 5°C–35°C	The maximum adsorption was 72.2 mg/g dry biomass at pH 6.0, contact time of 120 min, temperature of 25°C, and an initial concentration of 200 mg/L	[89]
	Cd(II)	*Chlamydomonas reinhardtii*	Contact time: 0–120 min, pH 2.0–7.0, initial metal concentration: 100 mg/L, biomass concentration: 0.2–1 g/L, temperature: 5°C–35°C	The maximum adsorption was 42.6 ± 0.5 mg/g dry biomass at pH 6.0, contact time of 120 min, temperature of 25°C, and an initial concentration of 100 mg/L	[89]
	Cd(II)	*Cystoseira indica*	Contact time: 0–24 h, pH 2.5–7, initial metal concentration: 0.5 mmol/L, biomass concentration 0.06–0.5 g/L, temperature: 25°C	The maximum sorption capacity was 19.4 mg/g at an optimum pH of 5.5, contact time of 120 min, temperature of 25°C, and biomass dosage of 2 g/L	[90]
	Cd(II)	*Anabaena sphaerica*	Contact time: 0–120 min, pH: 2.0–6.0, initial metal concentration: 50–300 mg/L, biosorbent dosage: 0.025–0.25 g, temperature: 25°C	The maximum biosorption capacity was 111.1 mg/g (85% removal) at pH 5.5, a contact time of 60 min, a temperature of 25°C, an initial metal ions concentration of 50 mg/L, and 10 g/L biosorbent dosage	[91]
	Ni(II)	*Cystoseira indica*	Contact time: 15–1,440 min, pH 2.5–7.0, initial metal concentration: 5–200 mg/L, biomass concentration: 0.006–0.48 g, temperature: 20°C–50°C	The maximum biosorption capacity was 10.1 mg/g at an optimum pH of 6.0, contact time of 120 min, temperature of 25°C, and biomass dosage of 2 g/L	[90]
	Ni(II)	*Oedogonium hatei*	pH 2.2–7, initial metal concentration: 10–400 mg/L, temperature: 25°C–45°C	The maximum adsorption capacity (untreated and acid-treated algae) was found to be 40.9 and 44.2 mg/g, respectively at a contact time of 80 min, pH of 5.0, an algal dose of 0.7 g/L, and 25°C temperature	[98]
	U(VI)	*Cystoseira indica* alga	Contact time: 0–300 min, pH: 2.0–7.5, initial metal concentration: 10–1,000 mg/L, biomass concentration: 0.2 g, temperature: 30°C	The maximum adsorption capacity was 454.5 mg/g on the Ca pre-treated, this was predicted by Langmuir isotherm at pH 4.0 and temperature 30°C	[99]
	Se(IV)	*Cladophora hutchinsiae*	Contact time: 5–120 min, pH: 2.0–8.0, initial metal concentration: 10–400 mg/L, biomass concentration: 1–20 g/L, temperature: 20°C–50°C	The maximum biosorption capacity was found to be 74.9 mg/g (96% biosorption removal) at pH 5.0, biomass concentration 8 g/L, contact time 60 min, and temperature 20°C	[100]

acceptable biosorbents for treating wastewater effluents, the 2-fold problem (waste disposal and effluent treatment) might be resolved [111]. Examples of industrial by-products are distillery sludge [112], fermentation wastes [113], activated sludges [114] and anaerobic sludges [37].

3.6. Agricultural-derived biosorbents

A considerable proportion of cellulose can be found in agricultural waste. Also present is lignin, which contains polar functional groups with a high potential for binding

Table 4
Biosorptive performance by fungal-derived biosorbents for the removal of heavy metals

Nature of biosorbent	Heavy metal	Biosorbent	Experimental conditions	Results description	References
Fungal-derived	Cu(II)	*Fomes fasciatus*	Contact time: 1–120 min, pH: 5.5, initial metal concentration: 10–100 mg/L, biomass concentration: 0.5–3 g/L, temperature: 26°C	There was a maximum biosorption capacity of 33.5 mg/g at a pH of 5.5, contact of 30 min, a biosorbent dose of 3.0 mg/g, and a temperature of 26°C	[105]
	Cr(VI)	*Termitomyces clypeatus*	pH 2.0–7.0, initial metal concentration: 100 mg/L, biomass concentration 8 g/L, temperature 30°C	There was a 100% removal efficiency with a pH of 2.0, contact time of 2,880 min, temperature of 30°C, initial concentration of 100 mg/L, and agitation speed of 150 rpm	[106]
	Cr(III)	*Saccharomyces cerevisiae*	Contact time: 0–6 h, pH: 4.5–6.0, initial metal concentration: 200 mg/L, biomass concentration: 0.5–14 g/L, temperature: 25°C–45°C	There was an 86.3 mg/g maximum removal with a contact time of 6 h, pH of 5.5, temperature of 35°C, and an initial concentration of 200 mg/L	[107]
	Cr(III)	*Saccharomyces cerevisiae*	Contact time: 0–120 min, pH: 2.0–8.0, biomass concentration: 1–40 g/L, temperature: 25°C	There was a maximum biosorption capacity of 105.2 mg/g (85% removal) at a biomass dosage of 10 g/L, pH of 5.0, and a contact time of 60 min	[97]

Table 5
Biosorptive performance by agricultural- and industrial-derived biosorbents for the removal of heavy metals

Nature of biosorbent	Heavy metal	Biosorbent	Experimental conditions	Results description	References
Agricultural-derived	Pb(II)	Olive cake	Contact time: 120 min, pH: 4.5–5.0, initial concentration: 25–400 mg/L, biomass concentration: 5 g/L, temperature: 20°C–70°C	Biosorption capacity of 42.3 mg/g with a contact time of 120 min, solid–liquid ratio of 5 g/L, a temperature of 20°C, and an initial concentration of 100 mg/L	[115]
	Cu(II)	*Carica papaya*	Contact time: 5–180 min, pH: 2.0–6.0, initial metal concentration: 5–500 mg/L, biomass concentration: 0.5–20 g/L, temperature: room	There was a 98% removal efficiency at a pH of 5.0, contact of 60 min, initial concentration of 10 mg/L, and temperature of 20°C	[116]
	Cu(II)	Wheat shell	Contact time: 0–175 min, pH: 2.0–7.0, initial metal concentration: 10–250 mg/L, biomass concentration 10–250 mg/L, temperature 25°C	There was a 99% removal efficiency (biosorption capacity – 0.1 mmol/g) at pH of 5.0, initial concentration of 10 mg/L, agitation speed of 250 rpm, temperature of 25°C, and a contact time of 120 min	[117]
	Cu(II)	*Eichhornia crassipes*	Contact time: 10–240 min, pH: 2.5–6.0, initial metal concentration: 2–25 mg/L, biomass concentration: 15 g/L, temperature: 25°C	The maximum biosorption capacity was 27.7 mg/g with a pH of 4.5, temperature of 25°C, contact time of 240 min, and an agitation speed of 10,000 rpm	[118]
	Cr(III)	Green coconut shell powder	pH: 2.0–9.0, initial metal concentration: 20–1,000 mg/L, biomass concentration: 5 g/L, temperature: 27°C	There was a maximum removal of 4.4 mg/g with an initial concentration of 20 mg/L, final concentration of 2.2 mg/L, temperature of 27°C, contact time of 60 min, and pH of 7.0	[119]

Table 5

Nature of biosorbent	Heavy metal	Biosorbent	Experimental conditions	Results description	References
Agricultural-derived	Cr(VI)	Green coconut shell powder	pH: 2.0–9.0, initial metal concentration: 20–1,000 mg/L, biomass concentration: 5 g/L, temperature: 27°C	There was an 86% removal efficiency with an initial concentration of 20 mg/L, final concentration of 2.3 mg/L, temperature of 27°C, contact time of 60 min, and pH of 2.0	[119]
	Zn(II)	Olive cake	Contact time: 120 min, pH: 4.5–5.0, initial concentration: 25–400 mg/L, biomass concentration: 5 g/L, temperature: 20°C–70°C	There was a 48% removal efficiency (4.1 mg/g – maximum biosorption capacity) with a contact time of 840 min, initial concentration of 50 mg/L, temperature of 20°C, and biosorbent dose of 5 g/L	[115]
	Zn(II)	*Carica papaya*	Contact time: 5–180 min, pH: 2.0–6.0, initial metal concentration: 5–500 mg/L, biomass concentration: 0.5–20 g/L, temperature: room	There was a 67% removal efficiency (max. biosorption capacity–13.6 mg/g) with a pH of 5.0, contact of 60 min, initial concentration of 1,000 ± 2 mg/L, temperature of 20°C, and agitation speed of 100 rpm	[116]
	Cd(II)	Sugar industry-derived biosorbent waste	Contact time: 0–150 min, initial metal concentration: 20 mg/L	There was a 96% removal efficiency with a contact time of 90 min and an initial concentration of 20 mg/L	[120]
	Cd(II)	*Carica papaya*	Contact time: 5–180 min, pH: 2.0–6.0, initial metal concentration: 5–500 mg/L, biomass concentration: 0.5–20 g/L, temperature: room	There was a 95% removal efficiency (max. biosorption capacity – 17.2 mg/g) with a pH of 5.0, contact of 60 min, and temperature of 20°C	[116]
Industrial-derived	Cr(VI)	Distillery sludge	Contact time: 0–160 min, pH: 3.0–10.0, initial metal concentration: 10–40 mg/L, biomass concentration: 0.05–2 g/L, temperature: 20°C–50°C	The maximum biosorption capacity of metal ions was 5.7 mg/g at pH 3.0 and a contact time of 120 min	[112]

metals, such as amino, carbonyl, alcoholic, phenolic, and ether groups [121]. Examples of agricultural waste biosorbents well reported include peat moss [122], straws [123], banana peels [124], sugar beet pulp [37], peanut skins [125], hazelnut shells [126], peanut hulls [127], corn cobs [128], coconut husks [129], and sawdust [130]. Agricultural waste products have been employed for biosorption from wastewater more frequently in recent decades due to their natural availability and the high degree of metal removal achieved in laboratory settings [131–133]. Sugarcane bagasse, for example, includes carboxylic and hydroxyl groups, demonstrating the ability to biosorb via ion exchange or complexation [134]. Reviewed studies involving agricultural waste as a biosorbent are presented in Table 5.

4. Biosorption studies

4.1. Batch laboratory studies

Over the past five decades, numerous research has been targeted towards elucidating metal-binding properties and biomass characteristics to enhance and optimise biosorption systems. Tables 2–5 present a summary of the reviewed results of biosorption investigations. The reported maximum biosorption capacities are strongly dependent on the characteristics of the biosorbent and the targeted adsorbate. Most of the reported studies were conducted to explicate the potential of a given biosorbent for a specific metal and to optimise the process of biosorption by varying fundamental parameters. Thus, the resulting capacities are not comparable to other biosorbents or other target metals. However, the versatility of biosorption is easily evident by the range of investigated biomasses and the spectrum of targeted heavy metals. A study of Tables 2–5 reveals the importance of pH in biosorption systems. For the biosorption of anionic species, the optimal pH range from 2–4. At the same time, cationic species lie within the range of 4.5–6.5. The optimal temperature varies from 20°C to 30°C. The influence of biosorbent dose and initial metal concentrations varies substantially and is strongly dependent on the concentration gradient created between the biomass and the target metal. At optimised operational parameters, efficiency is typically within the range of 85%–100%. The

pre-treatment of biosorbent is often initiated to enhance the physical and chemical sorption characteristics of the biomass. The particular pre-treatment process, together with the impact of competing ions, biomass viability, regeneration ability and experimental equipment, can be found in the corresponding references. The summarised data presented in Tables 2–5 can be of great importance to researchers in determining a suitable experimental range to begin biosorption investigations.

4.2. Batch pilot studies

Very few studies in the literature have reported on batch pilot-scale studies. Artola et al. [135] successfully developed a 3-zone batch contact settling pilot plant for the removal of Cu(II) by anaerobically digested sludge. A maximum metal uptake of 75.0 mg Cu(II)/g of total solids in the sludge was found for Cu/sludge feed ratios greater than 90.0 mg Cu(II)/g of total solids. A 0.037 m³ biosorption reactor was developed with a diameter of 0.3 m and a total height of 0.7 m. The vessel was divided into three operation zones: a clarification zone at the top, a continuously stirred zone where metal-biosorbent contact occurs and a bottom conic-shaped zone for settling. To avoid excess turbulence, which would have destroyed the biomass, mild mixing (4–5 rpm) using a rectangle paddle was employed in the contact zone. At a pH of 6.0–6.8, copper concentration varied from 50.0 to 250.0 mg/dm³. Laboratory-scale batch experiments revealed an equilibrium time of 30 min. Consequently, a heavy metal mean residence time of 0.5–3 h was used in the contact zone. The authors concluded that the results of the pilot plant experiments were in good agreement with predicted values from batch experiments. However, they did observe minor differences at high Cu/sludge feed ratios. This was attributed to insufficient contact between the heavy metal and the sludge.

4.3. Column laboratory steady-state studies

Some of the major hindrances to the application of biosorption at column level are increased head losses, the compressibility of column beds, channelling and disintegration of biosorbents. To overcome these limitations, several researchers have attempted to modify biosorbents to provide greater mechanical strength and dimensional stability. Yan and Viraraghavan [136] were able to successfully prepare a laboratory strain of *Mucor rouxii* (fungi) for column experiments through immobilisation of the biomass. The biomass was first processed for 30 min with 0.2 N NaOH solution, then washed, autoclaved for 30 min at 121°C, and then dried for 24 h at 60°C. The powdered biomass was then immobilised by adding 100 mL of N,N-dimethylformamide solution to a mixture of 14 g of powdered biomass and 7 g of polysulphone after it had been pulverised. A slurry developed after 16 h of rotational shaking at 125 rpm to completely dissolve the polysulphone in the N,N-dimethylformamide. This slurry was converted into spherical beads by passing it through a biomass immobilisation unit to produce beads between the range of 0.6 to 4.8 mm. An experimental biosorption column of diameter 1.27 cm and height of 40 cm was packed with 4.5 g biosorbent (bed depth of 29 cm). Column experiments for the removal of Pb(II) revealed a concentration of zero in the effluent for 20 bed volumes. Exhaustion of the column occurred after 100 bed volumes. For Pb, Zn, Cd, and Ni, the authors reported column biosorption capacities of 4.1, 1.4, 3.8, and 0.4 mg/g, respectively. The column was successfully regenerated using 0.05 N HNO₃. Sooksawat et al. [137] conducted biosorption column studies using untreated *Chara aculeolata* biomass for the sorption of Pb(II) and Cd(II). A glass column of 50 cm in length and 1 cm in diameter was used for the experiments. *C. aculeolata* was pulverised and sieved to produce particles that ranged in size from 0.2 to 0.6 mm. Varying biomass dosages (0.5, 1.0 and 1.5 g) and flow rate (30 to 60 mL/min) were examined. The column bed volumes and bed depths were 1.9, 3.5, and 5.2 mL and 3.3, 6.5, and 10.1 cm, respectively. The experimental setup was capable of reducing Pb(II) and Cd(II) concentrations from 10 mg/L to less than 0.02 mg/L. The column attained exhaustion after 2,500 bed volumes. The authors were successful in attaining three regenerations cycles using 0.1 M HCl as an eluent producing >98% recovery. The reported maximum sorption capacities were 105.6 and 37.9 mg/g for Pb(II) and Cd(II), respectively. Chen et al. [138] reported on the removal of Pb(II), Cd(II) and Hg(II) from solution using biosorption columns packed with immobilised *Microcystis aeruginosa*. Using a mortar and pestle, the dry biomass was ground to a size range of 0.5–0.71 mm. The authors used 3.2 g of the sieved material and combined it with 3% (w/v) sodium alginate and 100 mL of distilled deionised water to create beads. Through a syringe, drops of the sodium alginate-*Microcystis aeruginosa* mixture were injected into a 0.2 M CaCl₂ solution. After 2 h, the cross-linked alginate beads (2.0 mm in diameter) were removed. Biosorption columns of cross-sectional area 2 cm² were packed to a height of 10 cm. Influent was fed from the top of the bed at a rate of 0.75 mL/min. Removal efficiency of 90%, 90% and 80% was reported for Cd(II), Hg(II), and Pb(II), respectively. Similar successes in applying biosorbent at the column level have been reported by Cruz-Olivares et al. [139] for allspice residue, Pelit et al. [140] in the application of natural spider silk, and Abdolali et al. [141] for novel column-biosorbent comprising of tea waste, maple leaves and mandarin peel.

4.4. Column pilot steady-state studies

Biosorption columns have been identified as a potentially essential technique due to their simple design, relative ease of scaling-up procedures, and inexpensive and convenient operations. Further, it is the most commonly utilised adsorption method in large-scale wastewater treatment [51,101]. Since a fixed-bed (packed) is usually used, the experimental conditions such as bed height, length, flow rate and initial (inlet) concentration are often varied. Upgrading to pilot-scale systems allows researchers to discover the difficulties and limitations of applying biosorption in an industrial context, for example, the high expense of turning the biomass into a viable biosorbent material [142], that is, obtaining a steady supply of inexpensive raw biomass, challenges associated with biomass regeneration and reuse, and negative effects of coexisting ions on biosorptive ability [143]. According to Mikhaylov

et al. [144], scaling up involves the use of three key techniques; physical modelling, mathematical modelling, and scaling-up experiments. Calero et al. [145] further explained that scaling up first involves acquiring primary process parameters through testing, then picking the mathematical model which best meets the data and finally, the pilot-scale study is approached. Ronda et al. [146] conducted a study involving scaling-up to pilot. The authors used a continuous packed–bed laboratory column with an internal diameter of 1.5 cm and length of 23 cm and in the pilot experiment, an internal diameter of 5 cm and length of 56 cm. The various measures used to determine the scale-up, according to Inglezakis and Poulopoulous as cited in Ronda et al. [147] are presented below:

- Geometric similarity: the height-to-diameter ratio of the columns should been maintained.
- Kinematic similarity: the solution's physical parameters are kept constant in both columns to ensure a similar mass transfer regime.
- Dynamic similarity: The linear velocities in both columns should be nearly constant if the physical characteristics of the biosorbent (particle size and porosity) are kept constant, and the physical properties of the fluid are identical.

In a study by Calero et al. [145] involving the removal of Cr(III) onto olive stone in a fixed-bed, the authors varied column heights viz. 21.5 cm (300 g biomass), 42.5 cm (600 g biomass), and 62.0 cm (900 g biomass) at a flow rate of 28 mL/min. With the experiment initially completed at a laboratory-scale before attempting the pilot-scale, the authors noticed that the quantity of chromium removed (bed capacity) rose as bed height increased. This was attributed to the greater biosorbent dosages in larger beds with more surface area (more binding sites available for biosorption) and an improvement in the mass transfer zone development. Furthermore, the breakthrough time increased from 30 to 220 min with an increase in bed height from 21.5 to 62.0 cm. Similar trends were observed in studies for the removal of Pb(II) onto olive tree pruning [146]; biosorption of copper onto almond shell [147]; removal of chromium(VI) onto olive stone [148]; and the removal of zinc from industrial plating wastewater using hydrolysed olive cake [115].

Concerning the effect of flow rate, the removal of Pb(II) onto olive tree pruning was studied by Ronda et al. [146], where flow rate was varied from 44.4 to 88.8 mL/min at a bed height of 11.3 cm. The biosorption column was of height 56 cm and a diameter of 5 cm. The authors noted the breakthrough time reduced (from 195 to 75 min) as the flow rate started to rise (44 to 89 mL/min), which in turn made the column exhaustion occur faster (840 to 345 min). According to Hethnawi et al. [149], with high inlet flow rates, there is not enough time for the pollutants and the material to reach equilibrium. The front biosorption zone quickly moved to the bottom of the column, saturating the column earlier, leading to less metal ion contact time with the adsorbate binding sites and a decrease in the removal efficiency. Another study which had similar trends with the increase of flow rate was Cr(III) sorption onto olive stone; however, the authors noted that with a decrease in flow

rate, the residence time was increased because intraparticle diffusion becomes effective [145]. As a result, metal ions have enough time to penetrate and diffuse deeply into the pores, resulting in improved removal efficiency [150–152].

Calero et al. [145] reported on the effect of varying inlet concentration for the removal of Cr(III) onto olive stone at concentrations of 10, 20, 40 and 80 mg/L, pH of 4.0, flow rate of 14 mL/min, olive stone mass of 600 g, column diameter of 4.7 cm and bed height of 42.5 cm. The authors noted that the inlet concentration affected the operating characteristics, whereby, with an increase in inlet concentration, exhaustion occurred faster. Higher initial concentration resulted in a speedier breakthrough, while reduced concentration produced a larger treated volume and delayed breakthrough because the lower concentration gradient slowed transport due to a lower diffusion coefficient. At a concentration of 80 mg/L, the bed was saturated rapidly (330 min). The authors also noticed that as concentration increased from 10–80 mg/L, the biosorption capacity increased (0.15–0.3 mg/g), removal efficiency decreased (88%–25%), and breakthrough time decreased. Based on this analysis, they deduced that for concentrations higher than 40 mg/L, in order to increase breakthrough time, the bed height must be increased or the flow rate decreased. The dose–response model was successful in representing the full breakthrough curve. A comparison of the laboratory and pilot results showed Cr(III) removal was higher in the pilot (59%) than in laboratory studies (33%). However, the biosorption capacity was lower in the pilot (0.1 mg/g) than laboratory (0.4 mg/g). Similar trends were reported in the removal of Cr(VI) biosorbed onto olive stone by Martín-Lara et al. [148].

5. Effect of operational parameters on heavy metals biosorption

5.1. Effect of pH on biosorption

Vijayaraghavan and Yun [57] describe pH as one of the most important regulators of biosorption which influences the chemistry of the pollutants in solution, as well as the activity of functional groups on biosorbents and the competition with coexisting ions in solution. In a study by Ibrahim [97], four different marine algae were assessed for the removal of Co(II), Cd(II), Cr(III) and Pb(II). The pH was varied from 2.0–8.0 using 0.1 M NaOH or 0.1 M HNO_3, where the highest removal (98%) occurred at a pH of 5.0. As pH increased, the removal percentage decreased. The author explained that the biomass containing functional groups of carboxyl, which are acidic, was being influenced by pH. The surfaces became protonated at low pH (2.0–4.0) due to the high concentration of positively charged H^+ and H_3O^+ ions, which reduced the amount of accessible metal binding sites [153,154]. Deprotonation of carboxyl or other negatively charged groups, which causes the electrostatic attraction of positively charged metals, may be the cause of the rise in biosorption at pH 5.0 [154–155]. Because anionic hydroxide complexes compete with the active sites, efficiency may have decreased at higher pH values (6.0–8.0) [156–157]. Similar results were reported using wheat shell for the uptake of Cu(II) at pH 5.0 by Basci et al. [117]; yeast wastes for the uptake of Cu(II), Cd(II) and Pb(II) at pH 4.5–5.0 by Marques et al. [158]; *Micrococcus* sp. for the uptake of Cu(II) at pH 6.0

by Wong et al. [159]; and aerobic granular sludge for the uptake of Ni(II) at pH 6.0 by Xu et al. [160].

5.2. Effect of temperature

To further understand the sorption process, thermodynamic properties from the Gibb's free energy ($\Delta G°$) equation; enthalpy ($\Delta H°$) and entropy ($\Delta S°$) are often employed [161]. $\Delta G°$ shows the level of spontaneity, with negative values for a spontaneous process; $\Delta H°$ determines if the process is endothermic ($\Delta H° > 0$) or exothermic ($\Delta H° < 0$), and its size might also reveal the sort of sorption interaction that is taking place in the system. For example, in the case of physical adsorption (i.e., physisorption), enthalpy levels are generally in the range of 2.1–20.9 kJ/mol, whilst in the case of chemical adsorption (i.e., chemisorption) the values range from 20.9 to 418.4 kJ/mol. Lastly, positive values of $\Delta S°$ indicate that there is more unpredictability at the solid/solution contact and that the adsorbates have more flexibility. Negative values imply that the process occurred via an associative mechanism, leading to reduced chaos at the solid/solution interface, this could lead to adsorbate molecules escaping from the adsorbent surface and entering the solution [162,163]. Fadel et al. [163] studied the removal of manganese by *Saccharomyces cerevisiae* at a temperature range of 20°C–40°C and an agitation speed of 150 rpm. The results indicated that the range chosen did not have an impact on the sorption capacity. That said, in a study by Goyal et al. [164] for the removal of Cr(VI) and Fe(III) ions on *Streptococcus equisimilis*, *Saccharomyces cerevisiae* and *Aspergillus niger* using a temperature range of 25°C–40°C, 1,440 min and agitation speed of 400 rpm; the results showed a maximum biosorption capacity at 35°C–40°C (56.5 mg/g), 30°C–35°C (16.6 mg/g) and 45°C (101.0 mg/g), respectively. According to the authors, this was attributable to a higher affinity by sites for metal ions or an increase in binding sites on the relevant cell mass. Further, when the temperature was very high, there was a decrease in metal sorption due to the distortion of some sites on the cell surface. While at moderately high temperatures, the energy of the system enhances Cr(VI) attachment to the surface. Other studies which showed similar results were reported using marine bacterium for Pb(II) at 35°C (89%) by Mohapatra et al. [67]; *Bacillus* sp. for Cu(II) at 30°C (69%) by Rani et al. [66]; *Aspergillus* sp. for Hg(II) at 30°C (95%) by Abbas et al. [61] and *Micrococcus* sp. for nickel at 35°C (90%) by Shamim [165].

5.3. Effect of contact time

The contact duration between the biosorbent and the sorbate has no direct effect on biosorption capacity, although it can be a limiting factor. Under test conditions, extended contact time would enable the biosorbent material to exhibit its highest biosorption capacity [83]. The rate of biosorption is initially rapid since all of the active sites are vacant, and the metal ions have easy access [166]. However, as time passes, the rate of biosorption slows due to an increase in the percentage sorbent saturation [166–168]. In a study by Dahiya et al. [168], the authors reported a 50% elimination of Pb(II) in the first 60 min, followed by a gradual process up to a contact duration of 240 min when 92% was eliminated, with no significant change occurring beyond. Cu(II) exhibited a 30% removal in 60 min, then 88% after 300 min; nickel 28% (60 min), then 99% (300 min); and finally, Cs(II) 46% (60 min), then 98% (180 min). In the case of Co(II), more than 60% sorption was observed within 60 min and then a slow increase to eventually reach 97% removal in 180 min. The authors explained that extra-cellular binding was likely responsible for the initial quick sorption, while intracellular binding was probably responsible for the subsequent slower sorption. Ibrahim [97] showed a similar rapid rate of reaction for four marine algae onto Cd(II), Pb(II), Co(II) and Cr(III), where the biosorption efficiency was significantly increased by increasing the contact time up to 60 min, after which it remained more or less constant. Mohapatra et al. [67] studied the removal of Pb(II) using *Bacillus xiamenensis* with similar observation between 15–30 min, then equilibrium at 360 min. Wierzba and Latała [169] explained that some of the biosorbent binding sites were originally free, and the concentration of accessible Pb(II) ions was high. With the passage of time, the empty sites on the bacterial cell wall became gradually filled with metal ions, and the system achieved equilibrium given the lack of or extremely limited supply of free active sites. Several researchers noted that heavy metal sorption could be divided into two stages: a rapid initial phase followed by a much slower biosorption phase. The rapid initial metal biosorption process was directly linked to surface binding between negatively charged cell surface ligands and metal cations. The slower sorption rate was ascribed to interior metal penetration, which slows further uptake [170,171].

5.4. Effect of biosorbent dose

As biosorbents provide the binding sites for metal sorption, the dosage of biosorbents has a considerable impact on the biosorption process [172]. The amount and kind of biomass used in the biosorption process determine a variety of passive processes, including surface adsorption, coordination, chelation, precipitation, and ion exchange [173]. Mohapatra et al. [67] studied the removal of Pb(II) using live and dead biomass of *Bacillus xiamenensis*. The authors varied biomass dosage from 0.1–2.0 g/L. The following results were obtained; biosorption efficiency of 70%–97% (live) and 68%–96% (dead), with the dosage increasing from 0.1 to 1.0 g/L. The authors noticed that the biosorption efficiency increases as the dosage is increased. However, as the biomass dose was increased from 1.0 to 2.0 g/L, the biosorption rate remained constant, and the equilibrium time was reduced from 300 to 240 min. Due to the availability of more unbound surface ligands as biomass concentration increased, the adsorption rate increased significantly (up to 71% in 60 min) [173]. According to Abbas et al. [174], for the biosorption of Cr(III) and Cr(VI) by *Cassia fistula* (flowering plant biomass), biosorption was highly dependent on biomass concentration. The available metal was more quickly absorbed by biosorption sites at low concentrations, but at larger concentrations, intraparticle diffusion is required for metal ions to reach the biomass surface, and heavily hydrolyzed ions will diffuse more slowly.

5.5. Effect of initial concentration

In a batch biosorption system, the initial metal concentration is a critical component that provides an effective driving force for mass transfer. In a study by Oh et al. [175], the removal of Pb(II), Cd(II) and Cu(II) by *Pseudomonas stutzeri* was studied using an initial concentration of 50–300 mg/L and pH 2.0–6.0. The maximum biosorption obtained was 142.0 mg/g dry mass for Pb(II), 43.5 mg/g dry mass for Cd(II), and 36.2 mg/g dry mass for Cu(II) at an initial concentration of 300 mg/L. The authors noted that in all cases, there was a decline in biosorption percentage as the metal concentration increased. They explained that this was due to the high ratio of metal ions to free sites for biosorption. Other research that followed a similar pattern included Pb(II) on live and dead biomass *Bacillus xiamenensis* by Mohapatra et al. [67] and Pb(II) and Cu(II) on *Cladophora filamentous* macroalgae by Lee and Chang [176]. Yargıç et al. [177] studied Cu(II) sorption onto chemically treated tomato waste, *Solanum lycopersicum*. The authors noted the biosorption capacity raised when the initial concentration increased, whereas the metal ion removal efficiency reduced. According to Ozbay and Cinar [178], adsorbate molecules must first experience the boundary layer effect before diffusing from the boundary layer film onto the adsorbent surface and subsequently into the adsorbent's porous structure. Yargıç et al. [177] went on to explain that the biosorption concentration gradient was the driving force in overcoming mass transfer resistances between the adsorbent and adsorption medium, resulting in the observed increased biosorption capacity.

5.6. Effects of agitation speed

The formation of the external border and the distribution of the solute in the bulk solution can both be impacted by agitation speed [179]. A thicker solvent film layer forms around the adsorbent when the agitation speed is reduced, making the film layer a rate-controlling process [180]. It is important to note that the biosorbent's physical composition may be harmed by the effect of agitation speed [37]. In a study by Mohamad et al. [181] on Cu(II) removal using *Mesorhizobium amorphae*, the experiment ranged in agitation speeds from 60–210 × g. The biosorption capacity improved from 61.4 mg/g (31%) to 87.0 mg/g (44%), with the highest occurring at 150 × g, that is, when reaching equilibrium. Upon further raising the agitation speed, there was a decrease between 150–210 × g. Nuhoglu and Malkoc [180] also observed that the solvent film layer surrounding the adsorbent thickens at lower speeds, becoming a rate-controlling step, and thins at higher speeds. Other studies with similar results were Zn(II) and Pb(II) ions uptake using non-living biomass of *Phanerochaete chrysosporium* by Marandi et al. [182]; Cd(II), Mn(II), Ni(II), Pb(II), and Zn(II) ions uptake using *Aspergillus tamarii* by Şahin et al. [183]; Hexacyanoferrate(III) using dead biomass of the basidiomycete *Pleurotus mutilus* by Chergui et al. [184]; Chromium uptake using *Saccharomyces cerevisiae* by Parvathi and Nagendran [185]; Cd(II) and Pb(II) uptake using *Sargassum* sp. by Cruz et al. [186]. A study on mercury sorption using modified *Phoenix dactylifera* biomass had a maximum removal at 300 rpm (29.3 mg/g) and decreased at maximum agitation (14.0 mg/g), with the agitation speed varied from 0–400 rpm [187]. The author explained that this increased speed improves the uniform sorbate molecule distribution and aids in better contact between the sorbent and sorbate across the test. While the shearing of sorbate, most likely from the sorbent's surface, may have contributed to a drop at maximum agitation.

5.7. Effect of particle size

The effectiveness of biosorption is also significantly influenced by the size of the adsorbent particles [188–190]. Cu(II) biosorption on dried activated sludge with three different particle sizes was examined by Gulnaz et al. [191]. The biosorption capacities were 76.0, 70.0 and 66.0 mg/g for particle sizes <0.063, 0.63–1.25 and 1.25–2.50 mm, respectively. These results indicated as particle size increased, there was a decrease in the capacity; therefore, the authors selected the smaller particle size for further study. According to Chuah et al. [192], biosorption is a surface phenomenon; thus, smaller particles tend to have a higher efficiency because of the larger surface area. The uptake/saturation capacity per unit mass of biosorbent particles is improved by smaller particle size because it increases external surface area while creating more available binding sites [193,194]. This trend is seen in several studies, such as Zn(II) sorption onto the surface of non-living biomasses by Mishra et al. [195], Cd(II) removal using sawdust by Yu et al. [196], and Cu(II) and Pb(II) removal using tartaric acid modified rice husk by Wong et al. [197].

6. Modelling

6.1. Batch kinetic models

According to Muisa et al. [198], reaction kinetics is equally as significant as biosorption capacity in achieving optimal sorption performance. An efficient biosorbent is one that exhibits a quick removal rate in addition to possessing a large surface area, high porosity and high capacity [96,199,200]. Kinetic studies aid in explicating the rate-limiting steps in the reaction and the time for the reaction to reach equilibrium. Additionally, kinetic studies give crucial insight into potential biosorption mechanisms, which include possible transport mechanisms, viz. bulk transport, external/film diffusion, and intraparticle (surface and pore) diffusion, as well as possible attachment mechanisms, viz. physical, chemical or ion exchange. Some of the more important kinetic models [Eqs. (1)–(6)] applied in biosorption studies are presented in Table 6.

Sutherland's diffusion–chemisorption kinetic model was developed to replicate the biosorption of heavy metals onto heterogeneous materials [201,202]. The model assumes that diffusion controls the transport mechanism and chemisorption controls the attachment mechanism. The derivatives are obtained by equating the rate of change of concentration of the solid phase (q_t) as a function of the rate of mass transfer of adsorbate from the fluid phase to the adsorption site (K_{DC}); the equilibrium sorption capacity (q_e); and time to the power of $n-1$, where $n = 0.5$. The model is presented in Table 6, where K_{DC} (mg/g·t$^{0.5}$) is the diffusion–chemisorption constant, q_t (mg/g) is the mass of ions adsorbed per

Table 6
Kinetic models used to simulate biosorption reactions

Model	Equation	Eq. No.	References
Sutherland's diffusion–chemisorption (DC) model	$q_t = \dfrac{1}{\dfrac{1}{q_e} + \dfrac{t^{0.5-1}}{K_{DC}}} \, ; \, k_i = \dfrac{K_{DC}^2}{q_e}$	1	[202]
Weber and Morris intraparticle diffusion (ID) model	$q_t = K_{id}\left(t^{1/2}\right) + c \, ; \, K_{id} = \left[\dfrac{3q_e}{d_p}\right]\sqrt{\dfrac{D}{\pi}}$	2	[203]
Lagergren's pseudo-first-order (PFO) model	$q_t = q_e\left(1 - \exp^{-K_{PFO}t}\right)$	3	[206]
Ho's pseudo-second-order (PSO) model	$q_t = \dfrac{K_{PSO}q_e^2 t}{1 + K_2 q_e t} \, ; \, h = \left(K_{PSO}\right)q_e^2$	4	[207]
Elovich's model	$Q_t = \dfrac{1}{b}\ln\left(ab\right) + \dfrac{1}{b}\ln\left(t\right)$	5	[209]
Bangham's model	$\log\log\left(\dfrac{C_o}{C_o - Q_t m}\right) = \log\left(\dfrac{k_o m}{2.303V}\right) + \alpha\log t$	6	[212]

gram of sorbent at any time, and q_e (mg/g) is the adsorption at equilibrium. The initial slope of the kinetic curve was found to depend on the diffusion–chemisorption constants K_{DC} and q_e, where k_i (mg/g·t) is the initial reaction rate.

The intraparticle diffusion model presented in Table 6 proposes that the rate of intraparticle diffusion varies comparably with the half power of time [203]. According to Ofomaja [204], when the model is linearised, K_{id} (mg/g·t$^{1/2}$) is the rate constant of intraparticle transport, and the intercept c (mg/g) is taken to be comparative to the boundary layer thickness. If the rate-limiting step is intraparticle diffusion, a plot of solute adsorbed against the half power of time should return a straight line passing through the origin [203]. The constant K_{id} is also related to the intraparticle diffusivity, and d_p (cm) is the diameter of the particle [205].

In 1898, Lagergren, as cited by Ho and McKay [206], created a first-order rate equation to describe the kinetic progression of oxalic acid and malonic acid onto charcoal. Ho and McKay [206] described the equation as pseudo-first-order. The model assumes that physisorption limits the adsorption rate of the particles onto the adsorbent. The Lagergren equation is presented in Table 6, where K_{PFO} (1/min) is the pseudo-first-order rate constant.

The pseudo-second-order equation was developed to describe the adsorption of divalent metal ions onto peat moss [207]. According to Ho and McKay [208], the model assumes that removal is due to pseudo-second-order chemical reaction kinetics. The pseudo-second-order equation is presented in Table 6, where K_{PSO} is the pseudo-second-order rate (g/mg·min), and h is the initial sorption rate.

The Elovich equation was developed to describe chemical adsorption and is appropriate for systems with heterogeneous media [209]. According to the model, a is a constant related to the initial adsorption rate (mg/g·min), and b is a constant measuring surface coverage and chemisorption activation energy (mg/g). The model was simplified by Chien and Clayton [210] who made the assumption that $a \cdot b \cdot t \gg 1$ and parlayed the boundary conditions $q_t = 0$ at $t = 0$ and $q_t = q_t$ at any time $t = t$ [211]. The final form of the equation is presented in Table 6.

The Bangham's equation was developed on the assumption that pore diffusion was the only rate-controlling step during adsorption [212]. The equation is presented in Table 6, where C_o is the initial concentration of sorbate in solution (mg/L), V is the volume of the solution (mL), m is the mass of sorbent per litre of solution (g/L), and α (less than 1) and k_o (mL/L·g) are constants, which were calculated from the intercept and slope of the straight line plots. A good simulation of the experimental data by this equation would suggest that pore diffusion is rate-limiting [211,213,214].

Tables 7 and 8 summarise reported batch biosorption kinetic experiments and the models used to analyse the resulting data. Over 80% of the examined studies which matched their experimental data to kinetic models stated that the pseudo-second-order model produced the best fit, which implied that the biosorption process was driven by chemical sorption as opposed to physical sorption [215]. Approximately 13% of the reviewed studies reported either an equally good fit by the diffusion–chemisorption model and the pseudo-second-order model or a better fit by the diffusion–chemisorption model, which suggested that removal may have been controlled by both diffusion and chemisorption. The remaining reviewed studies found that pseudo-first-order model was able to provide the best fit implying the dominance of physisorption.

6.2. Batch isotherm models

Equilibrium isotherms [Eqs. (7)–(15)] are used extensively in the development of biosorption systems as well as in the assessment of the performance of biosorbents. This analysis indicates sorption capacity and provides some

Table 7
Reported studies of batch-laboratory kinetic experiments conducted and models used to analyse bacterial- and algal-derived biosorbents

Nature of biosorbent	Biosorbent	Heavy metal	Model used in study	Preferred model	References
Bacterial-derived	*Bacillus xiamenensis*	Pb(II)	PFO, PSO	PSO	[67]
	Bacillus subtilis composite	Pb(II), Cu(II), Zn(II)	PSO, DC	PSO, DC	[216]
	Deinococcus radiodurans biofilm	U(VI)	PFO, PSO, EE, IPD	PSO	[217]
	Maugeotia genuflexa	As(III)	PFO, PSO	PSO	[87]
	Lessonia nigrescens	As(V)	PFO	PFO	[88]
Algal-derived	*Chlamydomonas reinhardtii*	Pb(II)	PFO, PSO	PSO	[89]
	Nizimuddinia zanardini (FA-treated)	Pb(II)	PFO, PSO	PSO	[90]
	Anabaena sphaerica	Pb(II)	PFO, PSO	PSO	[91]
	Scenedesmus quadricauda	Cu(II)	PFO, PSO	PSO	[93]
	Laminaria digitata	Cr(III)	PFO, PSO	PSO	[94]
	Sargassum muticum	Cr(VI)	PFO, PSO	PSO	[95]
	Oedogonium hatei	Cr(VI)	PFO, PSO	PFO	[96]
	Nizimuddinia zanardini (FA-treated)	Ni(II)	PFO, PSO	PSO	[90]
	Oedogonium hatei	Ni(II)	PFO, PSO	PFO	[98]
	Cladophora hutchinsiae	Se(IV)	PFO, PSO	PSO	[100]
	Padina sp.	Sr(II)	PFO, PSO, IPD	PSO	[218]
	Padina sp.	U(VI)	PFO, PSO, IPD	PSO	[219]
	Ulva fasciata and *Sargassum* sp.	Cu(II)	PSO	PSO	[220]
	Bifurcaria bifurcata, Saccorhiza polyschides, Ascophyllum nodosum, Laminaria ochroleuca and *Pelvetia canaliculata*	Cd(II)	PSO	PSO	[221]
	Cystoseira indica, Nizmuddinia zanardini, Sargassum glaucescens and *Padina australis*	Ni(II)	PFO, PSO	PSO	[222]
	Caulerpa lentillifera	Cu(II), Cd(II), Pb(II)	PFO, PSO, IPD, EMT, VM	PSO	[223]
	Polysiphonia urceolata and *Chondrus ocellatus*	Cr(VI)	PFO, PSO	PSO	[224]

Pseudo-first-order: PFO, pseudo-second-order: PSO, intraparticle diffusion: IPD, diffusion–chemisorption: DC, Elovich equation: EE, Boyd kinetic equation: BKE, homogeneous particle diffusion model: HPDM, external mass transfer: EMT, Vermeulen's model: VM, zero-order: ZO, pore diffusion: PD, film diffusion: FD, Bangham's equation: BE

information about the affinity of the biosorbent for the metal ion species [105]. Mechanistic inferences are often cautioned as models such as the Langmuir and Freundlich were originally developed for gas adsorption. The effective design of sorption systems, according to Ho et al. [247], also depends on an accurate mathematical description of the equilibrium isotherm.

The Langmuir isotherm makes the assumption that each adsorption site on the adsorbent has the capacity to adsorb one molecule, producing a monolayer and that all sites have an equal affinity for molecules [248]. The model is presented in Table 9, where K_L is the Langmuir equilibrium constant (L/mg) and q_m is the maximum adsorption capacity (mg/g).

According to Sutherland et al. [249], Firth [as reported by Swan and Urquhart [250]] reported that De Saussure originally used the equation of the form $x = kc^{1/n}$ to model the adsorption of gases in 1814. Boedecker expanded its use in 1859 by extending it to solutions [250]. The adsorption isotherm was formally defined by Freundlich in 1906 as a specific case for non-ideal and reversible adsorption whereby

cations and anions are adsorbed onto the same surface simultaneously [251]. The equation is presented in Table 9, where K_F is the Freundlich constant related to adsorption affinity $((mg/g)(L/mg)^{1/n})$ and n_F is the Freundlich constant related to heterogeneity.

The Redlich–Peterson isotherm [252] is a hybrid isotherm which combines the characteristics of the Langmuir and the Freundlich isotherms. The model is designed to forecast both homogenous and heterogeneous adsorption systems. It is presented in Table 9, where K_{RP} is the Redlich–Peterson equilibrium constant; g_{RP} is the Redlich–Peterson exponent, and α_{RP} is the Redlich–Peterson isotherm constant.

The Sips isotherm [253] is a combined form of the Langmuir and Freundlich isotherms which was designed to predict heterogeneous adsorption systems without being constrained by the Freundlich isotherm model's rising adsorbate concentration. The model is presented in Table 9, where q_s is the Sips maximum adsorption capacity (mg/g), α_s is the Sips affinity constant, and n_s is the Sips index of heterogeneity.

Table 8
Reported studies of batch-laboratory kinetic experiments conducted and models used to analyse chitosan-, fungal-, and agricultural-derived biosorbents

Nature of biosorbent	Biosorbent	Heavy metal	Model used in study	Preferred model	References
Fungal-derived	*Fomes fasciatus*	Cu(II)	PFO, PSO, IPD, DC	DC	[202]
	Schizophyllum commune	Cu(II), Ni(II), Zn(II), Cr(VI)	PFO, PSO	PSO	[225]
	Penicillium notatum	Pb(II)	ZO, PFO, PSO	PSO	[226]
	Aspergillus niger	Cd(II), Zn(II)	PFO, PSO	PSO	[227]
	Turbinaria ornata	Cd(II)	PFO, PSO, IPD, EE	PSO, EE	[228]
	Aspergillus neoalliaceus	Pb(II)	PFO, PSO	PSO	[229]
	Saccharomyces cerevisiae	Co(II), Zn(II), Cu(II)	PFO, PSO, IPD	PSO	[230]
	Trichoderma sp.	Cd(II), Cr(VI), Cu(II), Pb(II)	PFO	PSO	[231]
Agricultural-derived	*Carica papaya*	Zn(II)	PFO, PSO	PSO	[116]
	Sugar industry waste (bagasse)	Cd(II)	PFO, PSO	PSO	[120]
	Carica papaya	Cd(II)	PFO, PSO	PSO	[116]
	Sugar industry waste (bagasse)	Fe(II)	PFO, PSO	PSO	[120]
	Carica papaya	Cu(II)	PFO, PSO	PSO	[116]
	Modified lemon peel	Ni(II)	PFO, PSO	PFO	[232]
	Pine tree cone	Cr(VI)	PFO, PSO, IPD, DC, PD, FD	DC, PSO	[233]
	Black rice husk ash	Cr(VI)	PFO, PSO, IPD, BKE, EE, DC, BE	PSO	[211]
	Modified pinecone powder	Cs	PFO, PSO, DC	DC	[234]
	Nauclea diderrichii	Cr(III), Pb(II)	PFO, PSO, DC, HPDM	PSO, DC	[235]
	Banana floret	Cu(II)	PFO, PSO, IPD, DC	DC	[236]
	White rice husk ash	Mn(II)	PFO, PSO, EE, DC, BE	PSO	[237]
	Oil palm fruit fiber	Cu(II), Pb(II), Ni(II), Sn(II)	PSO, DC	PSO	[238]
	Grape wastes, flax wool, flax mat, flax shive, barley straw, wheat straw	Cd(II)	PFO, PSO	PSO	[239]
	Rapeseed	Cr(VI)	PFO, PSO, IPD	PSO	[240]
	Lycopodium clavatum	Cr(VI)	PFO, PSO	PSO	[241]
	Hemp stalk	Pb(II)	PFO, PSO	PSO	[241]
	Chemically modified peat moss	Cu(II), Pb(II)	PFO, PSO, IPD, DC	DC	[122]
Chitosan-derived	Chitosan	Cu(II), Zn(II), Hg(II), As(III)	PFO, PSO, IPD	PSO	[243]
	Chitosan	Cr(III), Cr(VI)	PFO, PSO	PSO	[244]
	Chitosan/activated carbon composite	Pb(II), Cu(II), Cd(II)	PFO, PSO	PSO	[245]
	Modified chitosan	Cu(II), Zn(III), Cr(III)	PFO, PSO	PSO	[246]

Pseudo-first-order: PFO, pseudo-second-order: PSO, intraparticle diffusion: IPD, diffusion–chemisorption: DC, Elovich equation: EE, Boyd kinetic equation: BKE, homogeneous particle diffusion model: HPDM, external mass transfer: EMT, Vermeulen's model: VM, zero-order: ZO, pore diffusion: PD, film diffusion: FD, Bangham's equation: BE

The Toth isotherm is an empirical version of the Langmuir equation created to minimise the discrepancy between equilibrium data obtained through experimentation and the predicted value [254]. The most effective application of this model is for the description of heterogeneous adsorption systems that satisfy both the low and high-end boundaries of adsorbate concentration [255].

Table 9 gives the model's expression, where K_e is the Toth isotherm constant (mg/g), and n is the Toth isotherm exponent (mg/g). When $n = 1$, this equation reduces to the Langmuir isotherm equation. Because of this, the parameter n characterises the adsorption system's heterogeneity, and if it deviates further from unity (1), the system is considered heterogeneous [254].

Table 9
Isotherm models used to simulate biosorption reactions

Model	Equation	Eq. No.	References
Langmuir model	$q_e = \dfrac{q_m K_L C_e}{1 + K_L C_e}$	7	[248]
Freundlich model	$q_e = K_F C_e^{1/n_F}$	8	[251]
Redlich–Peterson model	$q_e = \dfrac{K_{RP} C_e}{1 + \alpha_{RP} C_e^{g_{RP}}}$	9	[252]
Sips model	$q_e = \dfrac{q_s (\alpha_s C_e)^{n_s}}{1 + (\alpha_s C_e)^{n_s}}$	10	[253]
Toth model	$\dfrac{q_e}{q_m} = \theta = \dfrac{K_e C_e}{\left[1 + (K_L C_e)^n\right]^{1/n}}$	11	[255]
Khan model	$q_e = \dfrac{q_{max} b_k C_e}{(1 + b_k C_e)^{a_k}}$	12	[256]
Temkin model	$q_e = \dfrac{RT}{b} \ln(K_T C_e)$	13	[257]
Dubinin–Radushkevich model	$q_e = q_{max}^{\left(-B_D \left[RT\ln\left(1 + \frac{1}{C_e}\right)\right]^2\right)}$	14	[260]
Radke–Prausnitz model	$q_e = \dfrac{q_{MRP} K_{RP} C_e}{(1 + K_{RP} C_E)^{MRP}}$	15	[261]

The Khan isotherm model was developed to describe bi-solute adsorption from pure dilute solutions [256]. This isotherm model is presented in Table 9, where a_k is the Khan isotherm model exponent, b_k is the model constant, and q_{max} is the Khan isotherm maximum adsorption capacity (mg/g).

The Temkin isotherm assumes that with increased surface coverage, the heat of adsorption of all molecules in the layer decreases linearly [257]. The model is valid only for an intermediate range of heavy metal ion concentrations [258]. The model is presented in Table 9, where b is the Temkin constant which is related to the heat of sorption (J/mol), R is the gas constant, and KT is the Temkin isotherm constant (L/g) [259].

For the most part, the Dubinin–Radushkevich isotherm is used to express the adsorption mechanism with a Gaussian energy distribution onto the surface of heterogeneous media [260]. The isotherm equation is presented in Table 9, where q_{max} (mg/g) is the Dubinin–Radushkevich monolayer capacity, and T (K) is the solution temperature. The value of B_D is related to the sorption energy E according to the equation: $E = 1/(2B_D)^{0.5}$ [259].

The Radke–Prausnitz model was formulated based on the concept of thermodynamic ideal solution [261]. According to Ayawei et al. [262] and Sivarajasekar and Baskar [263], it possesses a number of significant characteristics that make it more favoured in most adsorption systems at low adsorbate concentrations. The model is expressed in Table 9, where q_{MRP} is Radke–Prausnitz maximum adsorption capacity (mg/g), K_{RP} is Radke–Prausnitz equilibrium constant, and M_{RP} is Radke–Prausnitz model exponent.

Table 10 shows the application of isotherm models to simulate biosorption data from reported studies. The majority of the studies that were reviewed determined that the Langmuir isotherm model offered the best fit, which implies that points of valency on the surface of the biosorbent have equal affinities for molecules and are capable of adsorbing one molecule; as a result, the adsorbed layer will be one molecule thick [105]. Only a few studies revealed that the Freundlich isotherm model provided the best fit, and in those instances, it shows that sorption occurs onto heterogeneous surfaces. In their review of the history, present, and future patterns of biosorption, Park et al. [37] commented on similar trends.

6.3. Column models

Accurate prediction of the concentration-time profile or breakthrough curve for the effluent is necessary for the design of a column adsorption process to be successful [278]. In order to evaluate the effectiveness and applicability of columns for large-scale operations as well as to

Table 10
Reported studies of batch laboratory equilibrium experiments conducted and models used to analyse bacterial- and algal-derived biosorbents

Nature of biosorbent	Biosorbent	Heavy metal	Model used in study	Preferred model	References
Bacterial-derived	*Bacillus xiamenensis*	Pb(II)	Langmuir, Freundlich	Langmuir	[67]
	Bacillus thuringiensis strain OSM29	Cu(II), Cd(II), Cr(IV), Ni(II), Pb(II)	Langmuir, Freundlich	Langmuir, Freundlich	[264]
	Ochrobactrum anthropi	Cd(II), Cu(II), Cr(III)	Langmuir, Freundlich	Langmuir, Freundlich	[265]
	Enterobacter sp.	Cu(II), Cd(II)	Langmuir, Freundlich	Langmuir, Freundlich	[266]
	Serratia plymuthica	Ni(II)	Langmuir, Freundlich	Freundlich	[267]
	Escherichia coli	Ag, Cu(II), Fe(III)	Freundlich	Freundlich	[268]
Algal-derived	*Maugeotia genuflexa*	As(III)	Langmuir, Freundlich, Dubinin–Radushkevich	Langmuir	[87]
	Lessonia nigrescens	As(V)	Langmuir, Freundlich	Langmuir	[88]
	Chlamydomonas reinhardtii	Pb(II)	Langmuir, Freundlich	Freundlich	[89]
	Nizimuddinia zanardini	Pb(II)	Langmuir, Freundlich, Khan, Toth, Radke–Prausnitz	Freundlich, Radke–Prausnitz	[90]
	Anabaena sphaerica	Pb(II)	Freundlich, Langmuir, Dubinin–Radushkevich	Freundlich	[91]
	Scenedesmus quadricauda	Cu(II)	Langmuir, Freundlich, Dubinin–Radushkevich	Langmuir	[93]
	Laminaria digitata	Cr(III)	Langmuir, Freundlich	Langmuir	[94]
	Sargassum muticum	Cr(VI)	Langmuir, Freundlich, Temkin isotherm	Langmuir	[95]
	Oedogonium hatei	Cr(VI)	Langmuir, Freundlich	Langmuir	[96]
	Nizimuddinia zanardini	Ni(II)	Langmuir, Freundlich, Khan, Toth, Radke–Prausnitz	Freundlich, Radke–Prausnitz	[90]
	Oedogonium hatei	Ni(II)	Langmuir, Freundlich	Langmuir	[98]
	Cladophora hutchinsiae	Se(IV)	Freundlich, Langmuir, Dubinin–Radushkevich	Langmuir	[100]
	Padina sp.	Sr(II)	Langmuir, Freundlich, Sips	Langmuir	[218]
	Padina sp.	Sr(II)	Langmuir, Freundlich, Sips	Sips	[269]
	Caulerpa lentillifera	Cu(II), Cd(II), Pb(II)	Dubinin–Radushkevich, Sips, Langmuir	Langmuir	[223]
	Ulva fasciata and *Sargassum* sp.	Cu(II)	Langmuir	Langmuir	[220]
	Bifurcaria bifurcata, Saccorhiza polyschides, Ascophyllum nodosum, Laminaria ochroleuca and *Pelvetia canaliculata*	Cd(II)	Langmuir, Freundlich, Langmuir–Freundlich, Toth	Langmuir	[221]
	Cystoseira indica, Nizmuddinia zanardini, Sargassum glaucescens and *Padina australis*	Ni(II)	Langmuir, Freundlich	Langmuir	[222]
	Polysiphonia urceolata and *Chondrus ocellatus*	Cr(VI)	Langmuir, Freundlich	Langmuir, Freundlich	[224]

provide insight into the mechanism of sorption, a number of mathematical models have been developed [279]. The most popular models [Eqs. (16)–(22)] for simulating column biosorption data are shown in Table 12 in accordance with the reviewed journals, and Tables 13 and 14 show their applicability.

Table 11
Reported studies of batch laboratory equilibrium experiments conducted and models used to analyse chitosan-, fungal- and agricultural-derived biosorbents

Nature of biosorbent	Biosorbent	Heavy metal	Model used in study	Preferred model	References
	Penicillium janthinellum	Cr(VI)	Langmuir, Freundlich	Langmuir, Freundlich	[270]
	Trichoderma sp.	Cd(II), Cr(VI), Ni(II)	Langmuir, Freundlich	Langmuir	[271]
	Penicillium notatum	Pb(II)	Langmuir, Freundlich	Langmuir	[272]
Fungal-derived	*Turbinaria ornata*	Cd(II)	Freundlich, Langmuir, Temkin, Dubinin–Radushkevich	Langmuir	[273]
	Aspergillus neoalliaceus	Pb(II)	Langmuir, Freundlich	Langmuir	[229]
	Saccharomyces cerevisiae	Co(II), Zn(II), Cu(II)	Freundlich, Langmuir, Dubinin–Radushkevich	Dubinin–Radushkevich	[230]
	Fomes fasciatus	Cu(II)	Langmuir, Freundlich, Redlich–Peterson, Sips	Redlich Peterson, Sips	[116]
	Carica papaya	Zn(II)	Langmuir, Freundlich	Langmuir	[116]
	Carica papaya	Cu(II)	Langmuir, Freundlich	Langmuir	[116]
	Carica papaya	Cd(II)	Langmuir, Freundlich	Langmuir	[116]
	Green coconut shell	Cd(II)	Langmuir, Freundlich	Langmuir	[119]
	Neem bark	Pb(II)	Freundlich, Dubinin–Radushkevich	Freundlich	[274]
	Pine tree cone	Cr(VI)	Langmuir, Dubinin–Radushkevich	Langmuir	[233]
	Pine sawdust	Cu(II)	Langmuir, Freundlich	Langmuir	[275]
	Modified lemon peel	Ni(II)	Langmuir, Freundlich	Langmuir	[232]
Agricultural-derived	Biochar adsorbent made from agro-waste walnut shells	Ni(II)	Langmuir, Freundlich, Toth, Sips, Redlich–Peterson, Temkin, Dubinin–Radushkevich	Toth	[276]
	Banana floret	Cu(II)	Langmuir, Freundlich, Redlich–Peterson, Sips	Sips	[236]
	White rice husk ash	Mn(II)	Freundlich, Langmuir, Temkin, Dubinin–Radushkevich models	Langmuir	[237]
	Rapeseed	Cr(VI)	Langmuir, Freundlich	Freundlich	[240]
	Hemp stalk	Pb(II)	Freundlich, Langmuir, Temkin, Dubinin–Radushkevich	Langmuir, Freundlich	[242]
	Lycopodium clavatum	Cr(VI)	Freundlich, Langmuir, Temkin, Dubinin–Radushkevich	Langmuir	[241]
	Chitosan	Cu(II), Zn(II), Hg(II), As(III)	Langmuir	Langmuir	[243]
	Chitosan	Pb(II), Cd(II)	Langmuir, Freundlich	Freundlich	[277]
Chitosan-derived	Chitosan	Cr(III), Cr(VI)	Langmuir, Freundlich	Langmuir	[244]
	Chitosan/activated carbon composite	Pb(II), Cu(II), Cd(II)	Langmuir, Freundlich	Freundlich	[83]
	Modified chitosan	Cu(II), Zn(III), Cr(III)	Langmuir, Freundlich, Temkin	Langmuir	[246]

The Thomas model was created for adsorption processes in which there are no internal or external diffusion constraints [278,280]. The model ignores the effects of intraparticle mass transfer resistance and external film resistance and instead assumes that the rate of adsorption is controlled by the surface reaction between the adsorbate and the unused capacity of the adsorbent [278]. The Thomas model is presented in Table 12, where K_{TH} is the Thomas rate constant (L/mg·h), q_{TH} is the maximum capacity of adsorption (mg/g), and V is the volume of solution (L).

Table 12
Column models used to simulate biosorption reactions

Model	Equation	Eq. No.	References
Thomas model	$\dfrac{C_t}{C_o} = \dfrac{1}{1+\exp\left[\dfrac{k_{TH}}{Q}\left(q_{TH}m - C_o V\right)\right]}$	16	[291]
Yan model	$\dfrac{C_t}{C_o} = 1 - \dfrac{1}{1+\left[\dfrac{Q^2 t}{K_Y q_y m}\right]^{(K_Y C_o/Q)}}$	17	[281]
Bohart–Adams model	$\dfrac{C_t}{C_o} = e^{\left(K_{AB}C_o t - K_{AB}N_o \frac{H}{u}\right)}$	18	[282]]
Yoon–Nelson model	$\dfrac{C_t}{C_o - C_t} = \exp\left(K_{YN}t - K_{YN}\tau\right)$	19	[285]
Wolborska model	$\dfrac{C_t}{C_o} = \exp\left[\dfrac{\beta C_o t}{N_o} - \dfrac{\beta H}{u}\right]$	20	[287]
Bed depth service time model	$t = \dfrac{N_o}{C_o v}z - \dfrac{1}{C_o k_{AB}}\ln\left(\dfrac{C_0}{C}-1\right)$	21	[278]
Dose–response model	$\dfrac{C}{C_o} = 1 - \dfrac{1}{1+\left(\dfrac{C_o q_t}{q_o X}\right)^{\alpha}}$	22	[281]

The Yan model is an empirical model developed to minimise the errors resulting from the Thomas model, particularly at higher and lower periods of the breakthrough curve [281]. The non-linear form of the model is presented in Table 12, where K_Y is the Yan's rate constant (L/mg·h), and q_y is the maximum capacity of adsorption (mg/g).

The Bohart–Adams model [282] makes the assumption that the adsorption rate is proportional to the adsorbate concentration as well as the residual capacity of the adsorbent. Typically, the breakthrough curve's early phase (50% breakthrough) is described using the Bohart–Adams model [283,284]. The model is presented in Table 12, where K_{AB} is Bohart–Adams rate constant (L/mg·h), N_o is the saturation concentration of the column (mg/L), H is the packed column depth (cm), and u is the linear velocity which is flow rate per unit cross-sectional area (cm/h).

The Yoon–Nelson model [285] is a straightforward model built on the presumption that the likelihood of adsorption for each adsorbate molecule decreases at a rate that is proportional to both the likelihood of adsorbate adsorption and the likelihood of adsorbate breakthrough [55]. The adsorbent type, adsorbate parameters, or physical characteristics of the adsorption bed are not necessary for the model [286]. The Yoon–Nelson model is expressed in non-linear form as presented in Table 12, where k_{YN} is the Yoon–Nelson rate constant, (1/h) and τ (h) is the time required for 50% adsorbate breakthrough or time when $C_t/C_o = 0.5$.

The Wolborska model [287] represents the concentration distribution in the adsorbent bed for the low concentration portion (low C_t/C_o) of the breakthrough curve. The model is presented in Table 12, where β is the kinetic coefficient of external mass transfer (1/h) and N_o is the adsorbate concentration in both phases at equilibrium (mg/L).

In the fixed-bed analysis, the bed depth service time (BDST) model is a semi-empirical model that permits the fastest prediction of adsorbent performance. The BDST model is predicated on the idea that the surface reaction between the adsorbate and the unused capacity of the adsorbent controls the rate of sorption [278,288]. The model is presented in Table 12, where N_o is the adsorption capacity from BDST model (mg/L), and k_a is the rate constant in BDST model (L/mg·min).

The dose–response model [136] is based on mathematical concerns instead of mechanistic basics [289]. The model diminishes the error coming from the application of the Thomas model, notably at the lowest and greatest times of the breakthrough curve [290]. The model is presented in Table 12, where α is the model constant, q_0 is the maximum solute concentration in the solid phase (mg/g), X is the amount of adsorbent in the column (g), and Q is the flow rate (dm³/min).

Tables 13 and 14 summarise the applicability of column models in simulating the process of biosorption. The majority of the investigations under consideration, conducted at

Table 13
Reported studies of column batch and pilot experiments conducted and models used to analyse bacterial-, algal- and fungal-derived biosorbents

Nature of biosorbent	Biosorbent	Heavy metal	Level of study	Model used in study	Preferred model	References
Bacterial-derived	*Streptococcus equisimilis*	Cd(II)	Laboratory scale	Bohart–Adams, Yoon–Nelson, Wolborska	Bohart–Adams	[293]
	Streptococcus equisimilis	Cd(II)	Pilot scale	Bohart–Adams, Yoon–Nelson, Wolborska	Bohart–Adams	[293]
	Cystoseira indica alga	U(VI)	Laboratory scale	BDST, Thomas, Yan, Belter	BDST, Thomas, Yan, Belter	[294]
	Ascophyllum nodosum	Cd(II)	Laboratory scale	Bohart–Adams	Bohart–Adams	[295]
Algal-derived	*Sargassum wightii* biomass	Cu(II)	Laboratory scale	Thomas, Yoon–Nelson, Modified dose–response, BDST	Thomas, Yoon–Nelson, Modified dose–response	[296]
	Ulva reticulata	Cu(II), Co(II), Ni(II)	Laboratory scale	Thomas	Thomas	[2]
	Marine green algae	Cd(II)	Pilot scale	Bohart–Adams, Thomas, Yoon–Nelson	Thomas, Bohart–Adams	[297]
	Pleurotus cornucopiae	Pb(II)	Laboratory scale	Bohart–Adams, Thomas	Bohart–Adams, Thomas	[298]
	Mucor rouxii	Pb(II)	Laboratory scale	Thomas	Thomas	[136]
	Pleurotus cornucopiae (mushroom)	Cd(II)	Laboratory scale	Bohart–Adams, Thomas	Bohart–Adams, Thomas	[298]
	Mucor rouxii	Cd(II)	Laboratory scale	Thomas	Thomas	[136]
	Mucor rouxii	Zn(II)	Laboratory scale	Thomas	Thomas	[136]
	Spent mushroom substrate	Zn(II)	Laboratory scale	Yoon–Nelson, Thomas, Bohart–Adams, Wolborska	Yoon–Nelson	[299]
	Mucor rouxii	Ni(II)	Laboratory scale	Thomas	Thomas	[136]
Fungal-derived	*Pycnoporus sanguineus*	Pb(II), Cu(II), Cd(II)	Laboratory scale	BDST	BDST	[300]
	Pleurotus eryngii	Pb(II)	Laboratory scale	Thomas, BDST	Thomas, BDST	[301]
	Phanerochaete chrysosporium	Pb(II), Cu(II), Cd(II)	Laboratory scale	Bohart–Adams, Wolborska, Clark	Clark	[302]
	Modified *Agaricus bisporus*	Pb(II)	Laboratory scale	Bohart–Adams, Thomas, Yoon–Nelson	Thomas, Yoon–Nelson	[303]
	Spent mushroom substrate	Zn(II), Mn(II)	Pilot scale	Yoon–Nelson, Thomas, Bohart–Adams, Wolborska	Yoon–Nelson, Thomas	[299]
	Agaricus bisporus and *Pleurotus cornucopiae*	Cu(II), Cd(II), Pb(II), Ni(II), Zn(II)	Pilot scale	Bohart–Adams, Thomas, Yoon–Nelson	Thomas, Bohart–Adams	[298]

Table 14
Reported studies of column batch and pilot experiments conducted and models used to analyse chitosan- and agricultural-derived biosorbents

Nature of biosorbent	Biosorbent	Heavy metal	Level of study	Model used in study	Preferred model	References
Agricultural-derived	Blackcurrant seeds	Zn(II), Mn(II)	Laboratory scale	Thomas, Yoon–Nelson, Bohart–Adams, Wolborska	Yoon–Nelson, Thomas	[304]
	Azadirachta indica	Pb(II), Cu(II), Cr(VI), Zn(II), Ni(II), Cd(II)	Laboratory scale	Thomas, BDST, Bohart–Adams	Thomas	[305]
	Sugarcane bagasse	Pb(II), Cd(II)	Laboratory scale	Yoon–Nelson, Thomas, Dose–response	Thomas	[306]
	Chaff	Cu(II), Pb(II)	Laboratory scale	Thomas	Thomas	[307]
	Wheat bran	Se(IV), Se(VI)	Laboratory scale	BDST, Thomas, Yoon–Nelson	BDST	[308]
	Rapeseed biomass	Pb(II)	Laboratory scale	Thomas, Yoon–Nelson	Thomas, Yoon–Nelson	[309]
	Olive stone	Cr(III)	Pilot scale	BDST, Bohart–Adams, Thomas, Yoon–Nelson, Dose–response	BDST, Dose–response	[145]
	Multi-metal binding biosorbent – tea waste, maple leaves, and mandarin peel	Cd(III), Cu(II), Pb(II), Zn(II)	Pilot scale	Thomas, Dose–response, Yoon–Nelson	Thomas	[141]
Chitosan-derived	Chitosan-coated bentonite	Pb(II), Cu(II), Ni(II)	Laboratory scale	Bohart–Adams, Thomas, Yoon–Nelson	Bohart–Adams, Thomas, Yoon–Nelson	[310]
	Nanochitosan/sodium alginate/microcrystalline cellulose bead	Cu(II)	Laboratory scale	Thomas, Yoon–Nelson, Bohart–Adams	Thomas, Yoon–Nelson	[311]

laboratory and pilot scale, revealed an excellent fit of the Thomas model to the experimental data, suggesting that the sorption rate was controlled by the surface reaction between contaminant ions and vacant sites [292].

7. Desorption

7.1. Batch desorption studies

Desorption of heavy metals from metal-laden biosorbents opens the potential for recovering the metals while minimising process costs [294]. The usefulness of a biomass as a biosorbent is defined by its ease of regeneration and reuse in addition to its biosorptive capacity [312]. Desorption is generally conducted by contacting a suitable eluent with the metal-saturated biosorbent for a certain length of time until the eluent extracts the sorbate from the biosorbent. An appropriate eluent is essential for the desorption process, which is largely reliant on the adsorbate and the biosorbent [313]. Additionally, the eluent needs to be economical, environmentally benign, efficient, and not damaging to the properties of the biosorbent. Desorbing eluents are generally classified as chelating agents (EDTA), alkalis (sodium

hydroxide, sodium hydrogen carbonate, sodium carbonate, potassium hydroxide), and acids (hydrochloric acid, sulphuric acid, nitric acid, acetic acid) [314]). The following section discusses reported successes by researchers in desorbing and recovering heavy metals from biosorbents.

Sutherland and Venkobachar [315] reported on the desorption of Cu(II) from peat moss. They demonstrated that a distilled water wash could indicate if the metal ions were tightly bound to the biosorbent. Thus, ions released reflect that physical adsorption existed in the sorption process. Desorbed metal ions using competing ions revealed the possibility of ion exchange. Chelating agents such as EDTA are known to form soluble complexes with metal ions over the pH range of 2.0–12.0, and its application as an eluent reveals metal bound by chemisorption. The harsh wash by mineral acids such as HCl was shown to release metal ions bound by physical, chemisorption and ion exchange.

Reyes-Ledezma et al. [316] reported on the desorption of cobalt(II) from *Lemna gibba*. Strong acids, including 0.1 M HCL (hydrochloric acid), 0.1 M H_2SO_4 (sulfric acid), and 0.1 M HNO_3 (nitric acid) and alkaline compounds, including 0.1 M NaOH (sodium hydroxide), 0.1 M $NaHCO_3$ (sodium

bicarbonate), and 0.1M K_2HPO_4 (dipotassium phosphate) were employed as eluents. Eluent of volume 120 mL and the metal-laden biosorbent were added to an Erlenmeyer flask and agitated for 120 min at a speed of 140 rpm and a temperature of 18°C. After three cycles, the best performance was obtained with hydrochloric acid (100% desorption). The authors ascribed the mechanism to be electrostatic interaction. Saeed et al. [116] studied the desorption of Cu(II), Cd(II) and Zn(II) from papaya wood. Maximum desorption occurred after 60 min of wash with 0.1 N HCL. Copper desorbed about 75% in the first thirty (30) min. At equilibrium, desorbed amounts of copper(II), cadmium(II), and zinc(II) were 99%, 99%, and 99%, respectively. Regeneration studies revealed a decline in sorption capacity for zinc of 12% after 5 cycles. In a study by Sarı et al. [87], the authors desorbed As(III) from *Maugeotia genflexa* (dead green algae) using 0.5 M HCl, which produced a 96% recovery. Hossain et al. [317] reported on the recovery of Cu(II) from banana peel. Distilled water, 0.1 N H_2SO_4, 0.1 N HCl, 0.1 N HNO_3, 0.1 N NaOH, and 0.1 N CH_3COOH were utilised as eluents. Pre-adsorbed banana peel (0.5 g) was agitated at 120 rpm for 1,440 min in an Erlenmeyer flask. The amount of desorbed copper was measured in each of the mentioned eluents. After 9 adsorption–desorption cycles, 0.1 N H_2SO_4 with 94% desorbed was the optimum eluent. The biosorption capacity (32.4 mg/g) was unaffected after 7 cycles of use in the regeneration trials.

7.2. Pilot-scale desorption studies

Batch and column laboratory-scale studies have been extensively investigated over the past decades. To advance the biosorption process to industrial-scale application, several researchers have attempted to elucidate the desorption process at pilot-scale. Jakóbik-Kolon et al. [318] reported on the desorption of Zn(II) from hybrid pectin-guar gum. From laboratory-scale to pilot-scale, the authors increased biosorbent mass, height and diameter from 5 g, 15 mm and 11.2 cm to 16 kg, 240 mm and 130 cm, respectively. Acid solutions (0.1 M HNO_3 or 0.05 M H_2SO_4) were used for desorption experiments. Eluent was fed through the column at a constant flow rate of 30 L/h. Only 120 L of acid solution were required to remove the Zn(II) from the biosorbent after 5,900 L of the solution's influent volume had been filtered to the target level (2 mg/L). Thus, in one sorption–desorption step, the Zn(II) ions were subsequently concentrated 49 times [318]. After the first cycle, approximately 25% reduction in zinc removal capacity occurred; however, no further decrease was reported for the following 19 cycles. Raulino et al. [319] studied the desorption of multi-metal solution involving Cu(II), Ni(II) and Zn(II) from *Cocos nucifera*. In the experiment, approximately 20 L of eluent (0.5 mol/L HNO_3) was used in a PVC column (160 cm high × 62 cm ID). Almost all of the copper was desorbed (99%), whereas only 50% of the nickel and zinc were achievable. In a study by Long et al. [298], Pb(II) and Cd(II) were desorbed from modified *A. bisporus* and *P. cornucopiae*. Two plastic columns, each measuring 8.0 cm in diameter and 80 cm in length, were packed with biosorbent to a bed depth of 45 cm. The columns were used in series with 316 and 385 g biosorbent. The biosorption system when packed with the two mushrooms demonstrated the best performance with a treated volume of 156 L and a total metal uptake of 13.6 mg/g. Removal efficiencies of 95% were achieved for all metals in the outlet effluent using 3 L of 0.1 M HNO_3 at a flow rate of 30 mL/min.

8. Biosorption mechanisms

The development of biosorption for the removal and recovery of pollutants from aqueous solutions depends on a detailed understanding of the mechanisms through which biosorbents remove pollutants; yet, these mechanisms are typically poorly understood [320]. The biosorption process consists of a liquid phase (solvent, typically water) that contains dissolved species (adsorbate, metal) and a solid phase (sorbent, biosorbent, biological substance). Numerous mechanisms draw the latter and bind them because of the sorbent's high affinity for the adsorbate species.

Biomass used for biosorption can be dead (non-viable) or alive (viable). Metal ions become biosorbed to the surface of cells as a result of interactions with metal-functional groups on cell surfaces, such as carboxyl, phosphate, hydroxyl, amino, sulphur, sulphide, and thiol functional groups, among others [321]. This is known as passive biosorption, and uses any or all of the following metal binding mechanisms: coordination, complexation, ion exchange, physical adsorption (such as electrostatic), or inorganic microprecipitation [321]. This passive biosorption stage is reversible, where other ions, chelating agents, or acids can elute metal ions adsorbed to the surface. Active biosorption involves metal ions passing through the cell membrane and entering the cells [321]. Although it is easier to use dead biomass or its derivatives and the majority of metal uptake by non-living cells occurs passively [7,320,322], the impact of metabolic processes on sorption is frequently overlooked, especially if there is little biological input to the problem [17]. In addition to being divided into metabolism-dependent and non-metabolism-dependent categories, biosorption mechanisms can also be categorised according to where the metal is removed from solution: (i) extracellular accumulation/precipitation (occurs whether the organism is viable or dead); (ii) cell surface sorption or complexation (occurs whether the organism is viable or dead); and (iii) intracellular accumulation (requires microbial activity) [18].

Michalak et al. [108] outlined several analytical methods used to clarify the biosorption mechanism. Titration procedures make it simple to identify the functional groups on a material surface that have acidic or basic qualities as well as ion-exchange properties. In Fourier-transform infrared spectroscopy, the degree of band shifting in naturally occurring and metal-loaded biomass provides a clue as to how much functional groups interact with metal cations [108,155]. The distribution of various components on the surface of biomass can be studied using scanning electron microscopy and an energy-dispersive X-ray analytical system [323]. This method, in particular, enables the evaluation of morphological changes to the biomass surface (for instance, modifications to the structure of the cell wall following metal ion binding) [108,323]. The quantitative spectroscopic method of X-ray photoelectron spectroscopy analysis (XPS), sometimes referred to as electron spectroscopy

Table 15
Mechanisms of biosorption of heavy metals by various biosorbents

Heavy metal	Biosorbent	Elucidation of biosorption mechanisms	References
As(III)	*Maugeotia genuflexa*	The authors conducted characterization studies, kinetic and equilibrium modelling and thermodynamic analysis to gain mechanistic insight. Fourier-transform infrared spectroscopic examination revealed the presence of carboxyl, hydroxyl, and amide functional groups of the biomass and indicated that biosorption was mostly caused by ion exchange between the metal ions and the hydrogen atoms of the functional groups. Kinetic data followed the pseudo-second-order model suggesting that chemical sorption may be rate-controlling. Equilibrium data were best fitted to the Langmuir isotherm indicating monolayer sorption. The mean biosorption energy calculated using the Dubinin–Radushkevich isotherm implied chemical sorption. Thermodynamic parameters showed that the process was feasible, spontaneous and exothermic in nature. The authors concluded that biosorption of As(III) by algal biomass was predominantly chemical as ion exchange.	[87]
Pb(II)	*Anabaena sphaerica*	The authors conducted characterization studies and equilibrium modelling to gain mechanistic insight. Fourier-transform infrared spectra before and after sorption suggested the involvement amino, hydroxyl, carboxyl, and carbonyl functional groups. The equilibrium results were well represented the Langmuir and Freundlich isotherms. The mean biosorption energy calculated using the Dubinin–Radushkevich isotherm revealed that the biosorption involved valence forces and the sharing or exchange of electrons between the sorbent and sorbate. The authors concluded that biosorption of Cd(II) and Pb(II) onto the biomass of *Anabaena sphaerica* was predominantly ion exchange.	[91]
Cr(VI)	*Sargassum muticum*	The authors conducted characterization studies, kinetic and equilibrium modelling and thermodynamic analysis to gain mechanistic insight. Fourier-transform infrared spectra before and after loading of Cr(VI) indicated the participation of carboxyl, amino groups, hydroxy, amine, sulfonic acids and alcoholic groups in metal uptake. Kinetic data followed the pseudo-second-order model suggesting that chemical sorption was rate-controlling. Equilibrium data were well represented by both the Freundlich and Langmuir predictions. The correlation coefficients of the Langmuir curves, however, were noticeably greater suggesting that under the used experimental conditions, monolayer biosorption, as well as heterogeneous surface conditions, may coexist. Thermodynamic analysis suggested that the removal of Cr(VI) using *Sargassum sphaerice* was spontaneous and endothermic. The authors concluded that biosorption was predominantly chemical as ion exchange.	[95]
Cr(VI)	*Oedogonium hatei*	The authors conducted characterization studies, kinetic and equilibrium modelling and thermodynamic analysis to gain mechanistic insight. Fourier-transform infrared spectroscopy analysis revealed the involvement of amino, carboxylic, hydroxyl, and carbonyl groups in the sorption process. Equilibrium data were well described by both Langmuir and Freundlich adsorption isotherms, indicating both monolayer biosorption and heterogeneous surface conditions. Pseudo-first-order model did a good job of capturing biosorption dynamics. This suggested that although the process includes both boundary layer and intraparticle diffusion processes, film diffusion is primarily the rate-limiting phase. Thermodynamic parameters showed that biosorption was feasible, spontaneous and endothermic under studied conditions. The authors concluded that the process involving the rate-controlling step is much more complex involving both boundary layer and intraparticle diffusion processes.	[96]
Zn(II)	Powdered cow hooves	The authors conducted characterization studies, kinetic and equilibrium modelling and thermodynamic analysis to gain mechanistic insight. Fourier-transform infrared spectra before and after loading of Zn(II) highlighted the involvement of C=O and S−H functional groups. The second-order equation provides the best explanation for the biosorption of zinc onto cow hooves and suggests that chemisorption was the rate-determining process. Monolayer sorption was indicated by the equilibrium data's best match to the Langmuir isotherm. Since all values were less than 8 kJ/mol, the mean biosorption energy at all temperatures shows that physisorption predominated in the biosorption of zinc on cow hooves. Since chemisorption was previously identified as the rate-determining step by kinetic modelling, multiple biosorption mechanisms may be implicated. The process was deemed to be viable, spontaneous, and endothermic by thermodynamic analysis. The research also revealed certain structural alterations at the sorbate–sorbent interface and a significant affinity for Zn^{2+} ions in cow hooves. The authors concluded that biosorption of Zn(II) by powdered cow hooves can be described by both physical and chemical sorption.	[325]

Table 15

Heavy metal	Biosorbent	Elucidation of biosorption mechanisms	References
Cd(II)	*Nannochloropsis oculata*	The authors conducted characterization studies, kinetic and equilibrium modelling and thermodynamic analysis to gain mechanistic insight. Fourier-transform infrared spectra indicated that the functional groups predominantly involved in the biosorption were –OH, COO–, –CH and phosphate groups. The significant changes in the wave numbers of these specific peaks suggested that amido, hydroxyl and phosphate groups could be involved in the biosorption of Cd(II) onto *Nannochloropsis oculata*. Biosorption of Cd(II) by *Nannochloropsis oculata* followed pseudo-second-order kinetics. The Langmuir model was well-fitted by equilibrium data, which suggests that metal ion sorption onto *Nannochloropsis oculata* occurred at the functional groups or binding sites on the surface of the biomass, which is known as monolayer biosorption. The calculated thermodynamic parameters ($\Delta G°$, $\Delta H°$ and $\Delta S°$) showed that biosorption was feasible, spontaneous, chemical and exothermic. The authors concluded that biosorption of Cd(II) by *Nannochloropsis oculata* proceeds chemically.	[326]
Cu(II)	*Rosa damascena*	The authors conducted characterization studies, kinetic and equilibrium modelling and thermodynamic analysis to gain mechanistic insight. Following Cu^{2+} ion biosorption, there was a shift in the wavenumbers of the COOH, OH, and NH_2 groups, indicating that Cu^{2+} may have participated in the sorting process by forming complexes with functional groups on the biosorbent through electrostatic interactions and ion exchange. The Elovich kinetic model and the pseudo-second-order model performed well in fitting the biosorption data. Cu^{2+} biosorption was discovered to be influenced by the interaction of film and intraparticle diffusion. The experimental findings were best matched by the Langmuir and Dubinin–Radushkevich isotherm models, which revealed monolayer sorption. *Rosa damascena* primarily removed copper ions through chemisorption, according to the Dubinin–Radushkevich model's calculated value of E (9.13 kJ/mol). The thermodynamic parameters such as Gibbs free energy, enthalpy, and entropy suggested that sorption was spontaneous, feasible and endothermic. The authors concluded that biosorption of Cu^{2+} ions onto *Rosa damascena* biomass is controlled by both ion exchange and hydrogen bond formation.	[228]
Cd(II)	Leaf biomass of *Calotropis procera*	The authors conducted characterization studies, kinetic and equilibrium modelling and thermodynamic analysis to gain mechanistic insight. Fourier-transform infrared spectroscopy analysis revealed that hydroxy, amine, and alkane functional groups may have been involved in the biosorption of Cd(II), possibly through an ion-exchange process where the metal ions in the solution were transferred from the solution to the biosorbent, resulting in the formation of chemical bonds. Kinetic data followed the pseudo-second-order model suggesting that chemical sorption may have been rate-controlling. According to equilibrium studies, both the Freundlich and Langmuir isotherms accurately describe the biosorption of Cd(II) ions; however, the Langmuir model provided a better fit. Thermodynamic characteristics demonstrated that under experimental conditions, Cd(II) biosorption is viable, spontaneous, endothermic, and extremely disordered in nature. The authors concluded that biosorption was predominantly chemical as ion exchange.	[327]
Cd(II), Co(II)	*Thapsia transtagana* stems powder	The authors conducted characterization studies, kinetic and equilibrium modelling and thermodynamic analysis to gain mechanistic insight. The biosorption of Cd(II) and Co(II) onto the powdered stems of *Thapsia transtagana* may have been primarily caused by acidic functional groups, which were more prevalent than basic functional groups. The scanning electron microscopy showed a rough surface with variable pore size and shape distribution, which can facilitate the biosorption of metal ions on various biosorbent surfaces. The energy-dispersive X-ray spectrum showed that several minerals like potassium, calcium, and sodium were primarily linked with carbon (63.3%) and oxygen (31.5%). Biosorption of Cd(II) and Co(II) onto *Thapsia transtagana* stems powder was better described by the pseudo-first-order model instead of pseudo-second-order kinetic model. Biosorption of metals was best fitted by the Langmuir isotherm model. The loading of species onto the surface of *Thapsia transtagana* stems powder was suggested by thermodynamic analysis to be an exothermic removal process, and there was a reduction in randomness at the solid-solution interface. The authors made no conclusion regarding the predominant sorption mechanisms.	[328]

Table 15 (Continued)

Table 15

Heavy metal	Biosorbent	Elucidation of biosorption mechanisms	References
Se(II)	*Cladophora hutchinsiae*	The authors conducted characterization studies, kinetic and equilibrium modelling and thermodynamic analysis to gain mechanistic insight. According to Fourier-transform infrared spectroscopy measurements, the biosorption was mostly mediated by chemical interactions such as ion exchange between the metal ions and the hydrogen atoms of the carboxyl, hydroxyl, and amide groups of the biomass. The experimental data were well represented by the Lagergren's first order and pseudo-second-order kinetic models. According to the Dubinin–Radushkevich model's calculated mean biosorption energy, Se(IV) was biosorbed onto the biomass of *Cladophora hutchinsiae* through chemical ion exchange. According to the predicted thermodynamic characteristics, exothermic, spontaneous biosorption was possible. The authors concluded that biosorption was predominantly chemical ion exchange.	[100]
Cu(II)	Banana floret	The authors conducted characterization studies, kinetic and equilibrium modelling and thermodynamic analysis to gain mechanistic insight. Banana florets mostly comprise C, O, and K, with trace levels of Mg, S, Si, P, and Cl, according to an energy-dispersive X-ray analysis. The removal of the K, Mg, and Cl peaks upon biosorption indicates that it was involved in the sorption process. The diffusion–chemisorption model performed the best when simulating kinetic data. The Sips isotherm performed the best when simulating equilibrium data. Thermodynamic analysis revealed that the process was exothermic, spontaneously possible, and may have involved one or more of the following: hydrogen bonding, charge transfer, ligand-exchange, and ion bonds; direct and induced ion–dipole and dipole–dipole interactions; van der Waals interactions; hydrophobic bonding; and hydrophobic bonding. The authors concluded that while more than one process may be involved, intraparticle diffusion was the major attachment mechanism, and chemical sorption was the dominant transport mechanism.	[236]
Cd(II)	*Aspergillus nidulans*	The authors conducted kinetic and equilibrium modelling and thermodynamic analysis to gain mechanistic insight. Kinetic data were best simulated using the pseudo-second-order kinetic model suggesting that chemisorption may be the rate-limiting step that controls the biosorption process. Biosorption equilibrium data were best described by Langmuir isotherm model. The low values of $\Delta G°$ showed that sorption was both possible and spontaneous. The positive values of $\Delta S°$ indicate the sorbent's affinity for Cd(II) ions as well as the enhanced unpredictability at the solid/solution interface during sorption. The authors concluded that chemisorption may be the rate-limiting step that controls the biosorption process.	[329]
Pb(II)	*Enterobacter* sp.	The authors conducted characterization studies, kinetic and equilibrium modelling and thermodynamic analysis to gain mechanistic insight. Results from Fourier-transform infrared spectroscopy and XPS revealed that several oxygen-containing groups were primarily engaged in the biosorption process (–OH and –COOH groups). According to the theory, there was metal-ligand interaction after the addition of Pb(II) as a result of the contact between Pb–N and O–S–O with Pb(II). Kinetic data were best fitted by pseudo-second-order kinetic model indicating the chemisorption type sorption of Pb(II) onto *Enterobacter* sp. Equilibrium data were best represented by the Langmuir model at low concentrations and the Temkin isotherm at high concentrations. The computed $\Delta G°$ and $\Delta H°$ were –4.06 and 14.91 (kJ/mol), respectively, which indicated that the biosorption process was spontaneous and endothermic. The authors made no conclusion regarding the predominant sorption mechanisms.	[330]
Pb(II), Cd(II), Cu(II), Cr(VI)	Bark of *Prosopis spicigera*	The authors conducted characterization studies and kinetic and equilibrium modelling to gain mechanistic insight. Studies using Fourier-transform infrared spectroscopy technology suggested that the hydroxyl, carboxyl, and amino groups may be involved in the process of metal ion sorption. The porous characteristics of the *Prosopis spicigera* bark powder and its aptitude for heavy metal ion adsorption were confirmed by scanning electron micrographs. Kinetic studies fitted well to the pseudo-second-order equation indicating that chemical reactions may have been involved in the metal adsorption process. Both Freundlich and Langmuir isotherms fitted well to the adsorption data. The authors concluded that chemical reactions may be playing a role in the metal adsorption process.	[331]

Table 15 (Continued)

Table 15

Heavy metal	Biosorbent	Elucidation of biosorption mechanisms	References
Cu(II)	*Mesorhizobium amorphae*	The authors conducted characterization studies and equilibrium modelling to gain mechanistic insight. Numerous functional groups, including unsaturated alkenes, alkyls, and aromatic groups as well as O–H, N–H, C–H, C=O, –NH, –CN, C–N, and C–O, were found on the cell surface by Fourier-transform infrared spectroscopy analysis. These groups may have played a role in the interaction between the biosorbent and Cu(II). The sorption equilibrium was well-fitted by the Langmuir equation. The authors made no conclusion regarding the predominant sorption mechanisms.	[181]

for chemical analysis, offers important details on the elemental composition, empirical formula, and electronic state of the elements present in a material [108].

Additionally, adsorption kinetics, equilibrium and thermodynamics analysis have been extensively used to gain insights into the mechanisms of biosorption. Table 15 summarises the mechanistic insights obtained in a sliver of the reported studies. Functional groups varied amongst biosorbents but generally had a significant impact on metal uptake, which was attributed to ion exchange, electrostatic interaction, complexation or a combination of these mechanisms. The predominant kinetic model was the pseudo-second-order suggesting that chemical sorption was rate-controlling; however, several studies also reported the involvement of intraparticle diffusion or the dominance of physical sorption. The Langmuir model dominated among the equilibrium models implying monolayer adsorption. At the same time, various investigations reported that both the Freundlich and Langmuir isotherm models exhibit outstanding conformance, which suggests that monolayer biosorption and heterogeneous surface conditions may coexist under the used experimental conditions. In all reported instances, the sorption reactions were spontaneous and feasible but varied in terms of being endothermic or exothermic. According to Fomina and Gadd [11] and Vijayaraghavan and Balasubramanian [324], this variation in removal mechanisms is caused by the complexity of biomaterials as well as the experimental setup, and it is very likely that many mechanisms could exist at the same time.

9. Current trends and future research prospects

Despite the perceived benefits of biosorption (cheap capital and operating costs, reduced biological or chemical sludge, and biosorbent regeneration [12]), the majority of present studies have been restricted to laboratory-scale assessments. Further, many of these studies have been conducted using synthetic and single-ion wastewater or solutions in distilled water, which does not represent the characteristics of industrial effluents comprising coexisting and competing ions. Upgrading to pilot-scale systems allows researchers to discover the difficulties and limitations of applying biosorption in an industrial context. Such undertakings will allow for the consideration of the cost of turning biomass into a viable biosorbent material, the accessibility of a steady supply of raw biomass [143], and the challenges associated with heavy metal recovery and biomass

regeneration and reuse. The leaching of biosorbent-bound organics into treated effluent can be a significant drawback in biosorption applications, mainly because it can cause biosorption columns to clog, impact the quality of treated effluent and introduce an additional burden on treatment cost. Presently, this is not a major focal point in biosorption research and thus greater research attention is warranted. Recent advances in biosorption research have been focused on addressing the issues of biosorbent chemical and mechanical stability through immobilization of the biomass. Such modifications can enhance the separation of the sorbent from the medium [332], reduce channelling and reduce the build-up of pore water pressure in biosorption columns. Unfortunately, these modifications accompany a higher biosorbent cost and can lower biosorptive rates and capacities. Thus, greater research emphasis is needed to expound the optimization and influence of cost at the pilot and full-scale levels. In this review, it was evident that biosorption research continues unabated, however, it is also crucial to highlight that some of the reported literature lack sufficient methodological details to enable reproducibility and more comprehensible data interpretation.

10. Conclusion

The exceptional qualities of biosorbents, such as their abundance, high sorption capacities, and cost-effectiveness, make them a viable option to traditional technologies for the removal of heavy metals from solution. Key concepts affecting biosorption, such as the mechanisms by which different biosorbents remove heavy metals, the influence of experimental parameters on biosorption rate and capacity and the influence of coexisting and competing ions in synthetic solutions have been well established at the level of laboratory batch studies. However, despite the extensive works reported, many biosorbents are still at the developmental stage and yet to be applicable at an industrial scale. Further investigation in the direction of immobilization of biomass, regeneration of the biosorbent material, biosorption with real wastewater, leaching of organics and pilot studies are paramount in order to successfully utilize biosorption technologies in environmental remediation. The present study can be of great benefit to researchers in determining (1) a suitable experimental range to begin biosorption investigations, (2) gaps in the present research to aid in formulating a research agenda, (3) suitable eluents to promote heavy metal recovery and biosorbent reuse, and (4) protocols

and crucial operational parameters for the upgrading of existing batch-scale studies to pilot-scale.

Symbols

a	—	Elovich rate constant, mg/g·min
b	—	Elovich constant measuring surface coverage and chemisorption activation energy, mg/g
B_D	—	Dubinin–Radushkevich value related to sorption energy
b_k	—	Khan model constant
b_T	—	Temkin constant related to the heat of sorption, J/mol
C	—	Uniform concentration of the solute in the bulk of the liquid, mg/L
C_e	—	Equilibrium concentration in solution, mg/L
C_i	—	Concentration of the solute at the particle/liquid interface, mg/L
C_o	—	Initial metal ion concentration, mg/L
C_t	—	Concentration of metal ion at any time, mg/L
E	—	Dubinin–Radushkevich sorption energy
g_{RP}	—	Redlich–Peterson exponent
h	—	PSO initial rate
H	—	Packed column depth, cm
k_a	—	Rate constant in BDST model, L/mg·min
K_{AB}	—	Bohart–Adams rate constant, L/mg·h
k_i	—	DC initial rate, mg/g·t
K_{DC}	—	DC overall rate constant, mg/g·t$^{0.5}$
K_e	—	Toth isotherm constant, mg/g
K_F	—	Freundlich constant related to adsorption affinity, mg/g
K_{id}	—	ID rate constant, mg/g·t$^{1/2}$
K_L	—	Langmuir adsorption equilibrium constant, L/mg
k_o	—	Bhangam constant, mL/L·g
K_{PFO}	—	PFO rate constant, 1/min
K_{PSO}	—	PSO rate constant, g/mg·min
K_{RP}	—	Redlich–Peterson equilibrium constant
K_{RP}	—	Radke–Prausnitz equilibrium constant
K_T	—	Temkin isotherm constant, L/g
K_{TH}	—	Thomas rate constant, L/mg·h
K_Y	—	Yan's rate constant, L/mg·h
k_{YN}	—	Yoon–Nelson rate constant, 1/h
M	—	Biosorbent mass, g
M_{RP}	—	Radke–Prausnitz model exponent
N	—	Toth isotherm exponent, mg/g
n_F	—	Freundlich constant related to heterogeneity
N_o	—	Saturation concentration of the column, mg/L
n_s	—	Sips index of heterogeneity
Q	—	Flow rate, dm³/min
q_e	—	Equilibrium adsorption capacity, mg/g
q_L	—	Langmuir monolayer sorption capacity, mg/g
q_m	—	Maximum sorption capacity, mg/g
q_t	—	Adsorption capacity at any time, mg/g
q_s	—	Sips sorption capacity, mg/g
R	—	Universal gas constant, 8.314 J/K·mol
R_L	—	Separation factor
T	—	Reaction time, min
T	—	Absolute temperature in K
U	—	Linear velocity which is flow rate per unit cross-sectional area, cm/h
V	—	Volume, L
E_a	—	Activation energy
X	—	Amount of adsorbent in the column, g

Greek symbols

α_{RP}	—	Redlich–Peterson constant
α_k	—	Khan isotherm model exponent
A_s	—	Sips affinity constant
β	—	Kinetic coefficient of external mass transfer, 1/h
ΔG	—	Gibb's free energy change
ΔS	—	Entropy change
ΔH	—	Enthalpy change
α	—	Bhangam constant
τ	—	Time required for 50% adsorbate breakthrough or time when $C/C_o = 0.5$, h

References

[1] G. Oguntimein, Biosorption of heavy metals, dyes and contaminants emerging of concern by lignocellulosic biomass, J. Chem. Sci. Chem. Eng., 1 (2020) 28–55.

[2] K. Vijayaraghavan, J. Jegan, K. Palanivelu, M. Velan, Biosorption of cobalt(II) and nickel(II) by seaweeds: batch and column studies, Sep. Purif. Technol., 44 (2005) 53–59.

[3] J.H. Duffus, "Heavy metals" a meaningless term? (IUPAC Technical Report), Pure Appl. Chem., 74 (2002) 793–807.

[4] D.J. Jefferies, P. Firestone, Chemical analysis of some coarse fish from a Suffolk River carried out as part of the preparation for the first release of captive-bred otters, J. Otter Trust, 1 (1984) 17–22.

[5] B. Brown, M. Ahsanullah, Effect of heavy metals on mortality and growth, Mar. Pollut. Bull., 2 (1971) 182–187.

[6] J.W. Moore, Inorganic Contaminants of Surface Water, Springer, New York, 1991.

[7] B. Volesky, Biosorption and Biosorbents, B. Volesky, Ed., Biosorption of Heavy Metals, CRC Press, Boca Raton, 1990, pp. 36–48.

[8] M. Monachese, J.P. Burton, G. Reid, Bioremediation and tolerance of humans to heavy metals through microbial processes: a potential role for probiotics?, Appl. Environ. Microbiol., 78 (2012) 6397–6404.

[9] I. Ismail, T. Moustafa, Biosorption of Heavy Metals, D. Pathania, Ed., Heavy Metals: Sources, Toxicity and Remediation Techniques, Nova Science Publishers, New York, 2016, pp. 131–174.

[10] T. Ramachandra, N. Ahalya, R. Kanamadi, Biosorption: Techniques and Mechanisms, CES Technical Report 110, Centre for Ecological Sciences, Indian Institute of Science, Bangalore, 2005.

[11] M. Fomina, G.M. Gadd, Biosorption: current perspectives on concept, definition and application, Bioresour. Technol., 160 (2014) 3–14.

[12] D. Kratochvil, B. Volesky, Advances in the biosorption of heavy metals, Trends Biotechnol., 16 (1998) 291–300.

[13] T. Matsunaga, H. Takeyama, T. Nakao, A. Yamazawa, Screening of marine microalgae for bioremediation of cadmium-polluted seawater, J. Microtechnol., 70 (1999) 33–38.

[14] J.L. Zhou, Zn biosorption by *Rhizopus arrhizus* and other fungi, Appl. Microbiol. Biotechnol., 51 (1999) 686–693.

[15] K. Aftab, Development of Low-Cost Methodologies for the Removal of Some Toxic Metals (Pb, Zn) Using Fungal Biomass, (Ph.D. Thesis), Government College University, Faisalabad, 2005.

[16] E. Fourest, J.C. Roux, Heavy metal biosorption by fungal mycelial by-products: mechanisms and influence of pH, Appl. Microbiol. Biotechnol., 37 (1992) 399–403.

[17] G.M. Gadd, Biosorption: critical review of scientific rationale, environmental importance and significance for pollution treatment, J. Chem. Technol. Biotechnol., 84 (2009) 13–28.

[18] T. Muraleedharan, L. Iyengar, C. Venkobachar, Biosorption: an attractive alternative for metal removal and recovery, Curr. Sci., 61 (1991) 379–385.

[19] F.G.C. Landell, Dehydrated Hydrogel Microporous Pearls Made of Chitosan and Polyethylenglycol (PEG) and Process for the Manufacture Thereof, MX:2014009193:A, 2016.

[20] D. Li, X. He, Y. Tao, X. Wang, *Pseudomonas alcaliphila* MBR and Its Application in Bioreduction and Biosorption, US:8399237:B2, 2013.

[21] D.C. Tadic, P. Viedma, J.M.G. Sandoval, Biosorbents for the Extraction of Metals, US:8748153:B2, 2014.

[22] M.S. Pfeiffer, L.A.R. Araya, M.L.G. Vergara, Recombinant Bacterium Capable of Removing Mercury(II) Species, Cadmium(II) and Copper(II) in Presence of Other Heavy Metals From Polluted Sites, Product for the Bioremediation, Process of Obtaining the Product and Method of Bioremediation, US:8846376, 2014.

[23] T. Lewis, A. Paszczynski, R. Crawford, J. Sebat, M. Cortese, Methods and Compositions for Bioremediation, US:20030135032:A1, 2003.

[24] P.J. Oberholster, P.H. Cheng, Treatment of Wastewater, US:20160167994:A1, 2016.

[25] C. Rivasseau, E. Farhi, A. Atteia, D. Pro, Novel Radioresistant Alga of the Genus *Coccomyxa*, US:20180057383:A1, 2018.

[26] M.A. Kozubal, R.E. Macur, W.P. Inskeep, Acidophilic *Fusarium oxysporum* Strains, Methods of Their Production and Methods of Their Use, US:20180100171:A1, 2018.

[27] V.P. Prigione, G.C. Varese, L. Casieri, S. Voyron, A. Bertolotto, V.F. Marchisio, Use of *Rhizopus stolonifer* (Ehrenberg) Vuillemin in Methods for Treating Industrial Wastewaters Containing Dyes, US:7658849:B2, 2010.

[28] B. Volesky, Biosorption for the Next Century, in: Biohydrometallurgy and the Environment Toward the Mining of the 21st Century, Proceedings of the International Biohydrometallurgy Symposium, Elsevier, Amsterdam, 1999, pp. 161–170.

[29] J.P. Chen, L. Yang, Chemical modification of *Sargassum* sp. for prevention of organic leaching and enhancement of uptake during metal biosorption, Ind. Eng. Chem. Res., 44 (2005) 9931–9942.

[30] T.A. Davis, F.E.C. Ali, E. Giannitti, B. Volesky, A. Mucci, Cadmium biosorption by *S. fluitans*: treatment, resilience and uptake relative to other *Sargassum* spp. and brown algae, Water Qual. Res. J. Can., 39 (2004) 183–189.

[31] J.T. Matheickal, Q. Yu, Biosorption of lead(II) and copper(II) from aqueous solutions by pre-treated biomass of Australian marine algae, Bioresour. Technol., 69 (1999) 223–229.

[32] R. Dod, G. Banerjee, S. Saini, Adsorption of methylene blue using green pea peels (*Pisum sativum*): a cost-effective option for dye-based wastewater treatment, Biotechnol. Bioprocess Eng., 17 (2012) 862–874.

[33] M.A. Khosa, J. Wu, A. Ullah, Chemical modification, characterization, and application of chicken feathers as novel biosorbents, RSC Adv., 3 (2013) 20800–20810.

[34] I.A. Okoro, S.O. Okoro, Agricultural by products as green chemistry absorbents for the removal and recovery of metal ions from waste-water environments, Cont. J. Water Air Soil Pollut., 2 (2011) 15–22.

[35] J.M. Okuo, S.B. Sanni, S.U. Aigbedion, Selective biosorption of heavy metal ions from aqueous solutions by pre-treated Nigerian freshwater algae, Trends Appl. Sci. Res., 1 (2006) 83–90.

[36] M.S. Rahaman, A. Basu, M.R. Islam, The removal of As(III) and As(V) from aqueous solutions by waste materials, Bioresour. Technol., 99 (2008) 2815–2823.

[37] D. Park, Y.S. Yun, J.M. Park, The past, present, and future trends of biosorption, Biotechnol. Bioprocess Eng., 15 (2010) 86–102.

[38] D.W. O'Connell, C. Birkinshaw, T.F. O'Dwyer, Heavy metal adsorbents prepared from the modification of cellulose: a review, Bioresour. Technol., 99 (2008) 6709–6724.

[39] S. Patel, Potential of fruit and vegetable wastes as novel biosorbents: summarizing the recent studies, Rev. Environ. Sci. Biotechnol., 11 (2012) 365–380.

[40] W.S. Wan Ngah, M.A.K.M. Hanafiah, Removal of heavy metal ions from wastewater by chemically modified plant wastes as adsorbents: a review, Bioresour. Technol., 99 (2008) 3935–3948.

[41] C. Pathirana, A.M. Ziyath, K.B.S.N. Jinadasa, P. Egodawatta, S. Sarina, A. Goonetilleke, Quantifying the influence of surface physico-chemical properties of biosorbents on heavy metal adsorption, Chemosphere, 234 (2019) 488–495.

[42] C.J. Xin, N. Ngadi, Biosorption of chromium(VI) ions using sustainable eggshell impregnated *Pandanus amaryllifolius* roxb. adsorbent, PERINTIS eJournal, 8 (2018) 86–101.

[43] M.B. Ribeiro, J.V. Freitas, F.G. Nogueira, C.S. Farinas, Biosorption of phenolic compounds in lignocellulosic biomass biorefineries, Bioenergy Res., 14 (2021) 598–611.

[44] K.A. Shroff, V.K. Vaidya, Effect of pre-treatments on the biosorption of chromium(VI) ions by the dead biomass of *Rhizopus arrhizus*, J. Chem. Technol. Biotechnol., 87 (2012) 294–304.

[45] I. Vishan, B. Saha, S. Sivaprakasam, A. Kalamdhad, Evaluation of Cd(II) biosorption in aqueous solution by using lyophilized biomass of novel bacterial strain *Bacillus badius* AK: biosorption kinetics, thermodynamics and mechanism, Environ. Technol. Innovation, 14 (2019) 100323, doi: 10.1016/j.eti.2019.100323.

[46] W. Pranata Putra, A. Kamari, S. Najiah Mohd Yusoff, C. Fauziah Ishak, A. Mohamed, N. Hashim, I. Md Isa, Biosorption of Cu(II), Pb(II) and Zn(II) ions from aqueous solutions using selected waste materials: adsorption and characterisation studies, J. Encapsulation Adsorpt. Sci., 4 (2014) 25–35.

[47] O.A. Ramírez Calderón, O.M. Abdeldayem, A. Pugazhendhi, E.R. Rene, Current updates and perspectives of biosorption technology: an alternative for the removal of heavy metals from wastewater, Curr. Pollut. Rep., 6 (2020) 8–27.

[48] Environmental Protection Agency (USEPA), Fate, Transport, and Transformation Test Guidelines, Adsorption/Desorption (Batch Equilibrium), Washington, D.C., 2008.

[49] M. Zhao, J.R. Duncan, R.P. van Hille, Removal and recovery of zinc from solution and electroplating effluent using *Azolla filiculoides*, Water Res., 33 (1999) 1516–1522.

[50] A. Saeed, M. Iqbal, Bioremoval of cadmium from aqueous solution by black gram husk (*Cicer arietinum*), Water Res., 37 (2003) 3472–3480.

[51] B. Volesky, J. Weber, J.M. Park, Continuous-flow metal biosorption in a regenerable *Sargassum* column, Water Res., 37 (2003) 297–306.

[52] K.H. Chu, Improved fixed bed models for metal biosorption, Chem. Eng. J., 97 (2004) 233–239.

[53] Y. Sağ, Biosorption of heavy metals by fungal biomass and modeling of fungal biosorption: a review, Sep. Purif. Methods, 30 (2001) 1–48.

[54] O.P.A. Haapalainen, Binding of Heavy Metals and Nitrogenous Compounds From Wastewaters Via Biosorption, (M.Sc. Thesis), University of Oulu, 2014.

[55] Z. Aksu, F. Gönen, Biosorption of phenol by immobilized activated sludge in a continuous packed bed: prediction of breakthrough curves, Process Biochem., 39 (2004) 599–613.

[56] Z. Aksu, Application of biosorption for the removal of organic pollutants: a review, Process Biochem., 40 (2005) 997–1026.

[57] K. Vijayaraghavan, Y.S. Yun, Bacterial biosorbents and biosorption, Biotechnol. Adv., 26 (2008) 266–291.

[58] P. Le Cloirec, Y. Andres, Bioremediation of Heavy Metals Using Microorganisms, M. Fingerman, R. Nagabhushanam, Eds., Bioremediation of Aquatic and Terrestrial Ecosystems, Science Publishers, Plymouth, 2005, pp. 97–140.

[59] S. Papirio, L. Frunzo, M.R. Mattei, A. Ferraro, M. Race, B. D'Acunto, F. Pirozzi, G. Esposito, Heavy Metal Removal From Wastewaters by Biosorption: Mechanisms and Modeling, in: Sustainable Heavy Metal Remediation, Springer International Publishing, Cham, 2017, pp. 25–63.

[60] A. Adewuyi, Chemically modified biosorbents and their role in the removal of emerging pharmaceutical waste in the water system, Water, 12 (2020) 1551, doi: 10.3390/w12061551.

[61] S.H. Abbas, I.M. Ismail, T.M. Mostafa, A.H. Sulaymon, Biosorption of heavy metals: a review, J. Chem. Sci. Technol., 3 (2014) 74–102.

[62] H. Kinoshita, Y. Sohma, F. Ohtake, M. Ishida, Y. Kawai, H. Kitazawa, T. Saito, K. Kimura, Biosorption of heavy metals by lactic acid bacteria and identification of mercury binding protein, Res. Microbiol., 164 (2013) 701–709.

[63] D.A. John Wase, C. Forster, Biosorbents for Metal Ions, 1st ed., CRC Press, Boca Raton, FL, 1997.

[64] P. Vasudevan, V. Padmavathy, N. Tewari, S.C. Dhingra, Biosorption of heavy metal ions, J. Sci. Ind. Res., 60 (2001) 112–120.

[65] S.L.R.K. Kanamarlapudi, V.K. Chintalpudi, S. Muddada, Application of Biosorption for Removal of Heavy Metals From Wastewater, in: Biosorption, InTechOpen, London, 2018, pp. 70–116.

[66] M. Johncy Rani, B. Hemambika, J. Hemapriya, V. Rajesh Kannan, Comparative assessment of heavy metal removal by immobilized and dead bacterial cells: a biosorption approach, Afr. J. Environ. Sci. Technol., 4 (2010) 077–083.

[67] R.K. Mohapatra, P.K. Parhi, S. Pandey, B.K. Bindhani, H. Thatoi, C.R. Panda, Active and passive biosorption of Pb(II) using live and dead biomass of marine bacterium *Bacillus xiamenensis* PbRPSD202: kinetics and isotherm studies, J. Environ. Manage., 247 (2019) 121–134.

[68] R.F.L. Ribeiro, S.M.S. Magalhães, F.A.R. Barbosa, C.C. Nascentes, I.C. Campos, D.C. Moraes, Evaluation of the potential of microalgae *Microcystis novacekii* in the removal of Pb²⁺ from an aqueous medium, J. Hazard. Mater., 179 (2010) 947–953.

[69] A. Al-Gheethi, R. Mohamed, E. Noman, N. Ismail, O.A. Kadir, Removal of heavy metal ions from aqueous solutions using *Bacillus subtilis* biomass pre-treated by supercritical carbon dioxide, CLEAN – Soil Air Water, 45 (2017) 1700356, doi: 10.1002/clen.201700356.

[70] T. Tsuruta, Biosorption and recycling of gold using various microorganisms, J. Gen. Appl. Microbiol., 50 (2004) 221–228.

[71] W. Mwandira, K. Nakashima, S. Kawasaki, A. Arabelo, K. Banda, I. Nyambe, M. Chirwa, M. Ito, T. Sato, T. Igarashi, H. Nakata, S. Nakayama, M. Ishizuka, Biosorption of Pb(II) and Zn(II) from aqueous solution by *Oceanobacillus profundus* isolated from an abandoned mine, Sci. Rep., 10 (2020) 21189, doi: 10.1038/s41598-020-78187-4.

[72] P. Gupta, B. Diwan, Bacterial exopolysaccharide mediated heavy metal removal: a review on biosynthesis, mechanism and remediation strategies, Biotechnol. Rep., 13, (2017) 58–71.

[73] J.A. Morillo Pérez, R. García-Ribera, T. Quesada, M. Aguilera, A. Ramos-Cormenzana, M. Monteoliva-Sánchez, Biosorption of heavy metals by the exopolysaccharide produced by *Paenibacillus jamilae*, World J. Microbiol. Biotechnol., 24 (2008) 2699–2704.

[74] J.K. Biswas, A. Banerjee, B. Sarkar, D. Sarkar, S.K. Sarkar, M. Rai, M. Vithanage, Exploration of an extracellular polymeric substance from earthworm gut bacterium (*Bacillus licheniformis*) for bioflocculation and heavy metal removal potential, Appl. Sci., 10 (2020) 349, doi: 10.3390/app10010349.

[75] J. Nkoh, J. Yan, Z.N. Hong, R.K. Xu, M.A. Kamran, J. Jun, J.Y. Li, An electrokinetic perspective into the mechanism of divalent and trivalent cation sorption by extracellular polymeric substances of *Pseudomonas fluorescens*, Colloids Surf., B, 183 (2019) 110450, doi: 10.1016/j.colsurfb.2019.110450.

[76] M.I. Ansari, A. Malik, Biosorption of nickel and cadmium by metal resistant bacterial isolates from agricultural soil irrigated with industrial wastewater, Bioresour. Technol., 98 (2007) 3149–3153.

[77] Q. Li, W. Song, M. Sun, J. Li, Z. Yu, Composition change and adsorption performance of EPS from *Bacillus vallismortis* sp. induced by Na₂S, Ecotoxicol. Environ. Saf., 185 (2019) 109679, doi: 10.1016/j.ecoenv.2019.109679.

[78] S. Lu, X. Li, Y. Xi, H. Liu, Z. Zhang, Y. Huang, T. Xie, Y. Liu, B. Quan, C. Zhang, W. Xu, Insight the roles of loosely-bound and tightly-bound extracellular polymeric substances on Cu²⁺, Zn²⁺ and Pb²⁺ biosorption process with *Desulfovibrio vulgaris*, J. Colloid Interface Sci., 596 (2021) 408–419.

[79] P. Concórdio-Reis, M.A.M. Reis, F. Freitas, Biosorption of heavy metals by the bacterial exopolysaccharide FucoPol, Appl. Sci., 10 (2020) 6708, doi: 10.3390/app10196708.

[80] Saba, Y. Rehman, M. Ahmed, A.N. Sabri, Potential role of bacterial extracellular polymeric substances as biosorbent material for arsenic bioremediation, Biorem. J., 23 (2019) 72–81.

[81] J. Rincón, F. González, A. Ballester, M.L. Blázquez, J.A. Muñoz, Biosorption of heavy metals by chemically-activated alga *Fucus vesiculosus*, J. Chem. Technol. Biotechnol., 80 (2005) 1403–1407.

[82] L. Brinza, M. Dring, M. Gavrilescu, Marine micro and macro algal species as biosorbents for heavy metals, Environ. Eng. Manage. J., 6 (2007) 237–251.

[83] A. Ali Redha, Removal of heavy metals from aqueous media by biosorption, Arabian J. Basic Appl. Sci., 27 (2020) 183–193.

[84] I. Anastopoulos, G.Z. Kyzas, Progress in batch biosorption of heavy metals onto algae, J. Mol. Liq., 209 (2015) 77–86.

[85] T.A. Davis, B. Volesky, A. Mucci, A review of the biochemistry of heavy metal biosorption by brown algae, Water Res., 37 (2003) 4311–4330.

[86] R.H. Vieira, B. Volesky, Biosorption: a solution to pollution?, Int. Microbiol., 3 (2000) 17–24.

[87] A. Sarı, Ö.D. Uluozlü, M. Tüzen, Equilibrium, thermodynamic and kinetic investigations on biosorption of arsenic from aqueous solution by algae (*Maugeotia genuflexa*) biomass, Chem. Eng. J., 167 (2011) 155–161.

[88] H.K. Hansen, A. Ribeiro, E. Mateus, Biosorption of arsenic(V) with *Lessonia nigrescens*, Miner. Eng., 19 (2006) 486–490.

[89] I. Tüzün, G. Bayramoğlu, E. Yalçin, G. Başaran, G. Celik, M.Y. Arica, Equilibrium and kinetic studies on biosorption of Hg(II), Cd(II) and Pb(II) ions onto microalgae *Chlamydomonas reinhardtii*, J. Environ. Manage., 77 (2005) 85–92.

[90] M.M. Montazer-Rahmati, P. Rabbani, A. Abdolali, A.R. Keshtkar, Kinetics and equilibrium studies on biosorption of cadmium, lead, and nickel ions from aqueous solutions by intact and chemically modified brown algae, J. Hazard. Mater., 185 (2011) 401–407.

[91] A.M. Abdel-Aty, N.S. Ammar, H.H. Ghafar, R.K. Ali, Biosorption of cadmium and lead from aqueous solution by freshwater alga *Anabaena sphaerica* biomass, J. Adv. Res., 4 (2013) 367–374.

[92] F. Luo, Y. Liu, X. Li, Z. Xuan, J. Ma, Biosorption of lead ion by chemically-modified biomass of marine brown algae *Laminaria japonica*, Chemosphere, 64 (2006) 1122–1127.

[93] G. Bayramoğlu, M. Yakup Arica, Construction a hybrid biosorbent using *Scenedesmus quadricauda* and Ca-alginate for biosorption of Cu(II), Zn(II) and Ni(II): kinetics and equilibrium studies, Bioresour. Technol., 100 (2009) 186–193.

[94] I.M. Dittert, V.J.P. Vilar, E.A.B. da Silva, S.M.A.G.U. de Souza, A.A.U. de Souza, C.M.S. Botelho, R.A.R. Boaventura, Adding value to marine macro-algae *Laminaria digitata* through its use in the separation and recovery of trivalent chromium ions from aqueous solution, Chem. Eng. J., 193 (2012) 348–357.

[95] Y. González Bermúdez, I.L. Rodríguez Rico, E. Guibal, M. Calero de Hoces, M.Á. Martín-Lara, Biosorption of hexavalent chromium from aqueous solution by *Sargassum muticum* brown alga. Application of statistical design for process optimization, Chem. Eng. J., 183 (2012) 68–76.

[96] V.K. Gupta, A. Rastogi, Biosorption of hexavalent chromium by raw and acid-treated green alga *Oedogonium hatei* from aqueous solutions, J. Hazard. Mater., 163 (2009) 396–402.

[97] W.M. Ibrahim, Biosorption of heavy metal ions from aqueous solution by red macroalgae, J. Hazard. Mater., 192 (2011) 1827–1835.

[98] V.K. Gupta, A. Rastogi, A. Nayak, Biosorption of nickel onto treated alga (*Oedogonium hatei*): application of isotherm and kinetic models, J. Colloid Interface Sci., 342 (2010) 533–539.

[99] M.H. Khani, A.R. Keshtkar, B. Meysami, M.F. Zarea, R. Jalali, Biosorption of uranium from aqueous solutions by nonliving biomass of marine algae *Cystoseira indica*, Electron. J. Biotechnol., 9 (2006) 100–106.

[100] M. Tuzen, A. Sarı, Biosorption of selenium from aqueous solution by green algae (*Cladophora hutchinsiae*) biomass: equilibrium, thermodynamic and kinetic studies, Chem. Eng. J., 158 (2010) 200–206.

[101] R. Dhankhar, A. Hooda, Fungal biosorption--an alternative to meet the challenges of heavy metal pollution in aqueous solutions, Environ. Technol., 32 (2011) 467–491.

[102] Y. Göksungur, S. Uren, U. Güvenç, Biosorption of cadmium and lead ions by ethanol treated waste baker's yeast biomass, Bioresour. Technol., 96 (2005) 103–109.

[103] R. Say, N. Yılmaz, A. Denizli, Biosorption of cadmium, lead, mercury, and arsenic ions by the fungus *Penicillium purpurogenum*, Sep. Sci. Technol., 38 (2003) 2039–2053.

[104] G.M. Gadd, Accumulation and Transformation of Metals by Microorganisms, in: Biotechnology Set, Wiley-VCH Verlag GmbH, Weinheim, 2001, pp. 225–264.

[105] C. Sutherland, C. Venkobachar, Equilibrium modeling of Cu(II) biosorption onto untreated and treated forest macro-fungus *Fomes fasciatus*, Int. J. Plant Anim. Environ. Sci., 3 (2013) 193–203.

[106] L. Ramrakhiani, S. Khowala, Effect of pretreatment on hexavalent chromium biosorption and multimetal biosorption efficiency of *Termitomyces clypeatus* biomass, Int. J. Integr. Sci. Innov. Technol., 1 (2012) 7–15.

[107] I. Abd-Elsalam, Factorial design for some parameters affecting on chromium III uptake by *Saccharomyces cerevisiae*, Int. J. Appl. Biol. Pharm., 2 (2011) 33–40.

[108] I. Michalak, K. Chojnacka, A. Witek-Krowiak, State of the art for the biosorption process – review, Appl. Biochem. Biotechnol., 170 (2013) 1389–1416.

[109] J. Wang, C. Chen, Chitosan-based biosorbents: modification and application for biosorption of heavy metals and radionuclides, Bioresour. Technol., 160 (2014) 129–141.

[110] G. Crini, Recent developments in polysaccharide-based materials used as adsorbents in wastewater treatment, Prog. Polym. Sci., 30 (2005) 38–70.

[111] S. De Gisi, G. Lofrano, M. Grassi, M. Notarnicola, Characteristics and adsorption capacities of low-cost sorbents for wastewater treatment: a review, Sustainable Mater. Technol., 9 (2016) 10–40.

[112] K. Selvaraj, S. Manonmani, S. Pattabhi, Removal of hexavalent chromium using distillery sludge, Bioresour. Technol., 89 (2003) 207–211.

[113] R. Gulati, R.K. Saxena, R. Gupta, Fermentation waste of *Aspergillus terreus*: a potential copper biosorbent, World J. Microbiol. Biotechnol., 18 (2002) 397–401.

[114] Y. Liu, M.C. Lam, H.H. Fang, Adsorption of heavy metals by EPS of activated sludge, Water Sci. Technol., 43 (2001) 59–66.

[115] R. Fernández-González, M.Á. Martín-Lara, G. Blázquez, A. Pérez, M. Calero, Recovering metals from aqueous solutions by biosorption onto hydrolyzed olive cake, Water, 11 (2019) 2519, doi: 10.3390/w11122519.

[116] A. Saeed, M. Akhter, M. Iqbal, Removal and recovery of heavy metals from aqueous solution using papaya wood as a new biosorbent, Sep. Purif. Technol., 45 (2005) 25–31.

[117] N. Basci, E. Kocadagistan, B. Kocadagistan, Biosorption of copper(II) from aqueous solutions by wheat shell, Desalination, 164 (2004) 135–140.

[118] Z.R. Komy, W.H. Abdelraheem, N.M. Ismail, Biosorption of Cu²⁺ by *Eichhornia crassipes*: physicochemical characterization, biosorption modeling and mechanism, J. King Saud Univ. Sci., 25 (2013) 47–56.

[119] G.H. Pino, L.M.S. de Mesquita, M.L. Torem, G.A.S. Pinto, Biosorption of heavy metals by powder of green coconut shell, Sep. Sci. Technol., 41 (2006) 3141–3153.

[120] A. Kumar, O. Sahu, Sugar industry waste as removal of toxic metals from wastewater, World J. Chem. Edu., 1 (2013) 17–20.

[121] I.J. Alinnor, Adsorption of heavy metal ions from aqueous solution by fly ash, Fuel, 86 (2007) 853–857.

[122] C. Sutherland, B.S. Chittoo, C. Venkobachar, Application of an artificial neural network-genetic algorithm methodology for modelling and optimization of the improved biosorption of a chemically modified peat moss: kinetic studies, Desal. Water Treat., 84 (2017) 69–84.

[123] X. Han, C.F. Liang, T.Q. Li, K. Wang, H.G. Huang, X.E. Yang, Simultaneous removal of cadmium and sulfamethoxazole from aqueous solution by rice straw biochar, J. Zhejiang Univ.-Sci. B, 14 (2013) 640–649.

[124] J.R. Memon, S.Q. Memon, M.I. Bhanger, G.Z. Memon, A. El-Turki, G.C. Allen, Characterization of banana peel by scanning electron microscopy and FT-IR spectroscopy and its use for cadmium removal, Colloids Surf., B, 66 (2008) 260–265.

[125] O.I. Asubiojo, O.B. Ajelabi, Removal of heavy metals from industrial wastewaters using natural adsorbents, Toxicol. Environ. Chem., 91 (2009) 883–890.

[126] Y. Bulut, Z. Tez, Adsorption studies on ground shells of hazelnut and almond, J. Hazard. Mater., 149 (2007) 35–41.

[127] A. Hashem, E.S. Abdel-Halim, K.F. El-Tahlawy, A. Hebeish, Enhancement of the adsorption of Co(II) and Ni(II) ions onto peanut hulls through esterification using citric acid, Adsorpt. Sci. Technol., 23 (2005) 367–380.

[128] Y. Sun, P.A. Webley, Preparation of activated carbons from corncob with large specific surface area by a variety of chemical activators and their application in gas storage, Chem. Eng. J., 162 (2010) 883–892.

[129] I. Tan, A. Ahmad, B. Hameed, Optimization of preparation conditions for activated carbons from coconut husk using response surface methodology, Chem. Eng. J., 137 (2008) 462–470.

[130] Y. Bulut, Z. Tez, Removal of heavy metals from aqueous solution by sawdust adsorption, J. Environ. Sci., 19 (2007) 160–166.

[131] M.C. Ncibi, B. Mahjoub, M. Seffen, Investigation of the sorption mechanisms of metal-complexed dye onto *Posidonia oceanica* (L.) fibres through kinetic modelling analysis, Bioresour. Technol., 99 (2008) 5582–5589.

[132] Y. Safa, H.N. Bhatti, Biosorption of Direct Red-31 and Direct Orange-26 dyes by rice husk: application of factorial design analysis, Chem. Eng. Res. Des., 89 (2011a) 2566–2574.

[133] Y. Safa, H.N. Bhatti, Kinetic and thermodynamic modeling for the removal of Direct Red-31 and Direct Orange-26 dyes from aqueous solutions by rice husk, Desalination, 272 (2011b) 313–322.

[134] M.M. Dávila-Jiménez, M.P. Elizalde-González, A.A. Peláez-Cid, Adsorption interaction between natural adsorbents and textile dyes in aqueous solution, Colloids Surf., A, 254 (2005) 107–114.

[135] A. Artola, M.J. Martin, M. Balaguer, M. Rigola, Pilot plant biosorption in an integrated contact-settling system: application to Cu(II) removal by anaerobically digested sludge, J. Chem. Technol. Biotechnol., 76 (2001) 1141–1146.

[136] G. Yan, T. Viraraghavan, Heavy metal removal in a biosorption column by immobilized *M. rouxii* biomass, Bioresour. Technol., 78 (2001) 243–249.

[137] N. Sooksawat, M. Meetam, M. Kruatrachue, P. Pokethitiyook, D. Inthorn, Performance of packed bed column using *Chara aculeolata* biomass for removal of Pb and Cd ions from wastewater, J. Environ. Sci. Health. Part A Toxic/Hazard. Subst. Environ. Eng., 52 (2017) 539–546.

[138] J.Z. Chen, X.C. Tao, J. Xu, T. Zhang, Z.L. Liu, Biosorption of lead, cadmium and mercury by immobilized *Microcystis aeruginosa* in a column, Process Biochem., 40 (2005) 3675–3679.

[139] J. Cruz-Olivares, C. Pérez-Alonso, C. Barrera-Díaz, F. Ureña-Nuñez, M.C. Chaparro-Mercado, B. Bilyeu, Modeling of lead(II) biosorption by residue of allspice in a fixed-bed column, Chem. Eng. J., 228 (2013) 21–27.

[140] L. Pelit, F.N. Ertaş, A.E. Eroğlu, T. Shahwan, H. Tural, Biosorption of Cu(II) and Pb(II) ions from aqueous solution by natural spider silk, Bioresour. Technol., 102 (2011) 8807–8813.

[141] A. Abdolali, H.H. Ngo, W. Guo, J.L. Zhou, J. Zhang, S. Liang, S.W. Chang, D.D. Nguyen, Y. Liu, Application of a breakthrough biosorbent for removing heavy metals from synthetic and real wastewaters in a lab-scale continuous fixed-bed column, Bioresour. Technol., 229 (2017) 78–87.

[142] M. Tsezos, Z. Georgousis, E. Remoudaki, Mechanism of aluminum interference on uranium biosorption by *Rhizopus arrhizus*, Biotechnol. Bioeng., 55 (1997) 16–27.

[143] M. Tsezos, Biosorption of metals. The experience accumulated and the outlook for technology development, Hydrometallurgy, 59 (2001) 241–243.

[144] I. Mikhaylov, A. Averbuch, E. Tumarkin, I. Furmer, Chemical Technology, Part I, 3rd ed., MIR Publishers, Moscow, 1979.

[145] M. Calero, A. Ronda, A. Pérez, A. Yáñez, M.C. Trujillo, M.Á. Martín-Lara, The scale-up of Cr³⁺ biosorption onto olive

stone in a fixed bed column, Desal. Water Treat., 57 (2016) 25140–25152.

[146] A. Ronda, M.A. Martín-Lara, O. Osegueda, V. Castillo, G. Blázquez, Scale-up of a packed bed column for wastewater treatment, Water Sci. Technol., 77 (2018) 1386–1396.

[147] A. Ronda, M.A. Martín-Lara, E. Dionisio, G. Blázquez, M. Calero, Effect of lead in biosorption of copper by almond shell, J. Taiwan Inst. Chem. Eng., 44 (2013) 466–473.

[148] M.Á. Martín-Lara, M.C. Trujillo Miranda, A. Ronda Gálvez, A. Pérez Muñoz, M. Calero de Hoces, Valorization of olive stone as adsorbent of chromium(VI): comparison between laboratory- and pilot-scale fixed-bed columns, Int. J. Environ. Sci. Technol., 14 (2017) 2661–2674.

[149] A. Hethnawi, A.D. Manasrah, G. Vitale, N.N. Nassar, Fixed-bed column studies of total organic carbon removal from industrial wastewater by use of diatomite decorated with polyethylenimine-functionalized pyroxene nanoparticles, J. Colloid Interface Sci., 513 (2018) 28–42.

[150] R. Elangovan, L. Philip, K. Chandraraj, Biosorption of hexavalent and trivalent chromium by palm flower (*Borassus aethiopum*), Chem. Eng. J., 141 (2008) 99–111.

[151] G. Tenorio Rivas, Characterization of the Biosorption of Chromium with Olive Stone, (Ph.D. Thesis), University of Granada, 2006.

[152] M. Karimi, A. Shojaei, A. Nematollahzadeh, M.J. Abdekhodaie, Column study of Cr(VI) adsorption onto modified silica–polyacrylamide microspheres composite, Chem. Eng. J., 210 (2012) 280–288.

[153] P. Sar, S.F. D'Souza, Biosorption of thorium(IV) by a *Pseudomonas* biomass, Biotechnol. Lett., 24 (2002) 239–243.

[154] V.J.P. Vilar, C.M.S. Botelho, R.A.R. Boaventura, Lead uptake by algae *Gelidium* and composite material particles in a packed bed column, Chem. Eng. J., 144 (2008a) 420–430.

[155] V. Murphy, H. Hughes, P. Mcloughlin, Cu(II) binding by dried biomass of red, green and brown macroalgae, Water Res., 41 (2007) 731–740.

[156] P. Srinivasa Rao, S. Kalyani, K.V.N. Suresh Reddy, A. Krishnaiah, Comparison of biosorption of nickel(II) and copper(II) ions from aqueous solution by *Sphaeroplea* algae and acid treated *Sphaeroplea* algae, Sep. Sci. Technol., 40 (2005) 3149–3165.

[157] Y.P. Kumar, P. King, V.S.R.K. Prasad, Removal of copper from aqueous solution using *Ulva fasciata* sp.–a marine green algae, J. Hazard. Mater., 137 (2006) 367–373.

[158] P.A. Marques, H.M. Pinheiro, J. Teixeira, M.F. Rosa, Removal efficiency of Cu^{2+}, Cd^{2+} and Pb^{2+} by waste brewery biomass: pH and cation association effects, Desalination, 124 (1999) 137–144.

[159] M.F. Wong, H. Chua, W. Lo, C.K. Leung, P.H. Yu, Removal and recovery of copper(II) ions by bacterial biosorption, Appl. Biochem. Biotechnol., 91 (2001) 447–457.

[160] H. Xu, Y. Liu, J.H. Tay, Effect of pH on nickel biosorption by aerobic granular sludge, Bioresour. Technol., 97 (2006) 359–363.

[161] C. Escudero-Oñate, I. Villaescusa, The Thermodynamics of Heavy Metal Sorption onto Lignocellulosic Biomass, in: Heavy Metals, InTechOpen, London, 2018, pp. 235–251.

[162] A.C. Gonçalves Jr., D. Schwantes, M.A. Campagnolo, D.C. Dragunski, C.R.T. Tarley, A.K.D.S. Silva, Removal of toxic metals using endocarp of açaí berry as biosorbent, Water Sci. Technol., 77 (2018) 1547–1557.

[163] M. Fadel, N.M. Hassanein, M.M. Elshafei, A.H. Mostafa, M.A. Ahmed, H.M. Khater, Biosorption of manganese from groundwater by biomass of *Saccharomyces cerevisiae*, HBRC J., 13 (2017) 106–113.

[164] N. Goyal, S.C. Jain, U.C. Banerjee, Comparative studies on the microbial adsorption of heavy metals, Adv. Environ. Res., 7 (2003) 311–319.

[165] S. Shamim, Biosorption of Heavy Metals, in: Biosorption, InTechOpen, London, 2018, pp. 21–49.

[166] N.T. Abdel-Ghani, A.K. Hegazy, G.A. El-Chaghaby, *Typha domingensis* leaf powder for decontamination of aluminium, iron, zinc and lead: biosorption kinetics and equilibrium modeling, Int. J. Environ. Sci. Technol., 6 (2009) 243–248.

[167] W.M. Ibrahim, A.F. Hassan, Y.A. Azab, Biosorption of toxic heavy metals from aqueous solution by *Ulva lactuca* activated carbon, Egypt. J. Basic Appl. Sci., 3 (2016) 241–249.

[168] S. Dahiya, R.M. Tripathi, A.G. Hegde, Biosorption of heavy metals and radionuclide from aqueous solutions by pre-treated arca shell biomass, J. Hazard. Mater., 150 (2008) 376–386.

[169] S. Wierzba, A. Latała, Biosorption lead(II) and nickel(II) from an aqueous solution by bacterial biomass, Pol. J. Chem. Technol., 12 (2010) 72–78.

[170] S.N. Azizi, A. Hosseinzadeh Colagar, S.M. Hafeziyan, Removal of Cd(II) from aquatic system using *Oscillatoria* sp. biosorbent, Sci. World J., 2012 (2012) 347053, doi: 10.1100/2012/347053.

[171] A.A. Hamdy, Biosorption of heavy metals by marine algae, Curr. Microbiol., 41 (2000) 232–238.

[172] D. Kumar, J.P. Gaur, Metal biosorption by two cyanobacterial mats in relation to pH, biomass concentration, pretreatment and reuse, Bioresour. Technol., 102 (2011) 2529–2535.

[173] G. Ren, Y. Jin, C. Zhang, H. Gu, J. Qu, Characteristics of *Bacillus* sp. PZ-1 and its biosorption to Pb(II), Ecotoxicol. Environ. Saf., 117 (2015) 141–148.

[174] M. Abbas, R. Nadeem, M.N. Zafar, M. Arshad, Biosorption of chromium(III) and chromium(VI) by untreated and pretreated *Cassia fistula* biomass from aqueous solutions, Water Air Soil Pollut., 191 (2008) 139–148.

[175] S.E. Oh, S.H.A. Hassan, J.H. Joo, Biosorption of heavy metals by lyophilized cells of *Pseudomonas stutzeri*, World J. Microbiol. Biotechnol., 25 (2009) 1771–1778.

[176] Y.C. Lee, S.P. Chang, The biosorption of heavy metals from aqueous solution by *Spirogyra* and *Cladophora* filamentous macroalgae, Bioresour. Technol., 102 (2011) 5297–5304.

[177] A.Ş. Yargıç, R.Z. Yarbay Şahin, N. Özbay, E. Önal, Assessment of toxic copper(II) biosorption from aqueous solution by chemically-treated tomato waste, J. Cleaner Prod., 88 (2015) 152–159.

[178] E. Ozbay, A. Cinar, A Novel Approach to Smoothing on 3D Structured Adaptive Mesh of the Kinect-Based Models, in: Computer Science & Information Technology (CS & IT), Academy & Industry Research Collaboration Center (AIRCC), Tamil Nada, 2013, pp. 12–22.

[179] J.Y. Farah, N.S. El-Gendy, Performance, kinetics and equilibrium in biosorption of anionic dye Acid Red 14 by the waste biomass of *Saccharomyces cerevisiae* as a low-cost biosorbent, Turk. J. Eng. Environ. Sci., 37 (2013) 146–161.

[180] Y. Nuhoglu, E. Malkoc, Thermodynamic and kinetic studies for environmentally friendly Ni(II) biosorption using waste pomace of olive oil factory, Bioresour. Technol., 100 (2009) 2375–2380.

[181] O.A. Mohamad, X. Hao, P. Xie, S. Hatab, Y. Lin, G. Wei, Biosorption of copper(II) from aqueous solution using non-living *Mesorhizobium amorphae* strain CCNWGS0123, Microbes Environ., 27 (2012) 234–241.

[182] R. Marandi, F.D. Ardejani, H. Afshar, Biosorption of lead(II) and zinc(II) ions by pre-treated biomass of *Phanerochaete chrysosporium*, J. Min. Environ., 1 (2010) 9–16.

[183] İ. Şahin, S.Y. Keskin, C.S. Keskin, Biosorption of cadmium, manganese, nickel, lead, and zinc ions by *Aspergillus tamarii*, Desal. Water Treat., 51 (2013) 4524–4529.

[184] A. Chergui, R. Kerbachi, G.A. Junter, Biosorption of hexacyanoferrate(III) complex anion to dead biomass of the basidiomycete *Pleurotus mutilus*: biosorbent characterization and batch experiments, Chem. Eng. J., 147 (2009) 150–160.

[185] K. Parvathi, R. Nagendran, Biosorption of chromium from effluent generated in chrome-electroplating unit using *Saccharomyces cerevisiae*, Sep. Sci. Technol., 42 (2007) 625–638.

[186] C.C.V. Cruz, A.C.A. da Costa, C.A. Henriques, A.S. Luna, Kinetic modeling and equilibrium studies during cadmium biosorption by dead *Sargassum* sp. biomass, Bioresour. Technol., 91 (2004) 249–257.

[187] N. Rajamohan, M. Rajasimman, M. Dilipkumar, Parametric and kinetic studies on biosorption of mercury using modified *Phoenix dactylifera* biomass, J. Taiwan Inst. Chem. Eng., 45 (2014) 2622–2627.

[188] F.G. Helfferich, Principles of adsorption and adsorption processes, AlChE J., 31 (1985) 523–524.

[189] R.E. Treybal, Mass-Transfer Operations, 3rd ed., in: Adsorption and Ion Exchange, Mc-Graw Hill Company, Malaysia, 1981, pp. 568–569.

[190] R.C. Bansal, M. Goyal, Activated Carbon Adsorption, CRC Press, Boca Raton, 2005.

[191] O. Gulnaz, S. Saygideger, E. Kusvuran, Study of Cu(II) biosorption by dried activated sludge: effect of physico-chemical environment and kinetics study, J. Hazard. Mater., 120 (2005) 193–200.

[192] T.G. Chuah, A. Jumasiah, I. Azni, S. Katayon, S.Y. Thomas Choong, Rice husk as a potentially low-cost biosorbent for heavy metal and dye removal: an overview, Desalination, 175 (2005) 305–316.

[193] M. Riaz, R. Nadeem, M.A. Hanif, T.M. Ansari, K.U. Rehman, Pb(II) biosorption from hazardous aqueous streams using *Gossypium hirsutum* (cotton) waste biomass, J. Hazard. Mater., 161 (2009) 88–94.

[194] A. Şengil, M. Özacar, Competitive biosorption of Pb^{2+}, Cu^{2+} and Zn^{2+} ions from aqueous solutions onto valonia tannin resin, J. Hazard. Mater., 166 (2009) 1488–1494.

[195] V. Mishra, C. Balomajumder, V.K. Agarwal, Biosorption of Zn(II) onto the surface of non-living biomasses: a comparative study of adsorbent particle size and removal capacity of three different biomasses, Water Air Soil Pollut., 211 (2010) 489–500.

[196] L.J. Yu, S.S. Shukla, K.L. Dorris, A. Shukla, J.L. Margrave, Adsorption of chromium from aqueous solutions by maple sawdust, J. Hazard. Mater., 100 (2003) 53–63.

[197] K.K. Wong, C.K. Lee, K.S. Low, M.J. Haron, Removal of Cu and Pb by tartaric acid modified rice husk from aqueous solutions, Chemosphere, 50 (2003) 23–28.

[198] N. Muisa, I. Nhapi, W. Ruziwa, M.M. Manyuchi, Utilization of alum sludge as adsorbent for phosphorus removal in municipal wastewater: a review, J. Water Process Eng., 35 (2020) 101187, doi: 10.1016/j.jwpe.2020.101187.

[199] A. Bhatnagar, A.K. Minocha, Conventional and non-conventional adsorbents for removal of pollutants from water - a review, Indian J. Chem. Technol., 13 (2006) 203–217.

[200] S.P. Dubey, K. Gopal, J.L. Bersillon, Utility of adsorbents in the purification of drinking water: a review of characterization, efficiency and safety evaluation of various adsorbents, J. Environ. Biol., 30 (2009) 327–332.

[201] C. Sutherland, Removal of Heavy Metals from Water Using Low-Cost Adsorbents: Process Development, (Ph.D. Thesis), The University of the West Indies, St. Augustine, 2004.

[202] C. Sutherland, C. Venkobachar, A diffusion–chemisorption kinetic model for simulating biosorption using forest macro-fungus, *Fomes fasciatus*, Int. Res. J. Plant Sci., 1 (2010) 107–117.

[203] W.J. Weber Jr., J.C. Morris, Kinetics of adsorption on carbon from solution, J. Sanit. Eng. Div., 89 (1963) 31–59.

[204] A.E. Ofomaja, Intraparticle diffusion process for lead(II) biosorption onto *Mansonia* wood sawdust, Bioresour. Technol., 101 (2010) 5868–5876.

[205] A.R. Teixeira, C.C. Chang, T. Coogan, R. Kendall, W. Fan, P.J. Dauenhauer, Dominance of surface barriers in molecular transport through silicalite-1, J. Phys. Chem., 117 (2013) 25545–25555.

[206] Y.S. Ho, G. McKay, A comparison of chemisorption kinetic models applied to pollutant removal on various sorbents, Process Saf. Environ. Prot., 76 (1998a) 332–340.

[207] Y.S. Ho, G. Mckay, The kinetics of sorption of basic dyes from aqueous solution by sphagnum moss peat, Can. J. Chem. Eng., 76 (1998c) 822–827.

[208] Y.S. Ho, G. McKay, A kinetic study of dye sorption by biosorbent waste product pith, Resour. Conserv. Recycl., 25 (1999) 171–193.

[209] F.C. Wu, R.L. Tseng, R.S. Juang, Characteristics of Elovich equation used for the analysis of adsorption kinetics in dye-chitosan systems, Chem. Eng. J., 150 (2009) 366–373.

[210] S.H. Chien, W.R. Clayton, Application of Elovich equation to the kinetics of phosphate release and sorption in soils, Soil Sci. Soc. Am. J., 44 (1980) 265–268.

[211] V.G. Georgieva, M.P. Tavlieva, S.D. Genieva, L.T. Vlaev, Adsorption kinetics of Cr(VI) ions from aqueous solutions onto black rice husk ash, J. Mol. Liq., 208 (2015) 219–226.

[212] R. Subha, C. Namasivayam, Modeling of adsorption isotherms and kinetics of 2,4,6-trichlorophenol onto microporous $ZnCl_2$ activated coir pith carbon, J. Environ. Eng. Manage., 18 (2008) 275–280.

[213] V. Mishra, C. Balomajumder, V.K. Agarwal, Kinetics, mechanistic and thermodynamics of Zn(II) ion sorption: a modeling approach, CLEAN – Soil Air Water, 40 (2012) 718–727.

[214] A. Basker, P.S. Shabudeen, S. Daniel, P.V. Kumar, Adsorptive removal of malachite green from aqueous solution using areca husk carbon, Rasayan J. Chem., 7 (2014) 1–15.

[215] Y.S. Ho, G. Mckay, Kinetic models for the sorption of dye from aqueous solution by wood, Process Saf. Environ. Prot., 76 (1998b) 183–191.

[216] R. Mikutta, A. Baumgärtner, A. Schippers, L. Haumaier, G. Guggenberger, Extracellular polymeric substances from *Bacillus subtilis* associated with minerals modify the extent and rate of heavy metal sorption, Environ. Sci. Technol., 46 (2012) 3866–3873.

[217] T. Manobala, S.K. Shukla, T.S. Rao, M.D. Kumar, Kinetic modelling of the uranium biosorption by *Deinococcus radiodurans* biofilm, Chemosphere, 269 (2021) 128722, doi: 10.1016/j.chemosphere.2020.128722.

[218] M.H. Khani, Biosorption of strontium by a nonliving brown marine algae, *Padina* sp., Sep. Sci. Technol., 47 (2012) 1886–1897.

[219] M.H. Khani, Uranium biosorption by *Padina* sp. algae biomass: kinetics and thermodynamics, Environ. Sci. Pollut. Res. Int., 18 (2011) 1593–1605.

[220] S. Karthikeyan, R. Balasubramanian, C.S.P. Iyer, Evaluation of the marine algae *Ulva fasciata* and *Sargassum* sp. for the biosorption of Cu(II) from aqueous solutions, Bioresour. Technol., 98 (2007) 452–455.

[221] P. Lodeiro, B. Cordero, J.L. Barriada, R. Herrero, M.E. Sastre de Vicente, Biosorption of cadmium by biomass of brown marine macroalgae, Bioresour. Technol., 96 (2005) 1796–1803.

[222] H. Pahlavanzadeh, A.R. Keshtkar, J. Safdari, Z. Abadi, Biosorption of nickel(II) from aqueous solution by brown algae: equilibrium, dynamic and thermodynamic studies, J. Hazard. Mater., 175 (2010) 304–310.

[223] R. Apiratikul, P. Pavasant, Batch and column studies of biosorption of heavy metals by *Caulerpa lentillifera*, Bioresour. Technol., 99 (2008) 2766–2777.

[224] Y.X. Li, Y. Wang, F.J. Zhao, Kinetic and equilibrium studies of chromium(VI) biosorption by spent macro algae *Polysiphonia urceolata* and *Chondrus ocellatus*, Biotechnol. Biotechnol. Equip., 29 (2015) 498–505.

[225] A. Javaid, R. Bajwa, A. Javaid, Biosorption of heavy metals using a dead macro fungus *Schizophyllum commune* fries: evaluation of equilibrium and kinetic models, Pak. J. Bot., 42 (2010) 2105–2118.

[226] A. Khodabakhshi, F. Mohammadi-Moghadam, K. Shakeri, S. Hemati, Equilibrium and thermodynamic studies on the biosorption of lead(II) by living and nonliving biomass of *Penicillium notatum*, J. Chem., 2022 (2022) 1–9.

[227] Y.G. Liu, T. Fan, G.M. Zeng, X. Li, Q. Tong, F. Ye, M. Zhou, W.H. Xu, Y.E. Huang, Removal of cadmium and zinc ions from aqueous solution by living *Aspergillus niger*, Trans. Nonferrous Met. Soc. China, 16 (2006) 681–686.

[228] M.A. Fawzy, H.M. Al-Yasi, T.M. Galal, R.Z. Hamza, T.G. Abdelkader, E.F. Ali, S.H.A. Hassan, Statistical optimization, kinetic, equilibrium isotherm and thermodynamic studies of copper biosorption onto *Rosa damascena* leaves as a low-cost biosorbent, Sci. Rep., 12 (2022) 1–19.

[229] Y.D. Aracagök, Biosorption of lead by a soil isolate *Aspergillus neoalliaceus*, Arch. Microbiol., 204 (2022) 547, doi: 10.1007/s00203-022-03164-6.

[230] E. Savastru, D. Bulgariu, C.I. Zamfir, L. Bulgariu, Application of *Saccharomyces cerevisiae* in the biosorption of Co(II), Zn(II)

and Cu(II) ions from aqueous media, Water, 14 (2022) 976, doi: 10.3390/w14060976.

[231] S. Mushtaq, F.E. Bareen, A. Tayyeb, Equilibrium kinetics and thermodynamic studies on biosorption of heavy metals by metal-resistant strains of *Trichoderma* isolated from tannery solid waste, Environ. Sci. Pollut. Res. Int., 30 (2022) 10925–10954.

[232] M. Villen-Guzman, D. Gutierrez-Pinilla, C. Gomez-Lahoz, C. Vereda-Alonso, J.M. Rodriguez-Maroto, B. Arhoun, Optimization of Ni(II) biosorption from aqueous solution on modified lemon peel, Environ. Res., 179 (2019) 108849.

[233] A. Pholosi, E.B. Naidoo, A.E. Ofomaja, Intraparticle diffusion of Cr(VI) through biomass and magnetite coated biomass: A comparative kinetic and diffusion study, S. Afr. J. Chem. Eng., 32 (2020) 39–55.

[234] A.E. Ofomaja, A. Pholosi, E.B. Naidoo, Kinetics and competitive modeling of cesium biosorption onto chemically modified pine cone powder, J. Taiwan Inst. Chem. Eng., 44 (2013) 943–951.

[235] M.O. Omorogie, J.O. Babalola, E.I. Unuabonah, J.R. Gong, Hybrid materials from agro-waste and nanoparticles: implications on the kinetics of the adsorption of inorganic pollutants, Environ. Technol., 35 (2014) 611–619.

[236] C. Sutherland, A. Marcano, B. Chittoo, Artificial neural network-genetic algorithm prediction of heavy metal removal using a novel plant-based biosorbent banana floret: Kinetic, equilibrium, thermodynamics and desorption studies, In: Desalination and Water Treatment, InTechOpen, London, 2018, pp. 385–411.

[237] M.P. Tavlieva, S.D. Genieva, V.G. Georgieva, L.T. Vlaev, Thermodynamics and kinetics of the removal of manganese(II) ions from aqueous solutions by white rice husk ash, J. Mol. Liq., 211 (2015) 938–947.

[238] A. Obike, J. Igwe, C. Emeruwa, K. Uwakwe, C. Aghalibe, Diffusion–Chemisorption and Pseudo-Second-Order Kinetic Models for Heavy Metal Removal from Aqueous Solutions Using Modified and Unmodified Oil Palm Fruit Fibre, Chem. Sci. Int. J., 23 (2018) 1–13.

[239] P.M. Melia, R. Busquets, S. Ray, A.B. Cundy, Agricultural wastes from wheat, barley, flax and grape for the efficient removal of Cd from contaminated water, RSC Adv., 8 (2018) 40378–40386.

[240] P. Liu, Y. Gong, C. Yang, R. Ledesma-Amaro, Y.K. Park, S. Deng, Y. Wang, H. Wei, W. Chen, Biorefining of rapeseed meal: A new and sustainable strategy for improving Cr(VI) biosorption on residual wastes from agricultural byproducts after phenolic extraction, Waste Manag., 165 (2023) 70–81.

[241] A. Bilgic, A. Cimen, A.N. Kursunlu, A novel biosorbent functionalized pillar[5]arene: Synthesis, characterization and effective biosorption of Cr(VI), Sci. Total Environ., 857 (2023) 159312.

[242] J. Liu, C. Zhang, B. Tao, J. Beckerman, Revealing the roles of biomass components in the biosorption of heavy metals in wastewater by various chemically treated hemp stalks, J. Taiwan Inst. Chem. Eng., 143 (2023) 104701.

[243] M. Benavente, E. Álvarez, L. Moreno, J. Martinez, Removal of copper and zinc from gold ore tailings solutions using chitosan, In: II International Workshop on Process Hydrometallurgy, GECAMIN Ltda., Santiago 2008, pp. 139–152.

[244] N. Kano, K. Tanabe, M. Pang, Y. Deng, H. Imaizumi, Biosorption of chromium from aqueous solution using chitosan, J. Chem. Chem., 8 (2014) 1049–1058.

[245] A.S. Ali, A.M.A. Hassan, M.H. Nour, Equilibrium and Kinetics studies for Removal of Heavy Metals from simulated Wastewater using Chitosan/Activated carbon composite, Int. J. Res. Environ. Sci., 6 (2020) 12–27.

[246] H.Y. Sharef, N.A. Fakhre, Rapid adsorption of some heavy metals using extracted chitosan anchored with new aldehyde to form a schiff base, PLoS One, 17 (2022) 1–21.

[247] Y.S. Ho, J.F. Porter, G. McKay, Equilibrium isotherm studies for the sorption of divalent metal ions onto peat: Copper, nickel and lead single component systems, Water Air Soil Pollut., 141 (2001) 1–33.

[248] I. Langmuir, The constitution and fundamental properties of solids and liquids. Part 1. Solids, J. Am. Chem. Soc., 38 (1916) 2221–2295.

[249] C. Sutherland, B.S. Chittoo, C. Venkobachar, Application of ANN predictive model for the design of batch adsorbers - Equilibrium simulation of Cr(VI) adsorption onto activated carbon, Open Civ. Eng. J., 13 (2019) 69–81.

[250] E. Swan, A.R. Urquhart, Adsorption equations, J. Phys. Chem., 31 (1927) 251–276.

[251] H.M.F. Freundlich, Over the adsorption in solution, J. Phys. Chem., 57 (1906) 1100–1107.

[252] O. Redlich, D.L. Peterson, A useful adsorption isotherm, J. Phys. Chem., 63 (1959) 1024–1024.

[253] R. Sips, On the structure of a catalyst surface, J. Chem. Phys., 16 (1948) 490–495.

[254] J. Behbahani, Z.J. Behbahani, A new study on asphaltene adsorption in porous media, Petrol. Coal., 56 (2014) 459–466.

[255] M.S. Padder, C.B.C. Majunder, Studies on the removal of As(III) and As(V) through their adsorption onto granular activated carbon/MnFe2O4 composite: isotherm studies and error analysis, Compos. Interface, 23 (2012) 327–372.

[256] O. Amrhar, H. Nassali, M.S. Elyoubi, Two and three-parameter isothermal modeling for adsorption of crystal violet dye onto natural illitic clay: nonlinear regression analysis, J. Chem. and Pharm. Res., 7 (2015a) 892–903.

[257] D. Ringot, B. Lerzy, K. Chaplain, J.P. Bonhoure, E. Auclair, Y. Larondelle, *In-vitro* biosorption of ochratoxin A on the yeast industry by-products: comparison of isotherm models, Bioresour. Technol., 98 (2007) 1812–1821.

[258] H. Shahbeig, N. Bagheri, S.A. Ghorbanian, A. Hallajisani, S. Poorkarimi, A new adsorption isotherm model of aqueous solutions on granular activated carbon, World J. Modell. Simul., 9 (2013) 243–254.

[259] O. Amrhar, H. Nassai, M.S. Elyoubi, Application of nonlinear regression analysis to select the optimum absorption isotherm for methylene blue adsorption onto natural illitic clay, Bull. R. Soc. Sci. Liège, 84 (2015b) 116–130.

[260] A.O. Dada, A.P. Olalekan, A.M. Olatunya, O.J.I.J.C. Dada, Langmuir, Freundlich, Temkin and Dubinin–Radushkevich isotherms studies of equilibrium sorption of Zn²⁺ unto phosphoric acid modified rice husk, IOSR J. Appl. Chem., 3 (2012) 38–45.

[261] C.J. Radke, J.M. Prausnitz, Adsorption of organic solutes from dilute aqueous solution of activated carbon, Ind. Eng. Chem. Fundam., 11 (1972) 445–451.

[262] N. Ayawei, A.N. Ebelegi, D. Wankasi, Modelling and interpretation of adsorption isotherms, J. Chem., 2017 (2017) 1–11.

[263] N. Sivarajasekar, R. Baskar, Adsorption of basic red 9 onto activated carbon derived from immature cotton seeds: isotherm studies and error analysis, Desal. Water Treat., 52 (2014) 7743–7765.

[264] M. Oves, M.S. Khan, A. Zaidi, Biosorption of heavy metals by *Bacillus thuringiensis* strain OSM29 originating from industrial effluent contaminated north Indian soil, Saudi J. Biol. Sci., 20 (2013) 121–129.

[265] G. Ozdemir, T. Ozturk, N. Ceyhan, R. Isler, T. Cosar, Heavy metal biosorption by biomass of *Ochrobactrum anthropi* producing exopolysaccharide in activated sludge, Bioresour. Technol., 90 (2003) 71–74.

[266] W.B. Lu, J.J. Shi, C.H. Wang, J.S. Chang, Biosorption of lead, copper and cadmium by an indigenous isolate *Enterobacter* sp. J1 possessing high heavy-metal resistance, J. Hazard. Mater., 134 (2006) 80–86.

[267] R. Zanetti, S. Zecchin, M. Colombo, G. Borgonovo, S. Mazzini, L. Scaglioni, G. Facchetti, R. Gandolfi, I. Rimoldi, L. Cavalca, Ni²⁺ and Cu²⁺ biosorption by EPS-producing *Serratia plymuthica* strains and potential bio-catalysis of the organo–metal complexes, Water, 14 (2022) 3410.

[268] L. Xiao, X. Qu, D. Zhu, Biosorption of nonpolar hydrophobic organic compounds to *Escherichia coli* facilitated by metal and proton surface binding, Environ. Sci. Technol., 41 (2007) 2750–2755.

[269] M.H. Khani, Biosorption of strontium by *Padina* sp. algae biomass: process optimisation and equilibrium study, Int. J. Environ. Technol. and Manage., 16 (2013) 290–311.

[270] R. Kumar, N.R. Bishnoi, Garima, K. Bishnoi, Biosorption of chromium(VI) from aqueous solution and electroplating wastewater using fungal biomass, Chem. Eng. J., 135 (2008) 202–208.

[271] N.N.N.A. Rahman, M. Shahadat, F.M. Omar, A.W. Chew, M.O.A. Kadir, Dry *Trichoderma* biomass: biosorption behavior for the treatment of toxic heavy metal ions, Desal. Water Treat., 57 (2016) 13106–13112.

[272] A. Khodabakhshi, F.M. Moghadam, R. Abdizadeh, K. Shakeri, Biosorption of lead using *Penicillium notatum* dead biomass from aqueous solutions, Desal. Water Treat., 154 (2019) 296–304.

[273] M.A. Fawzy, H. Darwish, S. Alharthi, M.I. Al-Zaban, A. Noureldeen, S.H.A. Hassan, Process optimization and modeling of Cd^{2+} biosorption onto the free and immobilized *Turbinaria ornata* using Box–Behnken experimental design, Sci. Rep., 12 (2022) 3256, doi: 10.1038/s41598-022-07288-z.

[274] T.K. Naiya, A.K. Bhattacharya, S.K. Das, Adsorption of Pb(II) by sawdust and neem bark from aqueous solutions, Environ. Prog., 27 (2008) 313–328.

[275] C.I. Orozco, M.S. Freire, D. Gómez-Díaz, J. González-Álvarez, Removal of copper from aqueous solutions by biosorption onto pine sawdust, Sustainable Chem. Pharm., 32 (2023) 101016, doi: 10.1016/j.scp.2023.101016.

[276] V.G. Georgieva, L. Gonsalvesh, M.P. Tavlieva, Thermodynamics and kinetics of the removal of nickel(II) ions from aqueous solutions by biochar adsorbent made from agro-waste walnut shells, J. Mol. Liq., 309 (2020) 112788, doi: 10.1016/j.molliq.2020.112788.

[277] J.T. Bamgbose, S. Adewuyi, O. Bamgbose, A.A. Adetoye, Adsorption kinetics of cadmium and lead by chitosan, Afr. J. Biotechnol., 9 (2010) 2560–2565.

[278] R. Han, Y. Wang, X. Zhao, Y. Wang, F. Xie, J. Cheng, M. Tang, Adsorption of methylene blue by phoenix tree leaf powder in a fixed-bed column: experiments and prediction of breakthrough curves, Desalination, 245 (2009) 284–297.

[279] H. Patel, Fixed-bed column adsorption study: a comprehensive review, Appl. Water Sci., 9 (2019) 1–17.

[280] R.A. Hutchin, New method simplifies design of activated carbon systems, Chem. Eng., 80 (1973) 133–138.

[281] G. Yan, T. Viraraghavan, M. Chen, A new model for heavy metal removal in a biosorption column, Adsorpt. Sci. Technol., 19 (2001) 25–43.

[282] G.S. Bohart, E.Q. Adams, Some aspects of the behavior of charcoal with respect to chlorine, J. Am. Chem. Soc., 42 (1920) 523–544.

[283] T.A.H. Nguyen, H.H. Ngo, W.S. Guo, T.Q. Pham, F.M. Li, T.V. Nguyen, X.T. Bui, Adsorption of phosphate from aqueous solutions and sewage using zirconium loaded okara (ZLO): fixed-bed column study, Sci. Total Environ., 523 (2015) 40–49.

[284] S. Ayoob, A.K. Gupta, Sorptive response profile of an adsorbent in the defluoridation of drinking water, Chem. Eng. J., 133 (2007) 273–281.

[285] Y.H. Yoon, J.H. Nelson, Application of gas adsorption kinetics. I. A theoretical model for respirator cartridge service life, Am. Ind. Hyg. Assoc. J., 45 (1984) 509–516.

[286] M. Stojčić, D. Pamučar, E. Mahmutagić, Ž. Stević, Development of an ANFIS model for the optimization of a queuing system in warehouses, Information, 9 (2018) 240, doi: 10.3390/info9100240.

[287] A. Wolborska, Adsorption on activated carbon of p-nitrophenol from aqueous solution, Water Res., 23 (1989) 85–91.

[288] S. Singha, U. Sarkar, Analysis of the dynamics of a packed column using semi-empirical models: case studies with the removal of hexavalent chromium from effluent wastewater, Korean J. Chem. Eng., 32 (2015) 20–29.

[289] A.D. Dorado, X. Gamisans, C. Valderrama, M. Solé, C. Lao, Cr(III) removal from aqueous solutions: a straightforward model approaching of the adsorption in a fixed-bed column, J. Environ. Sci. Health., Part A, 49 (2014) 179–186.

[290] C.I.A. Ferreira, V. Calisto, M. Otero, H. Nadais, V.I. Esteves, Fixed-bed adsorption of tricaine methanesulfonate onto pyrolysed paper mill sludge, Aquacult. Eng., 77 (2017) 53–60.

[291] H.C. Thomas, Heterogeneous ion exchange in a flowing system, J. Am. Chem. Soc., 66 (1944) 1664–1666.

[292] N. Sazali, Z. Harun, N. Sazali, A review on batch and column adsorption of various adsorbent towards the removal of heavy metal, J. Adv. Res. Fluid Mech. Therm. Sci., 67 (2020) 66–88.

[293] F. Costa, T. Tavares, Diethylketone and Cd Pilot-Scale Biosorption by a Biofilm Supported on Vermiculite, in: WASTES – Solutions, Treatments and Opportunities II, CRC Press, London, 2018, pp. 139–145.

[294] M. Ghasemi, A.R. Keshtkar, R. Dabbagh, S. Jaber Safdari, Biosorption of uranium(VI) from aqueous solutions by Ca-pretreated *Cystoseira indica* alga: breakthrough curves studies and modeling, J. Hazard. Mater., 189 (2011) 141–149.

[295] B. Volesky, I. Prasetyo, Cadmium removal in a biosorption column, Biotechnol. Bioeng., 43 (1994) 1010–1015.

[296] K. Vijayaraghavan, D. Prabu, Potential of *Sargassum wightii* biomass for copper(II) removal from aqueous solutions: application of different mathematical models to batch and continuous biosorption data, J. Hazard. Mater., 137 (2006) 558–564.

[297] D. Bulgariu, L. Bulgariu, Potential use of alkaline treated algae waste biomass as sustainable biosorbent for clean recovery of cadmium(II) from aqueous media: batch and column studies, J. Cleaner Prod., 112 (2016) 4525–4533.

[298] Y. Long, Q. Li, J. Ni, F. Xu, H. Xu, Treatment of metal wastewater in pilot-scale packed bed systems: efficiency of single- vs. mixed-mushrooms, RSC Adv., 5 (2015) 29145–29152.

[299] Ł. Tuhy, M. Samoraj, Z. Witkowska, P. Rusek, K. Chojnacka, Conversion of spent mushroom substrate into micronutrient fertilizer via biosorption in a pilot plant, Ecol. Eng., 84 (2015) 370–374.

[300] Z. Zulfadhly, M.D. Mashitah, S. Bhatia, Heavy metals removal in fixed-bed column by the macro fungus *Pycnoporus sanguineus*, Environ. Pollut., 112 (2001) 463–470.

[301] F. Amin, F.N. Talpur, A. Balouch, H.I. Afridi, A.A. Khaskheli, Efficient entrapping of toxic Pb(II) ions from aqueous system on a fixed-bed column of fungal biosorbent, Geol. Ecol. Landscapes, 2 (2018) 39–44.

[302] K. Pakshirajan, T. Swaminathan, Continuous biosorption of Pb, Cu, and Cd by *Phanerochaete chrysosporium* in a packed column reactor, Soil Sediment Contam., 15 (2006) 187–197.

[303] Y. Long, D. Lei, J. Ni, Z. Ren, C. Chen, H. Xu, Packed bed column studies on lead(II) removal from industrial wastewater by modified *Agaricus bisporus*, Bioresour. Technol., 152 (2014) 457–463.

[304] M. Samoraj, Ł. Tuhy, P. Rusek, E. Rój, K. Chojnacka, Pilot plant conversion of blackcurrant seeds into new micronutrient fertilizer biocomponents via biosorption, Bioresources, 11 (2015) 400–413.

[305] H. Patel, Batch and continuous fixed bed adsorption of heavy metals removal using activated charcoal from neem (*Azadirachta indica*) leaf powder, Sci. Rep., 10 (2020) 16895, doi: 10.1038/s41598-020-72583-6.

[306] L.M. Vera, D. Bermejo, M.F. Uguña, N. Garcia, M. Flores, E. González, Fixed bed column modeling of lead(II) and cadmium(II) ions biosorption on sugarcane bagasse, Environ. Eng. Res., 24 (2018) 31–37.

[307] R. Han, J. Zhang, W. Zou, H. Xiao, J. Shi, H. Liu, Biosorption of copper(II) and lead(II) from aqueous solution by chaff in a fixed-bed column, J. Hazard. Mater., 133 (2006) 262–268.

[308] S.H. Hasan, P. Srivastava, M. Talat, Biosorption of lead using immobilized *Aeromonas hydrophila* biomass in up flow column system: factorial design for process optimization, J. Hazard. Mater., 177 (2010) 312–322.

[309] I. Morosanu, C. Teodosiu, C. Paduraru, D. Ibanescu, L. Tofan, Biosorption of lead ions from aqueous effluents by rapeseed biomass, New Biotechnol., 39 (2017) 110–124.

[310] W.C. Tsai, M.D.G. de Luna, H.L.P. Bermillo-Arriesgado, C.M. Futalan, J.I. Colades, M.W. Wan, Competitive fixed-bed adsorption of Pb(II), Cu(II), and Ni(II) from aqueous solution using chitosan-coated bentonite, Int. J. Polym. Sci., 2016 (2016) 1–11.

[311] Vijayalakshmi, Sangeetha, P.N. Sudha, Analysis of packed bed adsorption column with nanochitosan/sodium alginate/microcrystalline cellulose bead for copper(II) removal from aqueous solution, IOSR J. Pharm., (2017) 69–78.

[312] N. Bishnoi, Garima, Fungus – an alternative for bioremediation of heavy metal containing wastewater: a review, J. Sci. Ind. Res., 64 (2005) 93–100.

[313] A. Ghosh, M.G. Dastidar, A.T.R. Sreekrishnan, A.M. Asce, Recent advances in bioremediation of heavy metals and metal complex dyes: review, J. Environ. Eng., 142 (2015) 1–14.

[314] S. Lata, P.K. Singh, S.R. Samadder, Regeneration of adsorbents and recovery of heavy metals: a review, Int. J. Environ. Sci. Technol., 12 (2015) 1461–1478.

[315] C. Sutherland, C. Venkobachar, Regeneration of a chemically improved peat moss for the removal and recovery of Cu(II) and Pb(II) from aqueous solution, Desal. Water Treat., 178 (2020) 172–181.

[316] J.L. Reyes-Ledezma, E. Cristiani-Urbina, L. Morales-Barrera, Biosorption of Co^{2+} ions from aqueous solution by K_2HPO_4-pretreated duckweed *Lemna gibba*, Processes, 8 (2020) 1–21.

[317] M.A. Hossain, H.H. Ngo, W.S. Guo, T.V. Nguyen, Biosorption of Cu(II) from water by banana peel based biosorbent: experiments models of adsorption and desorption, J. Water Sustain., 2 (2012) 87–104.

[318] A. Jakóbik-Kolon, J. Bok-Badura, A. Milewski, K. Karoń, Long term and large-scale continuous studies on zinc(II) sorption and desorption on hybrid pectin-guar gum biosorbent, Polymers, 11 (2019) 96, doi: 10.3390/polym11010096.

[319] G.S.C. Raulinoa, C.B. Vidal, A.C.A. Lima, D.Q. Melo, J.T. Oliveira, R.F. Nascimento, Treatment influence on green coconut shells for removal of metal ions: pilot-scale fixed-bed column, Environ. Technol., 35 (2014) 1711–1720.

[320] F. Veglio, F. Beolchini, Removal of metals by biosorption: a review, Hydrometallurgy, 44 (1997) 301–316.

[321] J. Wang, C. Chen, Biosorption of heavy metals by *Saccharomyces cerevisiae*: a review, Biotechnol. Adv., 24 (2006) 427–451.

[322] Y. Madrid, C. Cámara, Biological substrates for metal preconcentration and speciation, Trends Anal. Chem., 16 (1997) 36–44.

[323] M.M. Figueira, B. Volesky, H.J. Mathieu, Instrumental analysis study of iron species biosorption by *Sargassum* biomass, Environ. Sci. Technol., 33 (1999) 1840–1846.

[324] K. Vijayaraghavan, R. Balasubramanian, Is biosorption suitable for decontamination of metal-bearing wastewaters? a critical review on the state-of-the-art of biosorption processes and future directions, J. Environ. Manage., 160 (2015) 283–296.

[325] I. Osasona, O.O. Ajayi, A.O. Adebayo, Equilibrium, kinetics, and thermodynamics of the biosorption of Zn(II) from aqueous solution using powdered cow hooves, ISRN Phys. Chem., 2013 (2013) 1–7.

[326] J. Kaparapu, M. Krishna Prasad, Equilibrium, kinetics and thermodynamic studies of cadmium(II) biosorption on *Nannochloropsis oculata*, Appl. Water Sci., 8 (2018) 1–9.

[327] B.J. Oyebamiji, L.C. Overah, A. Babarinde, V.O. Oninla, A. Olatunde, Kinetic, equilibrium and thermodynamic studies on the biosorption of Cd(II) from aqueous solutions by the leaf biomass of *Calotropis procera* – 'Sodom Apple', J. Appl. Sci. Environ. Manage., 15 (2011) 607–615.

[328] A. Machrouhi, M. Farnane, A. Elhalil, M. Abdennouri, H. Tounsadi, N. Barka, Heavy metals biosorption by *Thapsia transtagana* stems powder: kinetics, equilibrium and thermodynamics, Morrocan J. Chem., 7 (2019) 98–110.

[329] S. Maheswari, M. Vindyashree, A.G. Murugesan, Adsorption kinetics, equilibrium and thermodynamics studies for the removal of cadmium(II) ions from aqueous solution by *Aspergillus nidulans*, Int. J. Sci. Res. Pub., 6 (2016) 448–452.

[330] L. Liu, M. Xia, J. Hao, H. Xu, W. Song, Biosorption of Pb(II) by the resistant *Enterobacter* sp.: investigated by kinetics, equilibrium and thermodynamics, Arch. Environ. Prot., 47 (2021) 28–36.

[331] A. Sohail, S. Javed, M.U. Khan, A. Umar, W. Ulfat, J. Yaqoob, Biosorption of heavy metals onto the bark of *Prosopis spicigera*: a kinetic study for the removal of water toxicity, Am. Eurasian J. Toxicol. Sci., 7 (2015) 300–310.

[332] Z. Velkova, G. Kirova, M. Stoytcheva, S. Kostadinova, K. Todorova, V. Gochev, Immobilized microbial biosorbents for heavy metals removal, Eng. Life Sci., 18 (2018) 871–881.